ANALYSIS OF GENOME INTEGRITY AND CHROMATIN ARCHITECTURE IN HETEROCHROMATIN-DEFECTIVE MUTANTS OF *NEUROSPORA CRASSA*

by

TAKAHIKO SASAKI

(Under the Direction of Zachary Lewis)

ABSTRACT

Eukaryotic genomes are partitioned into functionally distinctive domains: euchromatin and heterochromatin. Euchromatin corresponds to transcriptionally active domains of chromosomes whereas heterochromatin is transcriptionally inert. Constitutive heterochromatin, typically marked by H3K9me3, is required for normal growth and development in eukaryotes. Previous studies in *Drosophila* showed that loss of heterochromatin mediated by H3K9 histone methyltransferases leads to genome instability characterized by global chromosomal rearrangements and increased copy number of repeats. Previous research in *Neurospora* indicates that loss of a component required for H3K9 methylation leads to sensitization of cells to a DNA damaging agent and growth defects. These observations suggest that heterochromatin components are required for normal genome integrity. A major goal of my dissertation has been to elucidate a role of heterochromatin components such as DIM-5 in genome maintenance and to identify the underlying mechanisms by which heterochromatin components ensure proper DNA repair and/or chromosomal replication in *Neurospora crassa*. In this dissertation, I describe how loss of DIM-5 or other heterochromatin components affect global chromatin architecture. I show evidence that *Δdim-5* strains suffer from genotoxic stress presumably caused by stalled DNA

replication forks or double-stranded DNA breaks. The endogenous stress activates the DNA damage checkpoint. I also show that *Δdim-5* strains form aberrant facultative heterochromatin that leads to spontaneous induction of the DNA damage response and growth defects. I demonstrate that, in *Δdim-5,* H3K27me3 distribution is completely switched to centromeres and AT-rich repetitive domains where constitutive heterochromatin normally occurs. This suggests that the recruitment process of the PRC2 complex responsible for H3K27me3 has changed in *Δdim-5,* disrupting global genome architecture. Removal of the PRC2 catalytic subunit *set-7* suppresses the MMS-hypersensitive phenotype and partially relieves the growth defects of *Δdim-5*. Moreover, I demonstrate that *Δdim-5* exhibits genetic interactions with *Δmi-2* and *Δcrf-6*. These findings show in greater detail that heterochromatin is required for genome integrity and defects in heterochromatin affect the global landscape of chromatin components and chromatin modification. This dissertation broadens our perspective of heterochromatin function and its importance in cell growth and development in eukaryotes.

INDEX WORDS: *Neurospora crassa*, Heterochromatin, Histone Lysine Methyltransferase, DNA methylation

ANALYSIS OF GENOME INTEGRITY AND CHROMATIN ARCHITECTURE IN HETEROCHROMATIN-DEFECTIVE MUTANTS OF *NEUROSPORA CRASSA*

by

TAKAHIKO SASAKI

B.S., The University of Alabama in Huntsville, 2007

A Dissertation Submitted to the Graduate Faculty of The University of Georgia in Partial Fulfillment of the Requirements for the Degree

DOCTOR OF PHILOSOPHY

ATHENS, GEORGIA

2015

ANALYSIS OF GENOME INTEGRITY AND CHROMATIN ARCHITECTURE IN HETEROCHROMATIN-DEFECTIVE MUTANTS OF *NEUROSPORA CRASSA*

by

TAKAHIKO SASAKI

Major Professor:	Zachary Lewis
Committee:	Anna Karls
	Michelle Momany
	Timothy Hoover
	Xiaoyu Zhang

Electronic Version Approved:

Julie Coffield
Interim Dean of the Graduate School
The University of Georgia
May 2015

DEDICATION

I dedicate this dissertation to my parents, Hiroo and Noriko who have been supporting the endeavor I have chosen to take on.

ACKNOWLEDGEMENTS

I thank my major advisor Zachary Lewis for providing wonderful projects for my graduate research. I also thank my advisory committee Dr. Anna Karls, Dr. Michelle Momany, Dr. Timothy Hoover and Dr. Xiaoyu Zhang for their support and guidance. I would like to thank my former major advisor Dr. Anne Summers for her support in my first research project and training at the Graduate school. For financial support I acknowledge the Department of Microbiology, the Graduate School, and Genetic Society of America. Finally, I would like to acknowledge my academic advisor at University of Alabama in Huntsville Dr. Maria Davis for giving me a chance to be a scientist.

TABLE OF CONTENTS

Page

LIST OF TABLES

Page

LIST OF FIGURES

Page

LIST OF ABBREVIATIONS

CPT Camptothecin

DSBs Double-stranded breaks

HATs Histone Acetyltransferases

HU hydroxyurea

KMTs Histone Lysine Acetyltransferases

MMS methyl methanesulfonate

SAM S-adenosylmethionine

VMM Vogel Minimal Medium

DIM Defective in DNA methylation

DCDC DIM-5,-7,-9, CUL4, DDB1, Complex

HCHC HP1, CDP-2, HDA-1 and CHAP

CHAPTER 1

INTRODUCTION AND LITERATURE REVIEW

My project is focused on investigating a role of heterochromatin components in genome integrity, using a tractable model organism *Neurospora crassa*. Many heterochromatin components have been identified by genetic screens or by protein co-purification followed by mass spectrometry in model organisms. Many studies have shown that components directing constitutive heterochromatin formation are required for genome integrity. Mutations in heterochromatin components have a link to human disease such as cancer. Despite its obvious importance, the molecular mechanisms by which heterochromatin components contribute to genome integrity remain elusive. The recent advance in sequencing technology allows us to study the genome-wide distribution of chromatin components. My review highlights the links between chromatin structure and function, featuring heterochromatin domains and the associated proteins.

Genetics and Epigenetics

Genetics is study of heredity in an organism. Its fundamental principle is that a gene is responsible for a final phenotype, and mutations within the gene are directly inheritable. This concept, however, does not explain some phenotypic variations of organisms in the same genetic background. For example, the Agouti mouse is obese and has a yellow hair color whereas its siblings of the same genotype have normal weight and dark grey coats (1). This variation can be explained by "epigenetic change" in the level of transcription of genes responsible for yellow

color development through loss of DNA methylation at cryptic promoters (2). This is one example showing that the final phenotype does not depend exclusively on genotypes. There has been a growing interest in studying these types of phenomena as they have links to human diseases such as cancer, and this interest has led to birth of epigenetics, which is the study of the inheritable traits or phenotypes that cannot be explained by an organism's genotype (3). Research in epigenetics is focused on interplay between genes and their products determining the outcome of growth and development. In epigenetics, chromatin is a focus of study because it regulates virtually all DNA based processes. For example, a number of factors such as nucleosome positioning, histone variants, histone modifications, DNA methylation, chromatin remodelers, and noncoding RNAs coordinate each other, affecting DNA replication, transcriptional states, and genome integrity (3-6). Epigenetic marks, such as DNA methylation, can be inheritable through mitosis and meiosis and transcriptional state is maintained through generation (3). Most importantly, chromatin and epigenetic processes play a pivotal role in differentiation of a single stem cell into various cell types (5, 7).

Eukaryotic genomes are packaged and organized into chromatin

Eukaryotic chromosomes are packaged and organized in a nucleus. The folding process is mediated by many cellular components. One of the key components is a DNA binding protein histone. Eukaryotes have several kinds of histones, H1, H2A, H2B, H3 and H4. These histones interact with DNA forming a stable complex called a nucleosome. Histones are basic, acid soluble proteins, which function as transcription regulators by restricting access of RNA polymerase onto DNA (8, 9). Nucleosome formation occurs all over the chromosomes and an array of nucleosomes lead to higher order chromatin structure in conjunction with other

chromatin components (10, 11). This chromosomal packaging is ubiquitous in eukaryotes perhaps because it enables them to carry more genetic material than bacteria. In fact, eukaryotic genomes typically range in size from small (10 Mbp yeast genome) to large 3 Gbp (human genome) whereas prokaryotic genomes are typically smaller (up to 10 Mb) (12).

Crystal structures of nucleosomes have been solved using histones from yeasts, *Drosophila*, *Xenopus* and human (13). The first high-resolution crystal structure of a nucleosome shows that the 146 bp of DNA wrapped around a histone octamer is comprised of 2 heterodimers each of H2A-H2B and H3-H4 (14). The bead-shaped structure has a diameter of about 100 Å and its height is 25 to 60 Å (13). The solvent accessible surface of a mononucleosome is about 74,000 $Å^2$ (13). Each histone contains 3 helices and two loops in the middle of sequence. Specifically, these domains are positioned between 27-88 of H2A, 34-98 of H2B, 64-131 of H3, and 31-93 of H4 from *Xenopus laevis* and conserved among eukaryotes (13, 14). These domains have the positively charged surface that facilitates histone-DNA interaction (13, 14). In addition, hydrogen bonds, ionic and non-polar interactions also contribute to formation of the core particle (13). An N-terminal tail of each histone and a C-terminal tail of H2A protrude from the nucleosome core particle. Unlike the core particle, these domains are flexible and can interact with various histone modifying enzymes and chromatin remodelers (6). Each N-terminal tail carries a strong net positive charge containing multiple arginine and lysine residues whereas the nucleosome surface is negatively charged due to the phosphate backbone (13). Nucleosomes create an excellent surface for binding of chromatin-associated proteins (13).

Nucleosome occupancy and positioning control transcription

Distributions of nucleosomes play an important role in transcription initiation and its regulation. Nucleosome positioning depends on DNA sequence, histone-DNA interaction, and nucleosome interacting proteins (15). An array of nucleosomes functions as a barrier for transcription, preventing nonspecific interaction between RNA polymerase II and DNA (16). Nucleosome formation is, in general, unfavorable at transcriptional start sites (TSS), enhancer and terminator regions where the homopolymeric DNA sequences such as poly(dA:dT) and poly(dG:dC) are present. This restricts transcriptional initiation to these sites (15). For example, the role of nucleosome occupancy in transcriptional regulation has been extensively studied in yeasts. Genome-wide mapping of nucleosomes in *Saccharomyces cerevisiae* has shown that nucleosome formation at upstream of open reading frames (ORFs) is depleted and the DNA sequence at the TSS is characterized by poly(dA:dT) tracts (17, 18). Transcription levels are correlated with the length of the poly(dA:dT) tracts, and introduction of poly(dA:dT) tracts are sufficient to disrupt repression of a gene by bypassing the requirement for a trans-acting transcriptional activator (19). Importantly, nucleosomes in promoter regions can be removed upon transcriptional activation as observed at the *pho5* locus (20, 21). These evidence suggests that eukaryotes control transcription by regulating nucleosome occupancy at TSS of promoter region, controlling the binding site of RNA polymerase.

Eukaryotic genomes are partitioned into functionally distinctive domains

In eukaryotes, the transcriptional activity of genes is tightly regulated through histone modifications. N-terminal tails of histones are heavily modified by a number of enzymes (22). Combination of the modifications can be viewed as a code that carries another layer of the

genetic information (6). Writers and erasers embed and edit a code whereas readers translate it into biological outputs. The code for active and repressive transcription is tightly regulated and restricted to particular regions of chromosomes (23).

Euchromatin is a highly decondensed form of chromatin that contains most of the transcriptionally active genes. Euchromatic domains are typically marked with di or tri-methylation at K4 of H3 (H3K4me2/3) that is well correlated with RNA polymerase II activity and hyperacetylation (24). In contrast, heterochromatin is a densely packaged form of chromatin. Heterochromatin was first defined based on its cytological properties (25), as these condensed parts of chromosomes are easily stained with certain basic dyes and can be visualized by electron microscopy (26). The molecular definition of heterochromatin is transcriptionally silent domains of genome where histones are hypoacetylated and chromatin is densely packaged (24). A number of studies suggest that heterochromatin domains are required for genome integrity and normal cell development.

Constitutive heterochromatin domains occur at pericentromeric and sub-telomeric regions where few genes are present (27). Its formation appears to be tightly restricted at the same genomic regions in all cell types(27). These domains are typically associated with tandem DNA repeats, although the DNA sequences are poorly conserved among eukaryotes. Hypoacetylation of histones and H3K9me2/3 are typically enriched in constitutive heterochromatin, leading to transcriptionally inactive regions of the genome (27).

Components required for pericentromeric transcriptional silencing have been identified through extensive genetic screens in many model organisms. In *Drosophila*, the position effect variegation (PEV) screen has been performed using a white mottled 4b (w^{4mb}) mutant to identify suppressor (Su(var)) and enhancer (E(var)) of variegation (28). The PEV screen utilizes the eye

color as a proxy for the chromatin state: red color for suppression of silenced w^{4mb} translocated next to heterochromatin, and white color for enhancing the silencing phenotype (28). Through the PEV screen, 60 Su(var) and 25 E(var) genes have been identified. Some of Su(var) genes are particularly important for formation of constitutive heterochromatin domains, including the H3K9 methyltransferase (Mtase) Su(var)3-9, heterochromatin protein 1 Su(var)2-5, histone deacetylases, RNA processing factors such as AGO2, and other chromatin associated proteins summarized in a review article (29). In contrast to Su(var), E(var) genes seem to be required for restricting the spread of heterochromatin and for defining the boundary between euchromatin and heterochromatin (28). Also, mouse homologs of the *Drosophila* heterochromatin components localize to constitutive heterochromatin domains based on fluorescent microscopy (29). The GFP-tagged homologs co-localize with the densely stained nuclear domains with DAPI that correspond to the constitutive heterochromatin containing more than 10,000 copies of A:T-rich satellite repeats (29). In *Schizosaccharomyces pombe*, exhaustive genetic screens using an ade6+ reporter fused to a centromeric repeat have been performed to find components required for silencing (30). RNAi components, H3K9 Mtase complex CLRC, yeast HP1-like protein Swi6 have been identified as core components of heterochromatin. In addition, splicing associated proteins Smd3, Saf1 and Saf5 and COP9 signalosome subunits Csn1 and Csn2 are found to be required for silencing (30). In *Neurospora*, screening of mutants defective in DNA methylation resulted in identification of constitutive heterochromatin components demonstrating that many heterochromatin regulators are conserved in animals and fungi (23). Constitutive heterochromatin forms at regions containing A:T-rich repetitive DNA sequences that have been mutated by repeat-induced point mutation (RIP). RIP is a unique genome defense system in *Neurospora* that introduces cytosine to thymine mutations in duplicated DNA sequences during

the sexual cycle. Heterochromatin structure in *Neurospora* is defined at the molecular level by hypoacetylated histones, H3K9me3, heterochromatin protein 1 (HP1) localization, and DNA methylation, similar to the heterochromatin signatures in plants and animals (31-34). In animals, plants, and fungi, repetitive DNA appears to be a common requirement for constitutive heterochromatin formation, although the exact signal directing assembly of the heterochromatin components is unclear.

Centromeres are essential features of eukaryotic chromosomes, as they play a pivotal role in chromosomal segregation facilitating chromosomal movement in mitosis and meiosis (35). Centromere sequences and their structural organization are rapidly evolving among eukaryotes, and they differ even between chromosomes in the same organism (35). For example, human centromeres ranges from 0.3 to 0.5 Mbp containing many 171 bp A:T-rich α-satellite repeats whereas *S. cerevisiae* has a small 125 bp centromere (35). *S. pombe* has three chromosomes and the centromeres of each chromosome differ structurally ranging 40 to 110 kbp in length (36). A major function of centromere is to provide a platform for assembly of a multiprotein complex kinetochore that consists of 80 proteins in human and at least 35 in yeasts (37, 38). The kinetochore is required for interaction of the centromere and microtubule spindle apparatus. The location of the centromere is determined by the presence of the histone H3 variant CenH3. Indeed, disruption of the centromere function by depleting CenH3 causes defects in assembly of centromere components and chromosomal segregation in many organisms including fungi, *Drosophila*, plants, and animals (39-42).

The *Neurospora* centromere is characterized by A:T- rich repetitive sequences and centromere proteins such as CenH3, CEN-C, CEN-T, and probably other counterparts found in other fungi and animals (43). It does not contain 170-nucleotide satellite repeats identified in

animals and plants. Instead, it contains many segments similar to LINE, copia, mariner, and gypsy transposable element families, all of which have been inactivated by RIP (43, 44). H3K9me3 and DNA methylation are enriched in centromere domain whereas euchromatic marker H3K4me2/3, which is typically observed at centromere core in other eukaryotes, is absent (43). Centromeric transcripts have been observed in many eukaryotes, but their functional roles remain unclear. Heterochromatin components, DIM-5 and HP1, are required for normal CenH3 positioning (43). Centromere organization and its components need further investigation to understand the centromere function in chromosomal segregation.

Facultative heterochromatin refers to domains of chromosomes where genes are transcriptionally silent but contain a subset of genes which are derepressed in response to environmental stimuli or particular developmental phases and are therefore responsible for controlling the complex developmental processes in eukaryotes. Although a number of genes involved in formation of facultative heterochromatin have been identified in many model organisms, the mechanisms for targeting components to specific genomic loci remain elusive. A core component of facultative heterochromatin is the polycomb repressive complex (PRC2) first identified in *Drosophila* (45). PRC2 components are conserved in some fungi, plants, and animals. PRC2 deposits a repressive mark H3K27me2/3, silencing a targeted locus presumably through interplay between compacting chromatin and other chromatin components. In addition to PRC2, animals have PRC1 complex responsible for monoubiquitylation of lysine 119 of H2A (H2AK119ub) and silencing (5). PRC1 is recruited to facultative heterochromatin domain through its subunit Pc/CBX that recognizes H3K27me3, and deposits H2AK119ub . However, it can also deposit H2AK119ub at the targeted loci independent of H3K27me3. Moreover, PRC1 silences a subset of targeted genes independent of its catalytic activity. Determinants of PRC1

and PRC2 recruitment are currently not well defined. Importantly, defective facultative heterochromatin leads to abnormal development in animals. *Drosophila* PRC2, composed of E(Z), Su(Z)12, ESC/ESCL, and P55, regulates expression of homeotic genes at a particular developmental stage. A mutation in PRC2 activity leads to disruption of transcriptional state in the developmental genes and results in abnormal segmentation. In mice, deletion of PRC2 components is lethal at the early embryonic stage (5). Deletion and overexpression of PRC2 have been observed in cancer cells and therefore have a link to carcinogenesis (46).

In fungi, facultative chromatin is associated with secondary metabolite production, and also has a link to pathogenesis. In *Fusarium graminearum*, H3K27 methylation silences genes required for the secondary metabolite synthesis and putative virulence factors (47). Absence of H3K27me3 causes growth defect and abnormal pigmentation (47). In *Cryptococcus neoformans*, an opportunistic fungus that causes cryptococcosis in immunocompromised patients, facultative heterochromatin occurs primarily at telomeric regions (48). Loss of catalytic subunit EZH2 does not affect growth and its effect on virulence remains unknown. Msl1 and Ccc1, subunits of *Cryptococcus* PRC2, are required for normal growth (48). In *Neurospora*, facultative heterochromatin occurs in sub-telomeric regions and in loci close to constitutive heterochromatin domains, covering 6.8% of genome (49). Core components of PRC2 are conserved and they consist of SET-7, EED, SU(Z)12, and NPF. SET-7 is the catalytic subunit of PRC2 required for H3K27me3. EED and SU(Z)12 are required for H3K27 methylation, whereas NPF is required at sub-telomeric regions and a subset of the facultative heterochromatin domains (49). A number of uncharacterized genes are marked by K27me3 and some of them are derepressed upon deletion of *set-7* (49). Most genes marked by K27me3 are conserved in other fungal species, but some are specific to *Neurospora*. Intriguingly, *Δset-7*, *Δeed*, *Δsuz12* mutants do not show growth defects,

whereas *Δnpf* mutant showed a slower growth rate (49). It appears that NPF has a function unrelated to facultative heterochromatin formation. Intriguingly, *Δset-7* forms false perithecia indicating that facultative heterochromatin regulates genes required during sexual cycle. Functions of genes marked by K27me3 need further characterization in *Neurospora*.

Telomeres are the ends of linear chromosomes that play a major role in genome maintenance and cell development. In animals and fungi with the exception of yeasts, telomeres are made up of well conserved hexamer repeats "TTAGGG", whereas typical plant telomeres contain an array of "TTTAGGG" (50). The telomere repeats are synthesized by telomerase reverse transcriptase using an RNA template. Telomeric components prevent chromosomal ends from being recognized as a substrate for DNA repair and homologous recombination. At least 40 proteins have been identified as telomere-associated proteins including heterochromatin components and DNA repair machineries. Purification of telomere-associated proteins yielded an additional 170 candidates (51). In the catalog of telomere components, shelterin complex plays a major role in telomere integrity. It consists of TRF1, TRF2, RAP1, TIN2, TPP1, and POT1, and binds to telomere DNA repeats preventing activation of the ATM- and ATR-dependent DNA damage response (50). In the absence of TRF2 or POT1, telomere regions triggers DNA damage response pathway through MRN complex and ATM (50). This leads to non-homologous end joining of chromosomal ends that cause duplication or deletion of chromosomal domains in mitosis (50). Heterochromatin mark H3K9me2/3 has been found at telomere regions in eukaryotes, therefore heterochromatic modification is thought to play a role in maintenance of telomere regions.

Eukaryotes regulate chromatin-based processes through histone modification and DNA methylation

Histones are well conserved DNA binding proteins in Eukaryotes, functioning as a core particle of a nucleosome. They are subjected to the extensive post-translational modifications such as acetylation, methylation and phosphorylation (22). These modifications frequently occur at histone N-terminal tails of histone H3 and H4 that extend beyond the surface of the nucleosome. They affect interaction partners at the histone-N-terminal tails and chromatin compaction. Interplay between H3K4 methylation and histone acetylation lead to the open chromatin structure allowing access of RNA polymerase II for transcription. In contrast to the euchromatin domains, H3K9, H3K27 methylation and hypoacetylation leads to a tightly packaged chromatin through interactions of a number of heterochromatin components, which results in transcriptionally inert regions. Thus, histone modification defines the landscape of functionally distinctive domains, regulating transcriptional activity of loci.

Histone Lysine methyltransferases (KMTs) catalyze the transfer of methyl-groups from s-adenosyl-methionine (SAM) to the primary amine of a lysine side chain of histones. KMTs harbor a SET (SU(var) Enhancer of Trithorax) domain that is responsible for mono, di, and tri-methylation of a lysine residue. SET domains are well conserved in most of eukaryotic KMTs (52). Crystal structures of KMTs have shown that a SET domain binds SAM and a peptide substrate, forming a channel required for the catalytic reaction of methyl-transfer. Remarkable similarities in structure of the catalytic pocket between various KMTs have been observed, revealing conserved residues at the catalytic site (53). For example, a well-conserved tyrosine residue at the channel is required for the catalytic reaction.

KMTs play an important role in chromatin architecture. Most eukaryotes have conserved lysine residues of histone H3: K4, K9, K27, K36, K79 (24). Each lysine has specialized enzymes for methylation and their enzymatic activities are well regulated, targeting a specific part of loci (54). For example, H3K4me2/3, K9me2/3, and K27me2/3 are mutually exclusive in most of chromosomal domains. Each methylated lysine facilitates the recruitment of a specific set of chromatin binding proteins. Readers of the marks, which typically contain chromodomain, plant homeodomain (PHD), tudor domain, and malignant brain tumor (MBT), localize to a particular locus through the methylated lysine and bring other interaction partners to the sites. For instance, HP1 is a highly conserved chromodomain containing protein required for heterochromatin formation and silencing but its isoform HP1a is also suggested to play a role in transcriptional activation (55). Purification of HP1 interaction partners in animals has shown that HP1 interacts with many proteins (56). Thus readers of methyl-lysine have a huge impact on the landscape of proteins associated with chromatin. Interplay of these factors affects other histone modifications, DNA methylation, and compaction of chromatin, leading to formation of specialized domains such as euchromaitn and heterochromatin. Tight regulation of KMTs is required for the proper control of transcriptional activation and silencing, and proper chromosomal replication and segregation. Although interaction partners of KMTs have been extensively identified by proteomic approaches in many eukaryotes, additional work is needed to understand how many KMTs are recruited to specific chromosomal loci.

Acetylation also contributes to chromatin structure and its transcriptional state. Histone acetylation occurs at almost all of lysine residues of histones and its general function is to open up the chromatin structure for transcriptional initiation. The first identified histone acetyltransferase was p55 from *Tetrahymena thermophile (57).* Yeast homolog of p55 is Gcn5, a

subunit of SAGA complex that promotes transcription at promoter regions through its acetylation activity all over the genome (58). In yeast, Gcn5 localizes to targeted loci through interaction with Tra1 and other transcriptional activators and through its bromodomain that is required for binding to acetylated lysine of histones (59). The Bromodomain is approximately 110 amino acids in length and forms an interaction surface specific for acetylated lysine. Crystral structures of 29 bromodomain proteins from human revealed the structurally conserved organization of a hydrophobic pocket that can accommodate binding of acetylated lysine residue of histone peptides (60). Gcn5 interacts with Ada2 and Ada3, acetylating multiple lysine residues of H3 and H2B, as it can acetylate K9, K14, K18 and K23 of H3 and lysines of H2B in vitro. This leads to relaxation of chromatin structure and recruitment of transcriptional factors and the preinitiation complex for transcription. Interestingly, Gcn5 has a genetic interaction with U2 snRNP proteins Msl1 and Lea1, and histone acetylation by Gcn5 is proposed to play a role in loading of the splicing components to the pre-mRNA during transcription. In *Drosophila*, Gcn5 and its interaction partners Ada2b and Ada3 are essential for viability. In mice, deletion of Gcn5 is lethal during embryogenesis (59). Thus acetylation of histones is required for proper transcriptional regulation and particularly important in normal development in animals.

DNA methylation plays a role in gene silencing, genome defense, imprinting and X-chromosome inactivation in eukaryotes (3). DNA methylation occurs at the 5-carbon position of cytosine at CG, CHG, CHH context where H is adenine, cytosine or thymine. In animals, DNA methylation has been observed across the genome with the exception of some transcription factor-binding sites and promoter regions. The majority of methylated cytosine is identified within the CG context which accounts for 70 - 80% of all CG nucleotides in a somatic cell (61). DNA methylation at the CHG and CHH context has been found exclusively in embryonic stem

cells and brain cells so far. In plants, most of methylated cytosines are identified in transposons and repetitive DNA sequence. DNA methylation occurs at 24% of CG, 6.7% of CHG, and 1.7% of CHH (62). In *Neurospora*, DNA methylation occurs at relics of transposons where AT-rich repetitive sequences are present, whereas other fungi, such as *S. pombe* and *Aspergilus nidulans*, lack DNA methylation (44). In *Neurospora*, approximately 2% of cytosines in the genome is methylated and removal of DNA methylation does not cause defects in growth and development (33).

How DNA methyltrasnferases are targeted to specific loci remains elusive in higher eukaryotes. In mammalian cells, DNMT3A and DNMT3B are DNA methyltransferases required for de novo DNA methylation at an early stage of embryonic development (63). Methylation of the cytosines is mitotically inherited into somatic cells through maintenance methylation by DNMT1, although other maintenance mechanisms appear to exist (64, 65). In *Neurospora*, DNA methylation is directed by K9me3 and established exclusively by a de novo DNA methyltransferase called DIM-2 (33).

RNA plays a pivotal role in chromatin structure and function

Small interfering RNA (siRNA) directs formation of repressive chromatin in *S. pombe* and plants. In *S. pombe*, RNA pol II transcribes repetitive sequences adjacent to centromere, producing a single-stranded centromeric RNA. RNA-dependent RNA polymerase complex (RDRC) associates with the centromeric RNA, synthesizing the complementary RNA strand. Dcr1 shortens the double stranded RNA to siRNA of 21 to 24 nt in length (66). The siRNA associates with Ago1 that forms RNA-induced initiation of transcriptional gene silencing (RITS) complex with Chp1 and Tas3 (67). RITS localizes at the centromeric domains, presumably

interacting with the non-coding centromeric RNA because interaction between RITS and single stranded RNA is required to induce heterochromatin formation. The histone H3K9 methylase complex (CLRC) associates with the RITS complex, depositing H3K9me2 at centromere domains (68). Chp1 in RITS and heterochromatin protein 1 homolog Swi6 can interact with H3K9me2 through their chromodomains. Interplay between RITS and CLRC leads to silencing of centromeres.

In plants, siRNA plays a role in genome maintenance and normal development, by directing DNA methylation (reviewed in (62). RNA polymerase IV (Pol IV) and RNA polymerase V have a primary role in production of siRNA. RNA-dependent RNA polymerase 2 (RDR2) is thought to process the single stranded RNA (ssRNA) produced by Pol IV into dsRNA. Dicer-like 3 (DCL3) trims the dsRNA into 24-nt siRNAs, the 3' ends of which are subjected to methylation by a RNA methyltransferase HEN3. Argonaute (AGO4) interacts with the siRNAs in the cytoplasm. AGO4-siRNA complex is recruited to the nascent Pol V transcripts through interaction with KTF1 and the complementary RNA sequences to the siRNAs. RNA directed DNA methylation 1 (RDM1) mediates interaction between DNA methyltransferase (DRM2) and AGO4. In turn, DRM2 methylates cytosines at CG, CHG, and CHH context, leading to the silencing of transposons and repetitive DNA. As this process inactivates the activity of transposon, siRNA-directed DNA methylation is a genome defense mechanism to maintain genome integrity. H3K9 methylation is deposited by SUVH4, SUVH5, and SUVH6, accompanying deacetylation of histones by HDA6, histone demethylases (JMJ14, LDL1, and LDL2), and deubiquitination of H2B by UBP26.

Long non-coding RNAs (LncRNAs) have been proposed to play a role in transcriptional regulation. LncRNAs are typically composed of more than 200 nucleotides that are not translated

into peptides. Many lncRNAs have been identified by RNA-seq and their expression level are usually low (69). These lncRNAs are transcribed from intergenic and intragenic regions and interact with many chromatin-associated proteins and genomic loci. lncRNA is thought to interact with both DNA and chromatin components to regulate transcriptional activation and repression. For example, it functions as an adaptor to facilitate interaction between histone modifying enzymes and DNA. HOTAIR is a 2.2 kb lncRNA transcribed from the intergenic region between HOXC11 and HOXC12 in human (70). Genome wide mapping of HOTAIR binding sites revealed that HOTAIR localizes to regions near loci marked byH3K27me3 in human cells. HOTAIR also interacts with PRC2 through its 5' domain and with a histone demethylase LSD1 through the 3' domain. Based on these data, it is proposed that HOTAIR recruits PRC2 and LSD1 to the targeted sites, coupling H3K27 methylation and H3K4 demethylation. Remarkably, increase in HOTAIR expression leads to the change in H3K27me3 localization whereas HOTAIR depletion inhibited cancer growth. Also, lncRNA Xist plays a role in X-chromosome inactivation through facilitating recruitment of PRC2 onto DNA (71). These indicate that lncRNA is required for a regulation of facultative heterochromatin formation. Another mechanism by which lncRNA controls transcription involves in inhibition of transcriptional activators. A lncRNA called growth arrest-specific 5 (Gas5) binds to the DNA binding domain of the glucocorticoid receptor, preventing transcriptional activation facilitated by glucocorticoid (72). This inhibition down-regulates glucocorticoid receptor targeted genes. Also, Lethe, a lncRNA highly up-regulated by proinflammatory cytokines or glucocorticoid receptor antagonist, can inhibit transcriptional activation by NF-kB through interaction with its subunit RelA (73).

Genome integrity is preserved by heterochromatin components

Maintenance of genome stability is essential for normal cell growth and development. Chromosomes are exposed to various biotic and abiotic stresses that challenge genome integrity. For example, abiotic stress from the environment, genotoxic chemicals and irradiation directly damages the DNA, whereas cells encounter biotic stresses from chromosomal replication and segregation as well as byproducts of cellular metabolism. These stresses cause DNA lesions and double stranded breaks (DSBs), which lead to genome instability when they are not repaired properly. Components involved in DNA replication, DNA repair, and cell cycle checkpoints coordinate each other to maintain genome integrity, ensuring accurate duplication of chromosomes. In fact, research has shown that defects in DNA replication or repair can lead to genome instabilities in the form of base substitutions, aberrant copy number of genes, loss of partial chromosome and gross chromosomal rearrangements (GCRs) (reviewed in (74-76). These genome instabilities are associated with human disease such as cancer and other genetic disorders. However, the molecular events that lead to the genome instability are largely unknown. Moreover, the cellular mechanisms that maintain normal genome stability are not completely understood.

Heterochromatin components are required for maintaining genome integrity. In humans, for example, a breast cancer susceptibility gene (BRCA1) interacts with HP1 and DNMT3B in an ATM-dependent manner (77). This interaction is required for normal heterochromatin structure and silencing (77). BRCA1 is strongly linked to breast and ovarian cancer (78). In mouse, a mutant of Suv39h has developmental defects in embryogenesis (79). Also, the mutation caused aberrant chromosomal segregation and abnormal spermatogenesis (79). In *Drosophila*, lack of the Su(var)3-9 required for H3K9me3 leads to dispersed nucleoli, formation of

extrachromosomal circular DNA (eccDNA) through homologous recombination (80, 81). Loss of H3K9 methylation also causes increase in copy number of repeats such as ribosomal DNA (rDNA) and satellite DNA (80, 81). In contrast to this observation, reduced copy number of rDNA in the Y-chromosome was observed in a Su(var)3-9 mutant (82). These observations illustrate that repeats are favorable substrates for illegitimate recombination when the heterochromatin is not properly maintained. It also indicates that heterochromatin might stabilize the repeats, preventing aberrant homologous recombination events. In *Neurospora*, DIM-5, a homolog of Su(var)3-9, is also required for heterochromatin formation and genome stability. Specifically, it has been shown that the DIM-5 deletion mutant was hypersensitivie to methyl methanesulfonate (MMS) and multiple copies of a transgene are not stably maintained in the absence of DIM-5. The copy number of *al-1* sequences integrated into *Δdim-5* by transformation decreased over generations whereas the wild-type strain did not lose any transgenic *al-1* repeats (83). Thus, defects in heterochromatin formation can result in genome instability, but the heterochromatin-based mechanisms that maintain genome integrity are not well understood.

Neurospora is a model organism suited for chromatin research

There are number of models used for chromatin research such as cancer cells, mice, *Drosophila*, *Caenorhabditis elegans*, maize, *Arabidopsis*, *T. thermophila* , *Neurospora*, *S.pombe*, *S. cerevisiae*, *C. neoformants*. *N. crassa* has been used as a tractable model organism for a long time, and is suited for chromatin study as described below. *N. crassa* should prove useful in modeling the mechanisms and maintenance of genome stability, which should shed light onto these functions in higher eukaryotes.

The underlying reason for the use of *Neurospora* as a model is because it allows one to do experiments that are difficult or impossible in other eukaryotes. First, known heterochromatin associated proteins that are essential for viability in higher eukaryotes are dispensable in *Neurospora*, which allows characterization of gene deletion mutants that are lethal in other common model organism such as mice or *Drosophila*. In addition, *Neurospora* genes have little redundancy in heterochromatin components, whereas animals and plants usually have multiple functional homologs. For example, human has 3 methyltransferases that target H3K9, whereas *Neurospora* has only one enzyme for this function. The lack of redundancy in *Neurospora* is due to repeat Induced Point mutation (RIP). RIP is a genome defense system that converts cytosine to thymine in both copies of DNA sequences if there are two copies of genes on a same chromosome. All sequences with more than 80% homology are subject to RIP except ribosomal DNA. RIP mutates all copies of transposons and homologus genes, resulting in a *Neurospora* genome devoid of the multi-copy gene families. Effects of a gene knockout are directly reflected to phenotype in haploid asexual cycle of *Neurospora*.

The molecular mechanisms of heterochromatin formation are well understood, and have previously been extensively studied in *Neurospora* species. In fact, *Neurospora* chromatin research provided first evidence that H3K9 methylation occurs upstream of DNA methylation. It has been conclusively demonstrated that heterochromatin forms at AT-rich repeat DNA sequences (44), that the protein DIM-5, a histone lysine methylatransferase (HKT), methylates lysine 9 of histone 3 (H3K9) (32), and that the protein HP1 recognizes the tri-methylated lysine 9 (H3K9me3) (31). HP1 then proceeds to recruit DIM-2, a DNA methyltransferase, which proceeds to methylate cytosines within heterochromatin domains (33). HP1 also recruits HDA-1, CDP-2, CHAP and the DMM complex to the sites. HP1, HDA-1, CDP-2, and CHAP (HCHC) is

required for silencing of constitutive heterochromatin, whereas the DMM complex is required which serves to prevent heterochromatin from spreading into adjacent euchromatin domains, presumably by actively demethylating H3K9me3 (84, 85). In addition, *Neurospora* is particularly useful for genomic studies of heterochromatin domains. Mapping of histone modifications and protein localization at the large array of repeats using Illumina sequencing is challenging in plants and animals as reads often map to multiple genomic locations (43). In *Neurospora*, all the repeats are relics of retrotransposons and almost all of reads can be mapped unambiguously to a single locus, even within repeat-rich domains such as centromeres and telomeres. H3K9 methylation, HP1 localization and DNA methylation, have been successfully mapped on a genome-wide scale. Thus, we know the locations of heterochromatic loci in the genome, the molecular composition of heterochromatin domains and the order of events that direct heterochroamtin assembly in *Neurospora* (Fig1.1).

It should be noted that *Neurospora* is a unique model organism in comparison to more commonly utilized yeast species such as *S. pombe*. Previous analysis and comparison of *N. crassa* genomic sequences have shown that it shares more than 500 genes with higher eukaryotes that are absent in the yeasts. In addition *N. crassa* has over 1400 genes that are more similar to their plant or animal orthologs than those of their yeast counterparts. In fact, *Neursopora* possesses a complex biology that is not present in yeasts: DNA methylation, light responsive transcriptional network and circadian clock. More importantly, key components involved in heterochromatin formation (H3K9 MTase and HP1) closely resemble those found in higher eukaryotes. The relative abundance of heterochromatin in *N. crassa* (>15%) is also more similar to higher eukaryotes (>30% for *Drosophila* and Human) than is found in the yeasts (<2%).Thus,

Neurospora should serve as a uniquely useful model in which to investigate the genome maintenance mechanisms of eukaryotic organisms.

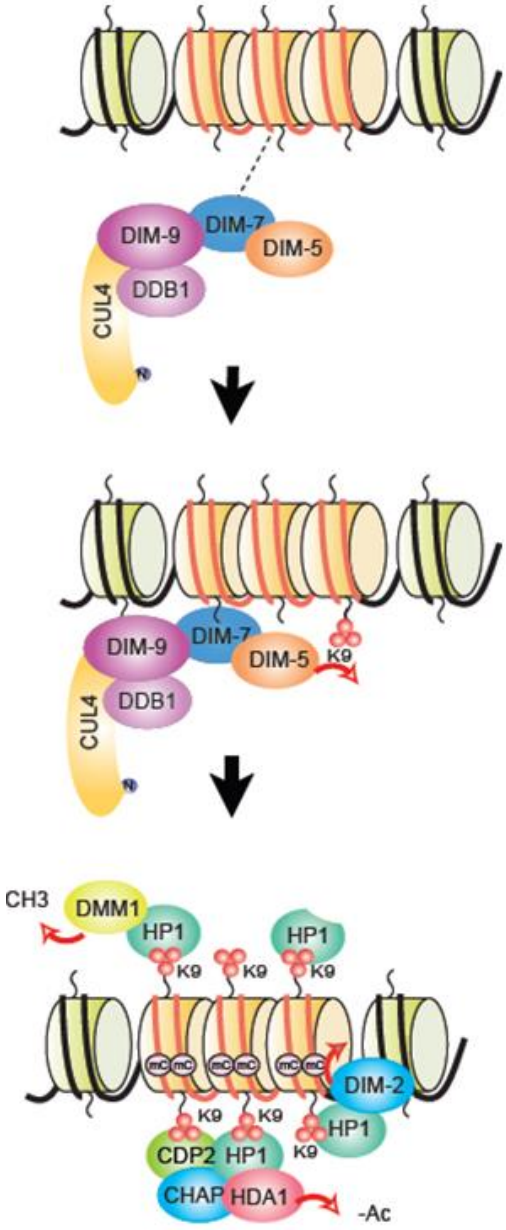

Fig 1.1 Constitutive heterochoromatin formation pathway in *Neurospora crassa* adapted from (86). DCDC associates with the AT-rich domains and DIM-5 tri-methylates H3K9. HP1, in turn, recognizes H3K9me3 and recruits HCHC, DMM1 and DIM-2 to the sites. DIM-2 methylates cytocines, leading to silencing of constitutive heterochromatin domains.

Rationale and objectives of this study

Previous work in *Neurospora* revealed that the methyltransferase complex DCDC, which is essential for H3K9 methylation and DNA methylation, is required for genome integrity. Deletion of individual DCDC components causes hypersensitivity MMS, whereas *Δhpo* and *Δdim-2*, both of which are defective in DNA methylation, show normal sensitivity. This suggests that DCDC is required for normal DNA replication or DNA repair. My dissertation project is focused on elucidation of underlying mechanism of defects in H3K9 methyltransferase mutant *Δdim-5* to enhance our knowledge of the DCDC function in genome maintenance. Outcome from my work will lead to a deeper understanding of molecular mechanisms of how heterochromatin functions.

The goal of chapter 2 is to investigate endogenous DNA damage in *Δdim-5*. We hypothesized that *Δdim-5* has a defects in DNA replication or fragile sites where DSBs frequently occur. We found that γH2A, a marker of replication fork stall and DSBs, is all over the genome in *Δdim-5*. This indicates that chromosomes in *Δdim-5* encounter the spontaneous DNA damage, activating DNA damage response pathway in normal growth condition. I was able to demonstrate that heterochromatin is required for normal genome integrity.

The goal of chapter 3 is to elucidate the underlying cause of defective genome maintenance in *Δdim-5*. I found that K27 methylation redistribute from facultative heterochromatin to constitutive heterochromatin in *Δdim-5*. MMS-hypersensitivity of *Δdim-5* was suppressed by deletion of gene required the K27 methylation *set-7*. The double mutant also partially suppressed the growth defect. The suppression suggests that K27 methylation at constitutive heterochromatin domains such as centromere has a toxic effect. It also indicates that PRC2 recruitment is completely misregulated in the absence of H3K9 methylation. I was able to

show that loss of H3K9 methylation causes a catastrophic effect on global chromatin architecture, leading to genome instability and growth defects. Components of constitutive heterochromatin are required for normal facultative heterochromatin formation.

The goal of chapter 4 is to identify the components causing toxicity in *Δdim-5*. I hypothesized that H3K27 redistribution in *Δdim-5* leads to recruitment of H3K27me3 binding proteins to constitutive heterochromatin leading to malfunction of the domains.
My results led to a model that core components of constitutive heterochromatin are required for normal chromatin architecture, restricting K27Kme3 at the normal facultative heterochromatin domains. Loss of the heterochromatin components such as DIM-5 and H3K9me3 leads to the redistribution of H3K27me3 to constitutive heterochromatin domains. I speculate that many components are mislocalized to centromere and normal centromere components are no longer function optimally or lose association with centromere.

Summary

In this dissertation, I used molecular and genomic approach to study genome maintenance. My findings expand our knowledge of how heterochromatin maintains genome integrity. My research provides a simple model of maintenance of chromatin architecture and importance of heterochromatin. This work might provide insights in the mechanism of genome instability in cancer.

References

1. **Dolinoy DC.** 2008. The agouti mouse model: an epigenetic biosensor for nutritional and environmental alterations on the fetal epigenome. Nutrition reviews **66 Suppl 1:**S7-11.

2. **Duhl DM, Vrieling H, Miller KA, Wolff GL, Barsh GS.** 1994. Neomorphic agouti mutations in obese yellow mice. Nature genetics **8:**59-65.

3. **Bird A.** 2002. DNA methylation patterns and epigenetic memory. Genes & development **16:**6-21.

4. **Gaydos LJ, Wang W, Strome S.** 2014. Gene repression. H3K27me and PRC2 transmit a memory of repression across generations and during development. Science **345:**1515-1518.

5. **Margueron R, Reinberg D.** 2011. The Polycomb complex PRC2 and its mark in life. Nature **469:**343-349.

6. **Strahl BD, Allis CD.** 2000. The language of covalent histone modifications. Nature **403:**41-45.

7. **Steffen PA, Ringrose L.** 2014. What are memories made of? How Polycomb and Trithorax proteins mediate epigenetic memory. Nature reviews. Molecular cell biology **15:**340-356.

8. **Shechter D, Dormann HL, Allis CD, Hake SB.** 2007. Extraction, purification and analysis of histones. Nature protocols **2:**1445-1457.

9. **Allfrey VG, Faulkner R, Mirsky AE.** 1964. Acetylation and Methylation of Histones and Their Possible Role in the Regulation of Rna Synthesis. Proceedings of the National Academy of Sciences of the United States of America **51:**786-794.

10. **Singh Sandhu K, Li G, Sung WK, Ruan Y.** 2011. Chromatin interaction networks and higher order architectures of eukaryotic genomes. Journal of cellular biochemistry **112:**2218-2221.

11. **Grigoryev SA.** 2012. Nucleosome spacing and chromatin higher-order folding. Nucleus **3:**493-499.

12. **Geer LY, Marchler-Bauer A, Geer RC, Han L, He J, He S, Liu C, Shi W, Bryant SH.** 2010. The NCBI BioSystems database. Nucleic acids research **38:**D492-496.

13. **McGinty RK, Tan S.** 2014. Nucleosome Structure and Function. Chemical reviews.

14. **Luger K, Mader AW, Richmond RK, Sargent DF, Richmond TJ.** 1997. Crystal structure of the nucleosome core particle at 2.8 A resolution. Nature **389:**251-260.

15. **Struhl K, Segal E.** 2013. Determinants of nucleosome positioning. Nature structural & molecular biology **20:**267-273.

16. **Radman-Livaja M, Rando OJ.** 2010. Nucleosome positioning: how is it established, and why does it matter? Developmental biology **339:**258-266.

17. **Yuan GC, Liu YJ, Dion MF, Slack MD, Wu LF, Altschuler SJ, Rando OJ.** 2005. Genome-scale identification of nucleosome positions in S. cerevisiae. Science **309:**626-630.

18. **Mavrich TN, Ioshikhes IP, Venters BJ, Jiang C, Tomsho LP, Qi J, Schuster SC, Albert I, Pugh BF.** 2008. A barrier nucleosome model for statistical positioning of nucleosomes throughout the yeast genome. Genome research **18:**1073-1083.

19. **Raveh-Sadka T, Levo M, Shabi U, Shany B, Keren L, Lotan-Pompan M, Zeevi D, Sharon E, Weinberger A, Segal E.** 2012. Manipulating nucleosome disfavoring sequences allows fine-tune regulation of gene expression in yeast. Nature genetics **44:**743-750.

20. **Boeger H, Griesenbeck J, Strattan JS, Kornberg RD.** 2004. Removal of promoter nucleosomes by disassembly rather than sliding in vivo. Molecular cell **14:**667-673.

21. **Korber P, Luckenbach T, Blaschke D, Horz W.** 2004. Evidence for histone eviction in trans upon induction of the yeast PHO5 promoter. Molecular and cellular biology **24:**10965-10974.

22. **Huang H, Sabari BR, Garcia BA, Allis CD, Zhao Y.** 2014. SnapShot: histone modifications. Cell **159:**458-458 e451.

23. **Rountree MR, Selker EU.** 2010. DNA methylation and the formation of heterochromatin in Neurospora crassa. Heredity **105:**38-44.

24. **Kouzarides T.** 2007. Chromatin modifications and their function. Cell **128:**693-705.

25. **Passarge E.** 1979. Emil Heitz and the concept of heterochromatin: longitudinal chromosome differentiation was recognized fifty years ago. American journal of human genetics **31:**106-115.

26. **Frenster JH.** 1971. Electron microscopic localization of acridine orange binding to DNA within human leukemic bone marrow cells. Cancer research **31:**1128-1133.

27. **Grewal SI, Jia S.** 2007. Heterochromatin revisited. Nature reviews. Genetics **8:**35-46.

28. **Schotta G, Ebert A, Dorn R, Reuter G.** 2003. Position-effect variegation and the genetic dissection of chromatin regulation in Drosophila. Seminars in cell & developmental biology **14:**67-75.

29. **Fodor BD, Shukeir N, Reuter G, Jenuwein T.** 2010. Mammalian Su(var) genes in chromatin control. Annual review of cell and developmental biology **26:**471-501.

30. **Bayne EH, Bijos DA, White SA, de Lima Alves F, Rappsilber J, Allshire RC.** 2014. A systematic genetic screen identifies new factors influencing centromeric heterochromatin integrity in fission yeast. Genome biology **15:**481.

31. **Freitag M, Hickey PC, Khlafallah TK, Read ND, Selker EU.** 2004. HP1 is essential for DNA methylation in Neurospora. Molecular cell **13:**427-434.

32. **Tamaru H, Zhang X, McMillen D, Singh PB, Nakayama J, Grewal SI, Allis CD, Cheng X, Selker EU.** 2003. Trimethylated lysine 9 of histone H3 is a mark for DNA methylation in Neurospora crassa. Nature genetics **34:**75-79.

33. **Tamaru H, Selker EU.** 2001. A histone H3 methyltransferase controls DNA methylation in Neurospora crassa. Nature **414:**277-283.

34. **Kouzminova EA, Selker EU.** 2001. *dim-2* encodes a DNA-methyltransferase responsible for all known cytosine methylation in Neurospora. EMBO Journal **20:**4309-4323.

35. **Cleveland DW, Mao Y, Sullivan KF.** 2003. Centromeres and kinetochores: from epigenetics to mitotic checkpoint signaling. Cell **112:**407-421.

36. **Wood V, Gwilliam R, Rajandream MA, Lyne M, Lyne R, Stewart A, Sgouros J, Peat N, Hayles J, Baker S, Basham D, Bowman S, Brooks K, Brown D, Brown S, Chillingworth T, Churcher C, Collins M, Connor R, Cronin A, Davis P, Feltwell T, Fraser A, Gentles S, Goble A, Hamlin N, Harris D, Hidalgo J, Hodgson G, Holroyd S, Hornsby T, Howarth S, Huckle EJ, Hunt S, Jagels K, James K, Jones L, Jones M, Leather S, McDonald S, McLean J, Mooney P, Moule S, Mungall K, Murphy L, Niblett D, Odell C, Oliver K, O'Neil S, Pearson D, Quail MA, Rabbinowitsch E, Rutherford K, Rutter S, Saunders D, Seeger K, Sharp S, Skelton J, Simmonds M, Squares R, Squares S, Stevens K, Taylor K, Taylor RG, Tivey A, Walsh S, Warren T, Whitehead S, Woodward J, Volckaert G, Aert R, Robben J, Grymonprez B, Weltjens I, Vanstreels E, Rieger M, Schafer M, Muller-Auer S, Gabel C, Fuchs M, Dusterhoft A, Fritzc C, Holzer E, Moestl D, Hilbert H, Borzym K, Langer I, Beck A, Lehrach H, Reinhardt R, Pohl TM, Eger P, Zimmermann W, Wedler H, Wambutt R, Purnelle B, Goffeau A, Cadieu E, Dreano S, Gloux S, Lelaure V, Mottier S, Galibert F, Aves SJ, Xiang Z, Hunt C, Moore K, Hurst SM, Lucas M, Rochet M, Gaillardin C, Tallada VA, Garzon A, Thode G, Daga RR, Cruzado L, Jimenez J, Sanchez M, del Rey F, Benito J, Dominguez A, Revuelta JL, Moreno S, Armstrong J, Forsburg SL, Cerutti L, Lowe T, McCombie WR, Paulsen I, Potashkin J,**

Shpakovski GV, Ussery D, Barrell BG, Nurse P. 2002. The genome sequence of Schizosaccharomyces pombe. Nature **415:**871-880.

37. **Westermann S, Cheeseman IM, Anderson S, Yates JR, 3rd, Drubin DG, Barnes G.** 2003. Architecture of the budding yeast kinetochore reveals a conserved molecular core. The Journal of cell biology **163:**215-222.

38. **Cheeseman IM, Desai A.** 2008. Molecular architecture of the kinetochore-microtubule interface. Nature reviews. Molecular cell biology **9:**33-46.

39. **Talbert PB, Masuelli R, Tyagi AP, Comai L, Henikoff S.** 2002. Centromeric localization and adaptive evolution of an Arabidopsis histone H3 variant. The Plant cell **14:**1053-1066.

40. **Howman EV, Fowler KJ, Newson AJ, Redward S, MacDonald AC, Kalitsis P, Choo KH.** 2000. Early disruption of centromeric chromatin organization in centromere protein A (Cenpa) null mice. Proceedings of the National Academy of Sciences of the United States of America **97:**1148-1153.

41. **Blower MD, Karpen GH.** 2001. The role of Drosophila CID in kinetochore formation, cell-cycle progression and heterochromatin interactions. Nature cell biology **3:**730-739.

42. **Stoler S, Keith KC, Curnick KE, Fitzgerald-Hayes M.** 1995. A mutation in CSE4, an essential gene encoding a novel chromatin-associated protein in yeast, causes chromosome nondisjunction and cell cycle arrest at mitosis. Genes & development **9:**573-586.

43. **Smith KM, Phatale PA, Sullivan CM, Pomraning KR, Freitag M.** 2011. Heterochromatin is required for normal distribution of Neurospora crassa CenH3. Molecular and cellular biology **31:**2528-2542.

44. **Lewis ZA, Honda S, Khlafallah TK, Jeffress JK, Freitag M, Mohn F, Schubeler D, Selker EU.** 2009. Relics of repeat-induced point mutation direct heterochromatin formation in Neurospora crassa. Genome research **19:**427-437.

45. **Schwartz YB, Pirrotta V.** 2013. A new world of Polycombs: unexpected partnerships and emerging functions. Nature reviews. Genetics **14:**853-864.

46. **Hock H.** 2012. A complex Polycomb issue: the two faces of EZH2 in cancer. Genes & development **26:**751-755.

47. **Connolly LR, Smith KM, Freitag M.** 2013. The Fusarium graminearum histone H3 K27 methyltransferase KMT6 regulates development and expression of secondary metabolite gene clusters. PLoS genetics **9:**e1003916.

48. **Dumesic PA, Homer CM, Moresco JJ, Pack LR, Shanle EK, Coyle SM, Strahl BD, Fujimori DG, Yates JR, 3rd, Madhani HD.** 2015. Product binding enforces the genomic specificity of a yeast polycomb repressive complex. Cell **160:**204-218.

49. **Jamieson K, Rountree MR, Lewis ZA, Stajich JE, Selker EU.** 2013. Regional control of histone H3 lysine 27 methylation in Neurospora. Proceedings of the National Academy of Sciences of the United States of America **110:**6027-6032.

50. **O'Sullivan RJ, Karlseder J.** 2010. Telomeres: protecting chromosomes against genome instability. Nature reviews. Molecular cell biology **11:**171-181.

51. **Dejardin J, Kingston RE.** 2009. Purification of proteins associated with specific genomic Loci. Cell **136:**175-186.

52. **Dillon SC, Zhang X, Trievel RC, Cheng X.** 2005. The SET-domain protein superfamily: protein lysine methyltransferases. Genome biology **6:**227.

53. **Upadhyay AK, Cheng X.** 2011. Dynamics of histone lysine methylation: structures of methyl writers and erasers. Progress in drug research. Fortschritte der Arzneimittelforschung. Progres des recherches pharmaceutiques **67:**107-124.

54. **Black JC, Van Rechem C, Whetstine JR.** 2012. Histone lysine methylation dynamics: establishment, regulation, and biological impact. Molecular cell **48:**491-507.

55. **Canzio D, Larson A, Narlikar GJ.** 2014. Mechanisms of functional promiscuity by HP1 proteins. Trends in cell biology **24:**377-386.

56. **Rosnoblet C, Vandamme J, Volkel P, Angrand PO.** 2011. Analysis of the human HP1 interactome reveals novel binding partners. Biochemical and biophysical research communications **413:**206-211.

57. **Brownell JE, Allis CD.** 1995. An activity gel assay detects a single, catalytically active histone acetyltransferase subunit in Tetrahymena macronuclei. Proceedings of the National Academy of Sciences of the United States of America **92:**6364-6368.

58. **Grant PA, Duggan L, Cote J, Roberts SM, Brownell JE, Candau R, Ohba R, Owen-Hughes T, Allis CD, Winston F, Berger SL, Workman JL.** 1997. Yeast Gcn5 functions in two multisubunit complexes to acetylate nucleosomal histones: characterization of an Ada complex and the SAGA (Spt/Ada) complex. Genes & development **11:**1640-1650.

59. **Koutelou E, Hirsch CL, Dent SY.** 2010. Multiple faces of the SAGA complex. Current opinion in cell biology **22:**374-382.

60. **Filippakopoulos P, Picaud S, Mangos M, Keates T, Lambert JP, Barsyte-Lovejoy D, Felletar I, Volkmer R, Muller S, Pawson T, Gingras AC, Arrowsmith CH, Knapp S.**

2012. Histone recognition and large-scale structural analysis of the human bromodomain family. Cell **149:**214-231.

61. **Ehrlich M, Gama-Sosa MA, Huang LH, Midgett RM, Kuo KC, McCune RA, Gehrke C.** 1982. Amount and distribution of 5-methylcytosine in human DNA from different types of tissues of cells. Nucleic acids research **10:**2709-2721.

62. **Law JA, Jacobsen SE.** 2010. Establishing, maintaining and modifying DNA methylation patterns in plants and animals. Nature reviews. Genetics **11:**204-220.

63. **Okano M, Bell DW, Haber DA, Li E.** 1999. DNA methyltransferases Dnmt3a and Dnmt3b are essential for de novo methylation and mammalian development. Cell **99:**247-257.

64. **Rhee I, Jair KW, Yen RW, Lengauer C, Herman JG, Kinzler KW, Vogelstein B, Baylin SB, Schuebel KE.** 2000. CpG methylation is maintained in human cancer cells lacking DNMT1. Nature **404:**1003-1007.

65. **Pradhan S, Bacolla A, Wells RD, Roberts RJ.** 1999. Recombinant human DNA (cytosine-5) methyltransferase. I. Expression, purification, and comparison of de novo and maintenance methylation. The Journal of biological chemistry **274:**33002-33010.

66. **Djupedal I, Kos-Braun IC, Mosher RA, Soderholm N, Simmer F, Hardcastle TJ, Fender A, Heidrich N, Kagansky A, Bayne E, Wagner EG, Baulcombe DC, Allshire RC, Ekwall K.** 2009. Analysis of small RNA in fission yeast; centromeric siRNAs are potentially generated through a structured RNA. The EMBO journal **28:**3832-3844.

67. **Verdel A, Jia S, Gerber S, Sugiyama T, Gygi S, Grewal SI, Moazed D.** 2004. RNAi-mediated targeting of heterochromatin by the RITS complex. Science **303:**672-676.

68. **Zhang K, Mosch K, Fischle W, Grewal SI.** 2008. Roles of the Clr4 methyltransferase complex in nucleation, spreading and maintenance of heterochromatin. Nature structural & molecular biology **15:**381-388.

69. **Mercer TR, Gerhardt DJ, Dinger ME, Crawford J, Trapnell C, Jeddeloh JA, Mattick JS, Rinn JL.** 2012. Targeted RNA sequencing reveals the deep complexity of the human transcriptome. Nature biotechnology **30:**99-104.

70. **Tsai MC, Manor O, Wan Y, Mosammaparast N, Wang JK, Lan F, Shi Y, Segal E, Chang HY.** 2010. Long noncoding RNA as modular scaffold of histone modification complexes. Science **329:**689-693.

71. **Lee JT.** 2009. Lessons from X-chromosome inactivation: long ncRNA as guides and tethers to the epigenome. Genes & development **23:**1831-1842.

72. **Kino T, Hurt DE, Ichijo T, Nader N, Chrousos GP.** 2010. Noncoding RNA gas5 is a growth arrest- and starvation-associated repressor of the glucocorticoid receptor. Science signaling **3:**ra8.

73. **Rapicavoli NA, Qu K, Zhang J, Mikhail M, Laberge RM, Chang HY.** 2013. A mammalian pseudogene lncRNA at the interface of inflammation and anti-inflammatory therapeutics. eLife **2:**e00762.

74. **Lambert S, Carr AM.** 2013. Impediments to replication fork movement: stabilisation, reactivation and genome instability. Chromosoma **122:**33-45.

75. **Aguilera A, Gomez-Gonzalez B.** 2008. Genome instability: a mechanistic view of its causes and consequences. Nature reviews. Genetics **9:**204-217.

76. **Cassidy LD, Venkitaraman AR.** 2012. Genome instability mechanisms and the structure of cancer genomes. Current opinion in genetics & development **22:**10-13.

77. **Filipponi D, Muller J, Emelyanov A, Bulavin DV.** 2013. Wip1 controls global heterochromatin silencing via ATM/BRCA1-dependent DNA methylation. Cancer cell **24:**528-541.

78. **Petrucelli N, Daly MB, Feldman GL.** 1993. BRCA1 and BRCA2 Hereditary Breast and Ovarian Cancer. *In* Pagon RA, Adam MP, Ardinger HH, Bird TD, Dolan CR, Fong CT, Smith RJH, Stephens K (ed.), GeneReviews(R), Seattle (WA).

79. **Peters AH, O'Carroll D, Scherthan H, Mechtler K, Sauer S, Schofer C, Weipoltshammer K, Pagani M, Lachner M, Kohlmaier A, Opravil S, Doyle M, Sibilia M, Jenuwein T.** 2001. Loss of the Suv39h histone methyltransferases impairs mammalian heterochromatin and genome stability. Cell **107:**323-337.

80. **Peng JC, Karpen GH.** 2009. Heterochromatic genome stability requires regulators of histone H3 K9 methylation. PLoS genetics **5:**e1000435.

81. **Peng JC, Karpen GH.** 2007. H3K9 methylation and RNA interference regulate nucleolar organization and repeated DNA stability. Nature cell biology **9:**25-35.

82. **Paredes S, Maggert KA.** 2009. Ribosomal DNA contributes to g
lobal chromatin regulation. Proceedings of the National Academy of Sciences of the United States of America **106:**17829-17834.

83. **Chicas A, Forrest EC, Sepich S, Cogoni C, Macino G.** 2005. Small interfering RNAs that trigger posttranscriptional gene silencing are not required for the histone H3 Lys9 methylation necessary for transgenic tandem repeat stabilization in Neurospora crassa. Molecular and cellular biology **25:**3793-3801.

84. **Honda S, Lewis ZA, Huarte M, Cho LY, David LL, Shi Y, Selker EU.** 2010. The DMM complex prevents spreading of DNA methylation from transposons to nearby genes in Neurospora crassa. Genes & development **24:**443-454.

85. **Honda S, Lewis ZA, Shimada K, Fischle W, Sack R, Selker EU.** 2012. Heterochromatin protein 1 forms distinct complexes to direct histone deacetylation and DNA methylation. Nature structural & molecular biology **19:**471-477.

86. **Lewis ZA, Adhvaryu KK, Honda S, Shiver AL, Knip M, Sack R, Selker EU.** 2010. DNA methylation and normal chromosome behavior in Neurospora depend on five components of a histone methyltransferase complex, DCDC. PLoS genetics **6:**e1001196.

CHAPTER 2

HETEROCHROMATIN CONTROLS γH2A LOCALIZATION IN *NEUROSPORA CRASSA*[1]

Sasaki T, Lynch KL, Mueller CV, Friedman S, Freitag M, Lewis ZA. 2014. Heterochromatin controls γH2A localization in *Neurospora crassa*. Eukaryotic cell 13:990-1000. [1]Reprinted here with permission of publisher.

Abstract

In response to genotoxic stress, ATR and ATM kinases phosphorylate H2A in fungi and H2AX in animals on a C-terminal serine. The resulting modified histone, called γH2A, recruits chromatin-binding proteins that stabilize stalled replication forks or promote DNA double-strand-break repair. To identify genomic loci that might be prone to replication fork stalling or DNA breakage in *Neurospora crassa*, we performed chromatin immunoprecipitation (ChIP) of γH2A followed by next-generation sequencing (ChIP-seq). γH2A-containing nucleosomes are enriched in *Neurospora* heterochromatin domains. These domains are comprised of A·T-rich repetitive DNA sequences associated with histone H3 methylated at lysine-9 (H3K9me), the H3K9me-binding protein heterochromatin protein 1 (HP1), and DNA cytosine methylation. H3K9 methylation, catalyzed by DIM-5, is required for normal γH2A localization. In contrast, γH2A is not required for H3K9 methylation or DNA methylation. Normal γH2A localization also depends on HP1 and a histone deacetylase, HDA-1, but is independent of the DNA methyltransferase DIM-2. γH2A is globally induced in*dim-5* mutants under normal growth conditions, suggesting that the DNA damage response is activated in these mutants in the absence of exogenous DNA damage. Together, these data suggest that heterochromatin formation is essential for normal DNA replication or repair.

Introduction

Heterochromatin is comprised of transcriptionally repressed, repetitive DNA sequences that remain condensed throughout the cell cycle (1). The condensed structure of heterochromatin and the repetitive nature of heterochromatic DNA sequences pose challenges to genome integrity during DNA replication and DNA repair. Repeated DNAs are hot spots for various types of genome instabilities because they can adopt non-B-form DNA structures that stall replication forks and because they are common sites of illegitimate recombination (2,–6). Such events can lead to mutations, gross chromosomal rearrangements, or copy number variations often associated with human diseases (7, 8). Despite their deleterious potential, repetitive DNA sequences make up a significant fraction of the genome in many eukaryotes, including many filamentous fungi (9,–12). These sequences likely persist in genomes because they perform essential functions in certain contexts. For example, the centromeres of most eukaryotes are flanked by large, repeat-rich heterochromatin domains (13), and centromeres of the filamentous fungus *Neurospora crassa* are completely heterochromatic (14, 15). Thus, cells limit deleterious effects of repetitive DNA sequences while preserving essential functions of heterochromatin domains.

Heterochromatin in mammals and *N. crassa* is enriched with specific molecular markers, including histone H3 lysine-9 methylation (H3K9me), heterochromatin protein 1 (HP1), and cytosine DNA methylation. In*Neurospora*, heterochromatin formation is initiated at A·T-rich repetitive DNA sequences by the H3K9 methyltransferase DIM-5 (defective in methylation 5), which exists in a multiprotein complex called DCDC (DIM-5/7/9–CUL4/DDB1 complex) (16,–19). According to proposed nomenclature conventions (20), DIM-5 is sometimes also referred to as KMT1 (lysine [K] methyltransferase 1), based on its structural and functional homologies

with the mammalian Suv39H1 (KMT1A) and Suv39H2 (KMT1B) enzymes. By methylating H3K9, DIM-5^{KMT1} creates a binding site for multiple HP1-containing complexes, including the DIM-2 DNA methyltransferase complex (21), the HCHC histone deacetylase complex (HP1-chromodomain protein 2 [CDP-2]-histone deacetylase 1 [HDA1] complex) (22), and a complex containing a putative histone demethylase, DMM-1 (DNA methylation modulator 1) (23). The combined activities of these complexes are required for proper establishment and maintenance of heterochromatin domains in *Neurospora*. These domains include centromeres, subtelomeric regions, and hundreds of dispersed heterochromatin regions scattered throughout the genome (14, 15).

Proper heterochromatin formation appears to be important for normal genome stability in several organisms, but how specific heterochromatin components contribute to genome maintenance is not well understood (4). In the fission yeast *Schizosaccharomyces pombe*, replication fork stalling is observed in heterochromatin domains (24), and Clr4^{KMT1} mutants, which lack H3K9me, exhibit high rates of illegitimate recombination within the repetitive ribosomal DNA (rDNA) locus (25). Cytological studies in *Drosophila melanogaster*revealed that H3K9me-deficient mutants exhibit spontaneous double-strand breaks (DSBs) in heterochromatin domains (4, 26,–28). H3K9me may promote genome stability through recruitment of HP1, as HP1 homologs in *Drosophila* and mammals contribute to the DNA damage response pathway through both H3K9me-dependent and -independent mechanisms (29,–38). Recent work in *Neurospora* indicates that H3K9 methylation is important for genome maintenance in this fungus as well. DCDC-deficient mutants are hypersensitive to the DNA-damaging agent methyl methanesulfonate (MMS) (16), suggesting that H3K9 methylation may be important for DNA replication or DNA repair. To investigate this possibility further, we examined γH2A—a well-

characterized marker of genotoxic stress—in wild-type strains and heterochromatin-deficient mutants.

In response to DNA replication stress or DNA DSBs, the mammalian H2A variant H2A.X is phosphorylated by ATM or ATR kinase on a serine near the C terminus (serine-139). The resulting modified histone, referred to as γH2AX, acts to stabilize stalled replication forks and facilitate double-strand-break repair (39). Fungi lack an H2A.X variant, but the core H2A protein contains an H2A.X-like sequence near the C terminus (SQEL). Similar to the situation in mammals, this C-terminal serine is phosphorylated by ATM and ATR kinases (Tel1 and Mec1 in *Saccharomyces cerevisiae*) to form γH2A in response to genotoxic stress (40). γH2A then recruits numerous chromatin-binding proteins to regulate genome stability (41).
Because γH2A accumulates around stalled replication forks and DSBs, this modified histone is often used as a marker of genome instability (42,–45). In budding and fission yeasts, genomewide analyses revealed that γH2A is enriched in heterochromatin domains during unperturbed vegetative growth (43, 45). Budding yeast (*S. cerevisiae*) lacks conserved features of heterochromatin, such as H3K9 methylation and HP1, but in *S. pombe*, γH2A was found to colocalize with H3K9me and HP1 (45). In the *S. pombe* $Clr4^{KMT1}$ mutant, γH2A enrichment was reduced in a heterochromatic region near the centromere and in a subtelomeric heterochromatin domain (45). In contrast, γH2A enrichment was unaffected in another heterochromatin domain, the silent mating-type locus. Thus, precisely how γH2A is directed to heterochromatin domains in either yeast species is not clear. In *Drosophila*, γH2A does not appear to be localized to heterochromatin domains in wild-type cells, but in H3K9-deficient mutants, high levels of γH2A are observed in heterochromatin domains, suggesting that heterochromatin-defective mutants suffer spontaneous DNA damage (26). In general, the functional and regulatory relationships

between γH2A and heterochromatin are not well understood. We performed genomic, molecular, and cytological analyses of γH2A in *Neurospora*. We show that γH2A is a component of heterochromatin in *Neurospora* and that γH2A is significantly induced in a heterochromatin-defective mutant under normal growth conditions. These data suggest that ATM or ATR kinase is hyperactivated in the absence of normal heterochromatin. We propose that a repressive chromatin structure at repetitive, A·T-rich DNA sequences is important for normal genome stability in *Neurospora*.

Materials and methods

Strains and growth media.

All *Neurospora* strains used in this study are listed in Table S2.1 in the supplemental material. Strains were grown at 32°C in Vogel's minimal medium (VMM) with 1.5% sucrose (46). Liquid cultures were shaken at 150 rpm. Crosses were performed on modified synthetic cross medium (46). For plating assays, *Neurospora* conidia were plated on VMM with 2.0% sorbose, 0.5% fructose, and 0.5% glucose. Where relevant, plates included 200 μg/ml hygromycin or 400 μg/ml Basta (47). LB medium supplemented with either ampicillin (50 μg/ml) or kanamycin (50 μg/ml) was used to grow *Escherichia coli*DH5α and XL1-Blue (48). Plasmids used for transformation were isolated using Qiagen miniprep kits.

Construction of H3K9 mutants.

Primers used for site-directed mutagenesis are listed in Table S2.2 in the supplemental material. Primers were designed using previously described criteria (49). H3K9 mutations to glutamine or arginine were introduced by PCR, using plasmid pK9L as the template (50, 51).

Plasmids containing *Neurospora* H3K9 mutations to glutamine or arginine were linearized with XbaI and introduced into *Neurospora* strain XStF9.1 by electroporation. This recipient strain contains the H3 coding sequence from *Fusarium graminearum* in place of the *Neurospora hH3* gene, as well as a deletion of *mus-51*. These features ensure that transformation leads to replacement of the entire *F. graminearum hH3* gene with the altered *Neurospora* H3 sequence. Homokaryotic H3 replacement strains were obtained by crossing primary transformants to the wild type. H3 replacement was confirmed by Southern blotting, followed by PCR and sequencing of the integrated DNA.

Molecular analyses.

Neurospora transformation (52), DNA isolation (53), protein isolation, histone isolation, and Western blotting (54) were performed as previously described. Southern blotting was performed as described previously (55), except that probe synthesis, hybridization, and detection were carried out using a North2South chemiluminescence hybridization and detection kit (Thermo). Chemiluminescent blots were imaged using a ProteinSimple FluorChem E imager. Primers used to generate probe templates are listed in Table S2.2 in the supplemental material. Chromatin immunoprecipitation (ChIP) was performed using 5-hour-old germinating conidia. Fifty-milliliter cultures containing 5×10^6 conidia/ml were grown for 5 h, and conidia were harvested by centrifugation. Conidia were washed once in phosphate-buffered saline (PBS), and chemical cross-linking was performed by incubating conidia in PBS containing 1% formaldehyde at room temperature on a rotating platform for 30 min. The reaction was quenched with 125 mM glycine. Conidia were washed with PBS twice and resuspended in lysis buffer (50 mM HEPES, pH 7.5, 140 mM NaCl, 1 mM EDTA, 1% Triton X-100, 0.1% deoxycholate). For

γH2A ChIP assays, the extraction buffer was supplemented with phosphatase inhibitor cocktail (Sigma). Chromatin was sheared by sonication, using an UltraSonic processor (duty cycle, 80; output, 3.5) (Heat System-Ultrasonics Inc.) to deliver 150 1-s pulses at 4°C. Lysates were centrifuged at 13,000 rpm for 5 min at 4°C. For γH2A-ChIP, 2 μl of anti-γH2A antibody (ab15083; Abcam) was used. For detection of H3K9 trimethylation (H3K9me3), 1 μl of antibody (Active Motif) was used. Protein A/G beads (20 μl) (sc-2003; Santa Cruz) were added to each sample. Following overnight incubation, beads were washed twice with 1 ml lysis buffer, once with lysis buffer containing 500 mM NaCl, once with 50 mM LiCl, and finally with TE (10 mM Tris-HCl, 1 mM EDTA). Bound chromatin was eluted in TES (50 mM Tris, pH 8.0, 10 mM EDTA, 1% SDS) at 65°C. Chromatin was de-cross-linked overnight at 65°C. The DNA was treated with RNase for 2 h at 50°C, treated with proteinase K for 2 h at 50°C, and extracted using phenol-chloroform. DNA pellets were washed with 70% ethanol and resuspended in TE buffer. Samples were then prepared for Illumina sequencing or subjected to analysis by quantitative real-time PCR.

qPCR and Illumina sequencing.

Primers used for quantitative PCR (qPCR) are listed in Table S2.2 in the supplemental material. DNAs obtained from ChIP assays were diluted 1:50 in H_2O for input samples and 1:10 in H_2O for samples immunoprecipitated with H3K9me3, H3K4me2, or γH2A antibody. For PCR, iTaq Universal SYBR green Supermix (Bio-Rad) was mixed with specific primer pairs, and 1 μl of the diluted ChIP DNA was added. qPCR was performed using an iCycler IQ instrument (Bio-Rad). Statistical analyses were performed in Microsoft Excel. For Illumina sequencing, libraries were prepared using half of the total immunoprecipitated fraction following

the instructions supplied with Illumina Tru-seq kits, except that genomic DNA adaptors were diluted 1:100 prior to ligation. Illumina sequencing was performed using an Illumina Hi-Seq 2000 genome analyzer at the University of Missouri DNA Core Laboratory.

Data analysis.

Sequence reads were mapped to the latest *Neurospora* genome annotation (version 12), available from the *Neurospora* genome database (11), by using bowtie2 (56). Read numbers were counted for 25-bp bins by using igvtools, and the read density was visualized using the Integrated Genome Viewer (IGV), available from the Broad Institute website (57, 58). We used IGV to normalize data to the total read number before plotting. To calculate normalized enrichment values, we created a custom feature annotation file containing genes, tRNAs, and DNA repeats. Repeated DNA sequences were identified by analyzing the*Neurospora* genome with RepeatScout (59). Repeat families were aligned to the *Neurospora* genome by using BLAT (60), and then coordinates were parsed using a custom perl script into a gene prediction format file that also contained coordinates for genes and tRNAs (downloaded from the Broad Institute genome database [11]). To calculate the normalized ChIP enrichment values (NLCS values) for each feature, we used EpiChIP software, which calculates enrichment values normalized for total read number and for length of the feature (61). Normalized H3K9me3, H3K4me3, and γH2A values for each feature were used to generate scatterplots and to calculate Pearson's correlation coefficients in Microsoft Excel. In addition, the NLCS values were used to plot the kernel density estimations for all features, genes, and repeats, using R (http://www.r-project.org). Where relevant, mapped reads were converted to bed format by use of bedtools software (62). Heterochromatin domains were classified as individual peaks by use of r-seg software

(http://smithlabresearch.org/software/rseg/). The coordinates of H3K9me peaks are listed in Table S2.3 in the supplemental material.

Immunofluorescence.

For cytological analysis of γH2A, we adapted a method previously described for*Aspergillus nidulans* (63). Conidia were inoculated into VMM containing 1.5% sucrose and incubated at 32°C for 12 h on coverslips or in an 8-well μ-Slide (Ibidi). Cells were fixed for 30 min in a solution containing 3.5% formaldehyde, 5% dimethyl sulfoxide (DMSO), 25 mM EGTA, and 5 mM $MgSO_4$. Fixed cells were washed with PBS three times, followed by a 90-min incubation in a 50% egg white solution containing 50 mM piperazine-*N*,*N*′-bis(2-ethanesulfonic acid) (PIPES), pH 6.7, 25 mM EGTA, 5 mM $MgSO_4$, 1 mM dithiothreitol (DTT), and 1 mg/ml of lyticase (purified from *Oerskovia xanthineolytica* [64]; generously provided by Vincent Starai, University of Georgia). Cells were washed again with PBS and incubated overnight at 4°C in a PBS solution containing the primary antibody (1:200 dilution of the Abcam anti-γH2A antibody described above). Cells were washed three times with PBSA (PBS supplemented with 0.1% bovine serum albumin [BSA]) and incubated for 50 min at room temperature in PBS containing a 1:200 dilution of the secondary antibody [Alexa Fluor 488–goat anti-rabbit IgG(H+L); Life Technologies]. Cells were washed with PBSA three times prior to imaging. Microscopy was performed using a DeltaVision II microscope equipped with a Delta Vision standard filter set, which includes fluorescein isothiocyanate (FITC) and tetramethyl rhodamine isocyanate (TRITC) filters for green and red fluorescence acquisition, respectively. Quantitative analysis of fluorescence intensities was performed using Softworx 1.3 software (Applied Precision).

Nucleotide sequence accession numbers.

Sequence data from this study are available through the NCBI Short Read Archives (accession no. SRP042169).

Results

γH2A is localized to heterochromatin domains in *Neurospora crassa*.

γH2A is a functionally conserved modification of H2A that acts to stabilize replication forks and facilitate double-strand-break repair in fungi and animals (43,–45, 65). To determine if γH2A is enriched at specific genomic locations in the filamentous fungus *Neurospora crassa*, we performed ChIP of γH2A followed by high-throughput sequencing (ChIP-seq). We used a previously characterized anti-γH2A antibody that was specific for both yeast and*Neurospora* γH2A proteins (H2A proteins phosphorylated on serine-129 and serine-131, respectively) (66,67). We also performed ChIP-seq experiments to detect two well-characterized chromatin modifications, H3K4me2 and H3K9me3, which are molecular markers of euchromatin and heterochromatin, respectively. As expected, H3K4me2 was enriched in active genes, while H3K9me3 was localized to A·T-rich, gene-poor heterochromatin domains (Fig. 1A). γH2A enrichment was highly correlated with heterochromatin domains identified by enriched H3K9 trimethylation (Fig. 2.1A and B); see Fig. S2.1 in the supplemental material). To validate the ChIP-seq results, we performed qPCR to examine γH2A at representative euchromatin (*hH4* and*cfp*) and heterochromatin (8:A6 and 9:E1) domains. qPCR results were fully consistent with our ChIP-seq data, confirming that γH2A is a component of heterochromatin domains in *Neurospora* (Fig. 1C). To confirm that the γH2A antibody was specific, we performed ChIP experiments using a γH2A-deficient strain in which the single H2A

gene was replaced with an H2A allele containing a serine-131-to-alanine substitution (66). Heterochromatic domains were not enriched in the *hH2A*^{S131A} strain when qPCR analyses were performed for representative heterochromatic and euchromatic regions (Fig. 1C). Similarly, heterochromatin domains were not enriched when the entire γH2A immunoprecipitate fraction was assayed by ChIP-seq (Fig. 1A and B; see Fig. S2.1), demonstrating that the γH2A antibody was specific for phosphorylated H2A serine-131.

To validate that γH2A is localized with H3K9me3 at divergent repeated sequences throughout the genome, we used EpiChIP software (61) to calculate the NLCS values for all features in the genome. Features included genes, tRNAs, and repeated DNA sequences. We generated a scatterplot to compare the NLCS values for H3K9me3 and γH2A or to compare H3K4me2 and γH2A in genes and repeats. H3K9me3 and γH2A were similarly enriched in repeats, while exhibiting low levels of enrichment in genes (Fig. 2.1D) (Pearson's correlation coefficient = 0.80). In contrast, H3K4me2 was enriched in many of the genes and exhibited no correlation with γH2A (Fig. 2.1D) (Pearson's correlation coefficient = −0.16). We also calculated the kernel density estimations to examine the relative frequencies of enriched and unenriched features for H3K4me2, H3K9me3, and γH2A. Plotting the kernel densities revealed a bimodal distribution for all three modifications. In each case, one peak corresponds to features with background levels of enrichment, while the second peak represents features enriched with the modification. We also plotted the kernel densities for genes or repeats alone. For H3K4me2, genes were distributed in two peaks, corresponding to background and enriched features, while repeats were distributed in a single background peak (see Fig. S2A in the supplemental material). For both H3K9me3 and γH2A, genes were distributed in a single peak corresponding to background enrichment. In contrast, repeats were distributed in a single peak corresponding to

enriched features (Fig. 2.2A and B). As expected, the kernel density estimation of γH2A enrichment in the *hH2A*^{S131A} strain produced a single peak corresponding to uniform background enrichment for all features across the genome (Fig. 2.2C). However, the enrichment value observed for repeats was slightly lower than that for genes due to a subtle bias against A·T-rich sequences observed in Illumina sequencing experiments (68, 69). Together, these data demonstrate that γH2A localizes to repeat-rich heterochromatin domains across the *Neurospora* genome.

H3K9 methylation is required for normal γH2A localization.

H3K9 methylation by DIM-5^{KMT1} is an early step in heterochromatin formation (50, 70). We were interested to learn if γH2A localization depends on DIM-5^{KMT1} or its enzymatic product, H3K9me3. We performed γH2A ChIP-seq experiments with a *dim-5* deletion strain and found that enrichment of γH2A was significantly reduced at all heterochromatin domains (see Fig. S2B in the supplemental material). Consistent with this apparent loss of enrichment, plotting the kernel density for γH2A enrichment in the *dim-5* strain revealed a single peak corresponding to uniform background enrichment across the genome for all features. We performed qPCR to validate the ChIP-seq data for representative heterochromatin domains on linkage groups (LG) II and V (Fig. 2.2E). We used primers to test enrichment adjacent to each domain (regions 90-1 and 230-1), at the edge of each domain (regions 90-2 and 230-2), and in the center of each domain (regions 90-3 and 230-3). qPCR data were fully consistent with the ChIP-seq data. γH2A enrichment was significantly reduced at both domains tested (peak 90 and peak 230) (see Table S3); however, a low level of γH2A in the center of the heterochromatin region remained (Fig. 2.2F) (Student's *t* test; $P < 0.008$ for region 90-2, $P < 0.008$ for region 90-3, $P < 0.0002$ for

region 230-2, and $P < 0.007$ for region 230-3). Together, these data suggest that γH2A localization is altered in the *dim-5* mutant strain. We next asked if γH2A enrichment depends on H3K9me3. It was previously reported that H3K9 is an essential residue in *Neurospora*, based on the observation that H3K9L mutants were not recovered from crosses in which the mutant *hH3* allele was integrated at an ectopic locus (51). We constructed H3K9-to-arginine (R) and H3K9-to-glutamine (Q) replacement alleles, which mimic unacetylated and acetylated lysine, respectively. Homokaryons were obtained for both alleles, demonstrating that H3K9 is not essential (see Fig. S2.3 in the supplemental material). As expected, both H3K9 substitution strains lacked DNA methylation (see Fig. S3), indicating that heterochromatin formation was defective. Both strains also exhibited severe growth defects, similar to *dim-5* strains (see Fig. S4). We next performed ChIP-seq experiments with these H3K9me3-deficient strains. Like the case in *dim-5* strains, γH2A was no longer enriched in repetitive sequences in these mutants (Fig. 2.3A and B). Loss of enrichment was evident across the entire genome (see Fig. S2C). Data for three representative heterochromatin regions are shown in Fig. 2.3B. We confirmed these data by performing ChIP-qPCR to assay γH2A enrichment at the 8:A6 heterochromatin region (Fig. 2.3C) (Student's *t* test; $P < 4 \times 10^{-5}$ for the $hH3^{K9Q}$ mutant and $P < 1.5 \times 10^{-5}$ for the $hH3^{K9R}$ mutant). These data show that heterochromatin formation directed by DIM-5 is required for normal localization of γH2A.

Normal γH2A localization depends on HP1.

HP1 binds methylated H3K9 and functions as a molecular scaffold to recruit additional chromatin-modifying enzymes to heterochromatin domains (21). *Neurospora*HP1 forms distinct complexes with the histone deacetylase HDA1 and the DNA methyltransferase (MTase) DIM-2

(22, 54). To determine if HP1, HDA1, or DIM-2 is required for proper control of γH2A localization, we performed ChIP-qPCR experiments using deletion strains that lack these proteins. As expected based on prior work, enrichment of H3K9me3 was abolished at the 8:A6 region in the *hpo* and *hda-1* strains but not in the *dim-2* strain. Similarly, γH2A was lost from the 8:A6 region in the *hpo* and *hda-1* strains but not in the*dim-2* strain (Fig. 2.4A) (Student's *t* test; $P < 0.0001$ for the *hpo* strain and $P < 1.0 \times 10^{-7}$ for the *hda-1* strain). We also performed qPCR to examine γH2A enrichment at the same representative regions on LGII and LGV as those examined above (peaks 90 and 230). For both regions, γH2A enrichment was lost at the edge of the heterochromatin domain in the *hpo* and *hda-1* strains (Student's *t* test; $P < 0.001$ for region 90-2 in the*hpo* strain, $P < 0.001$ for region 90-2 in the *hda-1* strain, $P < 0.002$ for region 230-2 in the *hda-1* strain, and $P < 0.003$ for region 230-2 in the *hpo* strain). The *dim-2* strain exhibited a small decrease in γH2A enrichment at the edge of the LGV domain (region 230-2), but the observed difference was not statistically significant. The *dim-2* strain also failed to exhibit significant differences in the level of γH2A enrichment in the centers of these heterochromatin domains (Fig. 2.4B and C). Enrichment was slightly reduced in the centers of the LGII and LGV regions in the *hda-1* strain (Fig. 2.4C) (Student's *t* test; $P < 0.013$ for region 90-3 and $P < 0.025$ for region 230-3). Enrichment appeared to be slightly reduced in the middle of the LGV domain in the *hpo*strains, but this difference was not statistically significant (Fig. 2.4C) (Student's *t* test; $P < 0.17$ for region 230-3). These data suggest that the HCHC complex contributes to normal localization of γH2A. However, the loss of enrichment in the HCHC-deficient strains was less severe than that in the *dim-5* mutants at the regions tested. This suggests that another H3K9me-binding protein may be important for normal γH2A localization. In contrast, DNA methylation is not required for γH2A enrichment at heterochromatin domains.

γH2A is not required for H3K9 methylation or DNA methylation.

Since γH2A is enriched in heterochromatin domains, we tested the possibility that γH2A regulates H3K9me3 or DNA methylation. qPCR experiments revealed similar enrichments of H3K9me3 at the 8:A6 region in both wild-type and*hH2A*^{S131A} strains (Fig. 2.3C). To confirm this, we performed ChIP-seq experiments to examine H3K9me3 in the *hH2A*^{S131A} strain. These analyses revealed that H3K9 methylation patterns were qualitatively similar in the wild type and the *hH2A*^{S131A} strain (Fig. 2.5A). To next determine if γH2A was required for proper control of DNA methylation, genomic DNAs from the wild-type and *hH2A*^{S131A} strains were digested with the methylation-sensitive enzyme BfuCI and the methylation-insensitive isoschizomer DpnII. The digested DNAs were analyzed by Southern blotting to examine DNA methylation at known methylated regions (8:A6, 8:G3, and centromere VII) (71). The membrane was also probed for the unmethylated H3 gene to confirm that the DNAs had been digested completely. Wild-type patterns of DNA methylation were observed for all four loci (Fig. 2.5B). These data show that γH2A is not required for H3K9 trimethylation or cytosine DNA methylation.

γH2A is induced in the *dim-5* strain.

We asked if the loss of γH2A enrichment observed in the *dim-5* strain corresponded to a global reduction in γH2A levels. We isolated total histones from the wild-type, *dim-5*, and*hH2A*^{S131A} strains. As a control, we also isolated histones from the same strains following exposure to the DNA-damaging agent MMS, and we performed Western blotting to examine the level of γH2A in each strain. To ensure equal loading, gels were stained with Coomassie brilliant blue, and we performed Western blotting using antibodies that recognize H3K4me2, which was previously demonstrated to be unchanged in the *dim-5* background (54). In the wild type, γH2A

levels are low in minimal medium, but exposure to MMS leads to induction of γH2A, as observed previously (66). In contrast, analysis of the *dim-5* strain revealed that γH2A levels were significantly elevated in minimal medium (Student's *t* test; $P = 0.02$). γH2A levels remained high following exposure to MMS (Fig. 2.6). No signal was observed for the $hH2A^{S131A}$ strain.

These data appeared to be inconsistent with our ChIP-seq data, which suggested an apparent loss of enrichment in the *dim-5*, $H3^{K9R}$, and $H3^{K9Q}$ strains (Fig. 2.2 and 2.3). However, overall increased γH2A levels in euchromatin would also result in the loss of relative γH2A enrichment observed in H3K9me3-deficient strains. To test this possibility, we performed immunofluorescence assays to visualize γH2A localization in the wild-type and *dim-5* strains. Both strains contained an H1-RFP reporter construct to enable visualization of nuclei. In wild-type cells, the observed fluorescence was similar to that for the $hH2A^{S131A}$ strain, consistent with the low levels of γH2A observed in Western blot experiments (Fig. 2.7A; see Fig. S4 in the supplemental material). In contrast, nuclei in *dim-5* cells were intensely stained with the γH2A antibody (Fig. 2.7A). γH2A appeared to be enriched throughout *dim-5* nuclei, although some nuclei displayed nonuniform γH2A staining (Fig. 2.7B). Immunofluorescence assays revealed that γH2A accumulated in wild-type nuclei following exposure to the DNA-damaging agent MMS (see Fig. S5), demonstrating that this method is able to detect elevated levels of γH2A in wild-type cells. We quantified green and red fluorescence in wild-type and *dim-5* nuclei grown in minimal medium (Fig. 2.7C). These data confirmed that *dim-5* strains exhibit a significant induction of γH2A under normal growth conditions, consistent with defective DNA replication or repair in these strains. We next asked if γH2A misregulation is responsible for the drug sensitivity of *dim-5* strains. We tested colony survival of wild-type, *dim-5*, $hH2A^{S131A}$, and *dim-5*;$hH2A^{S131A}$ strains on MMS and the topoisomerase inhibitor camptothecin. Double-mutant

strains were more sensitive than either single mutant, suggesting that DIM-5 regulates additional factors, along with γH2A, to promote proper DNA replication or repair (see Fig. S6).

Discussion

γH2A associates with heterochromatin in *Neurospora*.

We found that γH2A is a component of heterochromatin domains in wild-type *Neurospora* cells. Similar results were observed in *S. cerevisiae* and *S. pombe* (43, 45, 72), suggesting that γH2A is a conserved heterochromatin component in fungi, or at least in the ascomycetes. These data raise the possibility that γH2A is enriched in heterochromatin in other eukaryotes as well. Like the case in other organisms that have been studied, *Neurospora* γH2A is generated by ATM and ATR kinases in response to replication stress or DNA damage (66, 67). The MRN complex (Mre11, Rad50, and Nbs1) orchestrates ATM recruitment and activation at double-strand breaks (73, 74), while ATR is activated by accumulation of single-stranded DNA (ssDNA) (75). Because ssDNA can accumulate during various repair processes, ATR is able to respond to a variety of different types of DNA damage and genotoxic stresses. For example, ssDNA is generated during end resection of a double-strand break and at stalled replication forks, where the replicative helicase is thought to become uncoupled from DNA polymerase (76). It is possible that the heterochromatin structure leads to stalled replication forks in the wild type, thereby activating ATR kinase. Studies from *S. cerevisiae* show that γH2A overlaps regions that stall replication forks, including heterochromatin domains, and that recruitment of γH2A to heterochromatin depends on Sir3 (43, 72, 77). In *S. pombe*, heterochromatin-associated γH2A depends on the checkpoint kinase RAD3 (a homolog of ATR) (45). Certain DNA-binding proteins can inhibit replication fork progression (5). Thus, the tightly packaged nucleosomes

found in heterochromatin may act as a natural impediment to replication forks. Indeed, analysis of replication intermediates by two-dimensional gel electrophoresis revealed stalled replication forks in heterochromatin domains of wild-type *S. pombe* cells (24). However, it remains possible that H2A kinases, such as ATR and ATM, are recruited directly to heterochromatin domains. Further studies are needed to determine the mechanisms responsible for γH2A deposition in heterochromatin in wild-type cells.

In yeasts and animals, γH2A functions as a signal to recruit proteins that stabilize stalled replication forks or regulate DNA repair (41, 78, 79). For example, *S. pombe* Brc1 binds to γH2A via its BRCT domains to enable recovery from replication stress (78). *Neurospora* heterochromatin domains are comprised of AT-rich repetitive sequences that can adopt non-B-form DNA structures, such as cruciforms or hairpins. Such structures are known to stall replication forks in bacterial, yeast, and mammalian cells (80). It is therefore possible that γH2A functions to recruit proteins to stabilize replication forks that encounter natural sequence impediments found in heterochromatin domains. On the other hand, repeated DNA sequences can also provide substrates for illegitimate recombination, leading to chromosome rearrangements. Work with*Drosophila* revealed distinct DSB repair mechanisms in heterochromatin and euchromatin (32). The*Neurospora dim-5* mutant exhibits elevated rates of illegitimate recombination between heterochromatin-associated transgenes arranged in tandem (81). Thus, γH2A may recruit proteins to regulate the type of DNA repair that occurs in heterochromatin. The mammalian γH2A-binding protein PTIP binds 53BP1 to suppress homologous recombination (HR) and promote nonhomologous end joining (NHEJ) (82, 83), consistent with this possibility. The *Neurospora* genome encodes 10 BRCT domain-containing

proteins (11). Future studies are required to determine if any of these proteins are localized to heterochromatin and, if so, what functions they might perform at these genomic regions. While γH2A is best known for its response to replication stress and DNA damage, it is possible that this modified histone performs other functions at heterochromatin domains. Recent work with *S. cerevisiae*suggested that γH2A is important for long-range interactions between silent mating-type loci (77), raising the possibility that γH2A contributes to three-dimensional organization of the nucleus. On the other hand, γH2A may play a role in transcriptional silencing. The mammalian γH2A-binding protein MDC1 (mediator of DNA damage checkpoint 1) appears to be important for silencing sex chromosomes during male meiosis (84). In *S. cerevisiae*, the homolog of Brc1, Esc4/Rtt107, was implicated in silencing because it binds to the silencing protein SIR3 (85). In *S. pombe*, the γH2A-binding protein Brc1 is required for normal transcriptional silencing of a reporter gene embedded in pericentromeric heterochromatin (86). It is likely, however, that this protein contributes to silencing independently of γH2A, as γH2A itself is not required for silencing or for normal heterochromatin formation in *S. pombe* (45). We found that γH2A is not required for normal H3K9me3 or DNA methylation in *Neurospora*, demonstrating that heterochromatin formation does not depend on phosphorylation of H2A serine-131. In particular, we found that DNA methylation at the 8:A6 region is not affected in the *Neurospora H2A*^{S131A} mutant. This result suggests that γH2A is not required for transcriptional silencing, because this locus frequently loses DNA methylation in mutants that affect transcriptional silencing (15, 22, 54).

Heterochromatin formation is required for normal genome stability in *Neurospora*.

The DCDC complex is required for growth on the DNA-damaging agent MMS (16), suggesting that this complex is required for normal DNA replication or repair. In this study, we found that Δ*dim-5* strains have high levels of γH2A during normal replicative growth. These data suggest that Δ*dim-5* strains suffer spontaneous DNA damage during replication, perhaps due to frequent replication fork collapse. γH2A in *S. cerevisiae* and *S. pombe* heterochromatin-deficient mutants has been analyzed by ChIP. *S. cerevisiae sir3* mutants show reduced enrichment of γH2A in heterochromatin (72), and for *S. pombe*, it was reported that γH2A enrichment in centromeres and subtelomeric regions depends on Clr4, a homolog of DIM-5^{KMT1} (45, 87). Based on the results obtained with *S. pombe*, it was suggested that H3K9 methylation by Clr4 is required for γH2A deposition in heterochromatin. Similarly, we observed reduced enrichment of γH2A at heterochromatin domains in the Δ*dim-5* strain. Taken together, our results suggest that heterochromatin-deficient *Neurospora* mutants do not exhibit reduced γH2A in heterochromatin but, rather, display elevated levels of γH2A throughout the genome. This interpretation is fully consistent with our global analyses of γH2A by Western blotting and immunofluorescence assays, as well as with our ChIP-seq analyses. It is possible that *S. pombe* heterochromatin mutants display a similar induction of γH2A. The reported loss of heterochromatin-associated γH2A in Clr4 mutants was determined by normalizing γH2A enrichment in heterochromatin domains to a euchromatic control locus. Thus, in *S. pombe*, loss of enrichment may result from increased γH2A in euchromatin, as observed in our experiments. This would be consistent with recent work showing that heterochromatin components are required for proper genome integrity of centromeres in the absence of fork stability components (88).

In *Drosophila* mutants lacking the DIM-5 homolog Su(var)3-9, γH2A is induced in foci that colocalize with heterochromatin (26, 27). Our results show that γH2A is dramatically induced in the *dim-5* strain and appears to be found throughout the nucleus. Given that γH2A is induced by stalled replication forks and by DSBs, these data suggest that DIM-5 is required for DNA replication or repair in *Neurospora*. This interpretation is supported by previous work demonstrating that DIM-5-deficient cells are hypersensitive to the DNA-damaging agent MMS (16). It is possible that DIM-5 is a global regulator of genome stability. However, γH2A is deposited in extremely large domains around DSBs (0.5 to 2 Mb in human cells) (42). In yeast, γH2A can spread to the undamaged domains close to the site of damage both in *cis* and in *trans*, presumably because ATR modifies serine-129 of H2A in close proximity (89). Our results may indicate that the Δ*dim-5*strain accumulates DSBs in heterochromatin domains, leading to massive spread of γH2A into euchromatin. Such a model is supported by recent analyses of *Drosophila* mutants defective for H3K9 methylation (4, 26,27). These *Drosophila* mutants exhibit spontaneous DNA damage, including double-strand breaks, and suffer frequent genome rearrangements. These defects are presumably due to defective replication of heterochromatin-associated repeat sequences. Future studies are required to determine how heterochromatin might function to preserve genome integrity. The *Neurospora* genome includes abundant heterochromatin domains that share important molecular features with higher eukaryotes. Given these similarities with other eukaryotes, future work with *Neurospora* is likely to lead to important insights regarding the relationships between heterochromatin and genome maintenance.

Acknowledgements

We thank Shin Hatakeyama and Shuuitsu Tanaka at Saitama University for providing the *H2A*^{S131A} strain. This work was funded in part by a grant to Z.A.L. from the March of Dimes Foundation (grant 5-FY14-89) and by a grant to M.F. from the National Institutes of Health (grant GM097637).

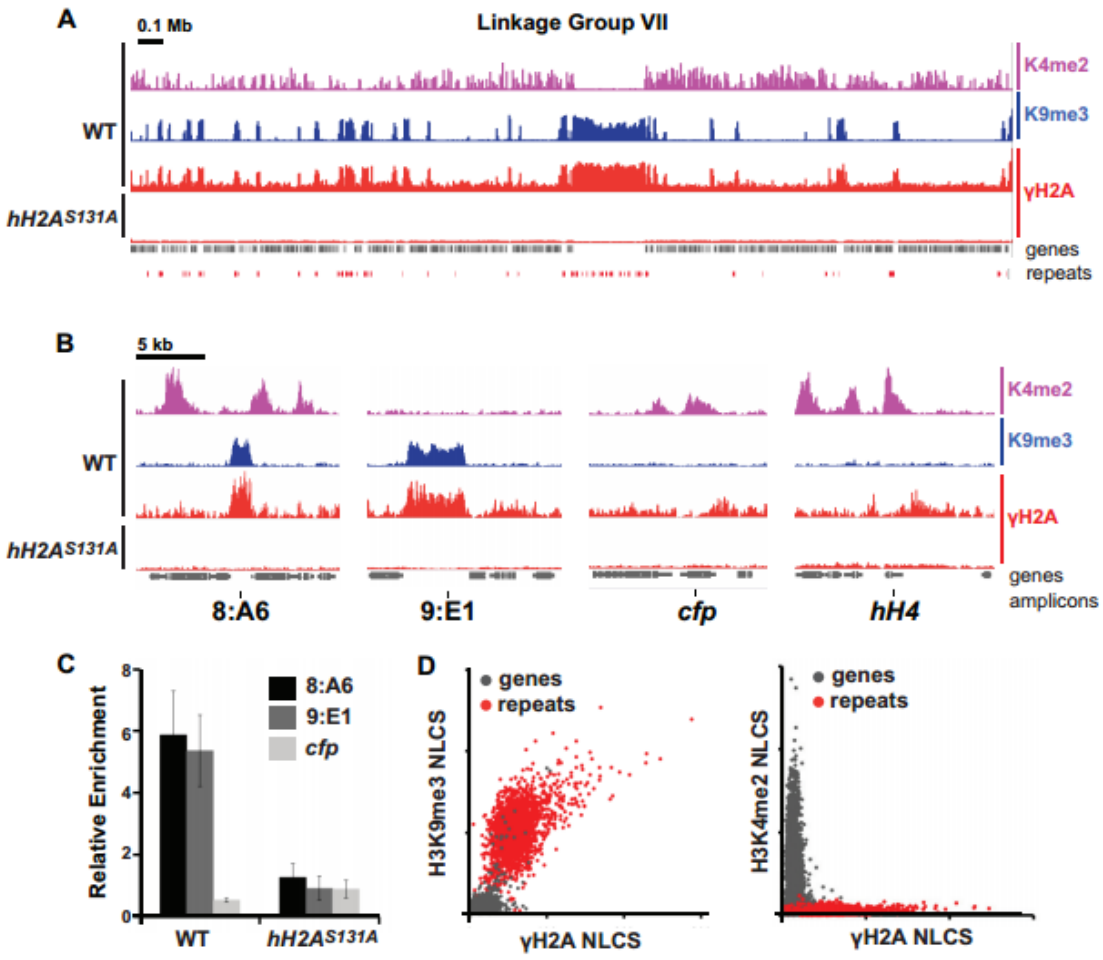

Figure 2.1 γH2A is a heterochromatin component in *Neurospora*. (**A**) ChIP-seq enrichment across Linkage Group VII is shown for H3K4me2, H3K9me3, and γH2A in the wildtype strain and for γH2A in the negative control *hH2A*^{S131A} strain. The strain is indicated on the left of the histogram and the antibody used to perform ChIP-seq is indicated on the right. The positions of genes (grey) and degenerate DNA repeats (red) are shown at the bottom of the plot. The scale bar at the top indicates 0.1 Mb. (**B**) ChIP-seq enrichment patterns for representative heterochromatin (8:A6 and 9:E1) and euchromatin (H4 and CFP) domains are shown. The scale bar indicates 5 kb. Genes are shown in grey beneath each plot. The positions of PCR amplicons used to validate enrichment are indicated with a black line beneath each plot. (**C**) Quantitative real time-PCR

analysis of the representative regions shown in B. The relative enrichment of 8:A6, 9:E1, and *cfp* was determined by normalizing the indicated region to the *hH4* gene. (**D**) Scatter plots comparing enrichment of γH2A and H3K9me3 (left) or γH2A and H3K4me2 (right) are shown. The normalized ChIP enrichment value (NLCS) obtained for the indicated antibody was plotted for each genomic feature. Genes and tRNAs are shown in grey and repeats are shown in red.

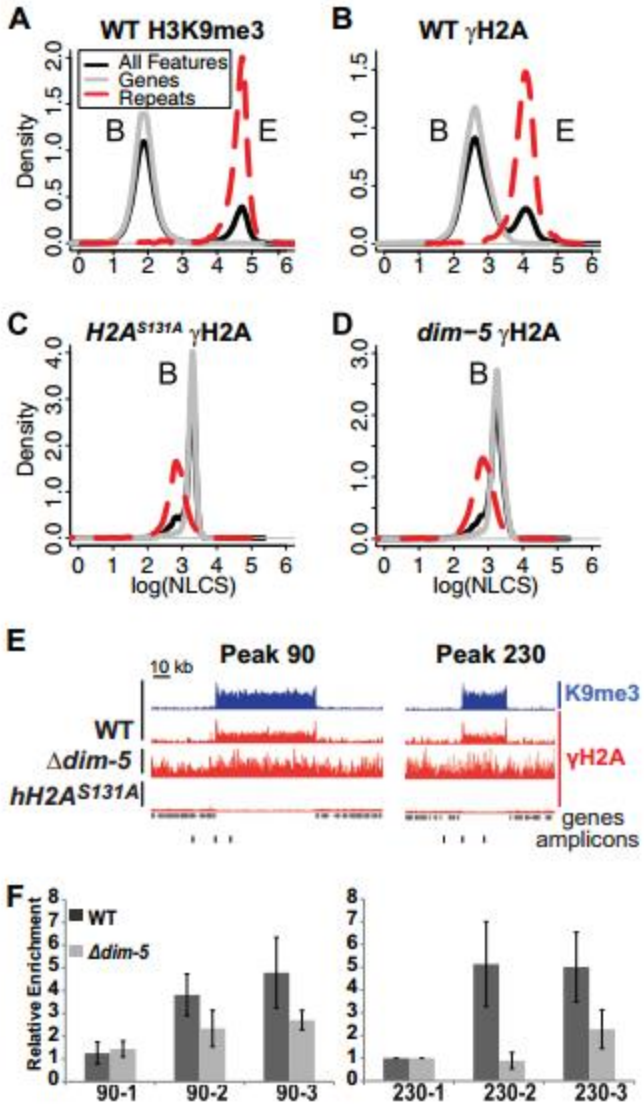

Figure 2.2 Enrichment of γH2A depends on DIM-5. (**A - D**) The distribution (kernel density estimation; density) of normalized read counts (NLCS) is shown for all genomic features (genes and repeats; black), genes only (grey), and repeats only (red). In wildtype, two peaks are observed for both H3K9me3 and γH2A, corresponding to features with background signal (‘‘B’’; genes) and features enriched for the modification (‘‘E’’; repeats). In *hH2A*^{S131A} and *Δdim-5* strains, all features exhibit background levels of γH2A enrichment. (**E**) ChIP-seq data for H3K9me3 and γH2A are shown for wildtype, *Δdim-5*, and *hH2A*^{S131A} strains at two representative regions. The strain is indicated on the left of the histogram, and the antibody used

to perform ChIP-seq is indicated on the right. The scale bar indicates 10 kb. Genes are shown in grey beneath each plot. The positions of PCR amplicons used to validate the ChIP-seq experiment are indicated with a black line beneath the plot. (**F**) γH2A ChIP samples were subjected to qPCR to analyze enrichment at each of the amplicons shown in E. Relative enrichment was determined by normalizing the enrichment value at each region to the euchromatic flank adjacent to each peak (90-1 or 230-1).

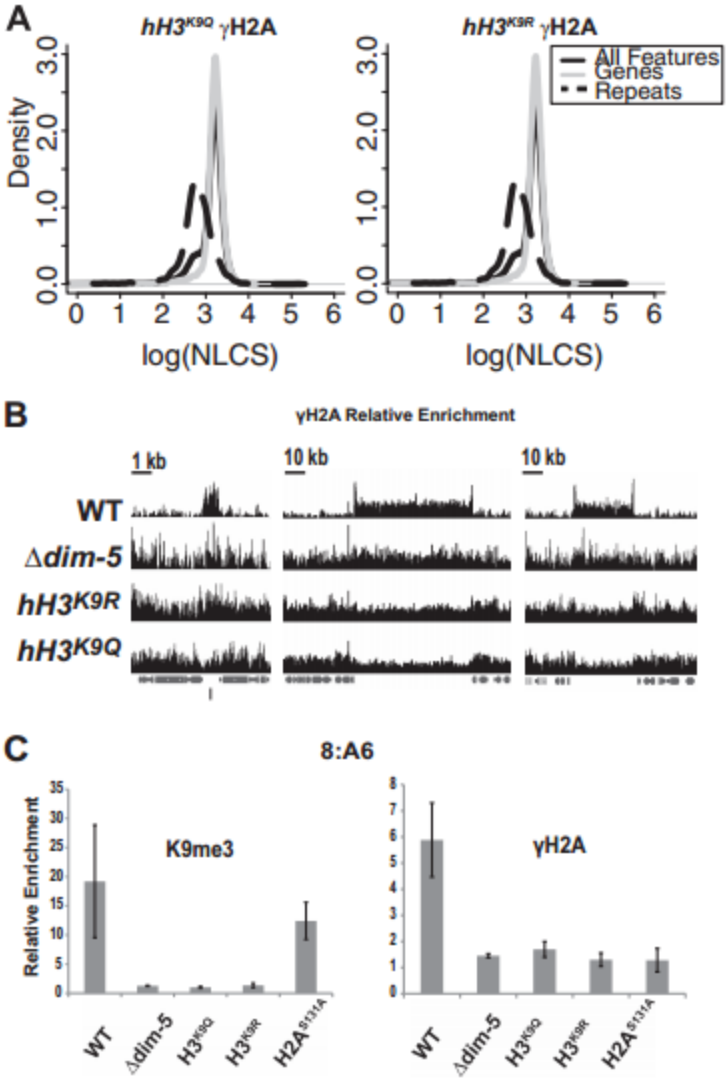

Figure 2.3 H3K9me3 is required for γH2A enrichment. (**A**) The distribution (kernel density estimation; density) of normalized read counts (NLCS) is shown for all genomic features (genes and repeats), genes only, and repeats only for strains harboring H3K9 substitution alleles. In both strains, all features display equivalent background levels of γH2A enrichment. (**B**) ChIP-seq data for γH2A are shown for wildtype, *Δdim-5*, and two strains harboring H3K9 substitution alleles at two representative regions (peak 90 and peak 230). A scale bar at the top of each graph indicates the size of the region plotted. Genes are shown in grey beneath each plot. The position of the 8:A6 PCR amplicon used to validate the ChIP-seq experiment is indicated with a black line

beneath the plot. (**C**) γH2A ChIP samples were subjected to qPCR to analyze enrichment at the 8:A6 region. Relative enrichment was determined by normalizing the enrichment value at 8:A6 to the *hH4* gene.

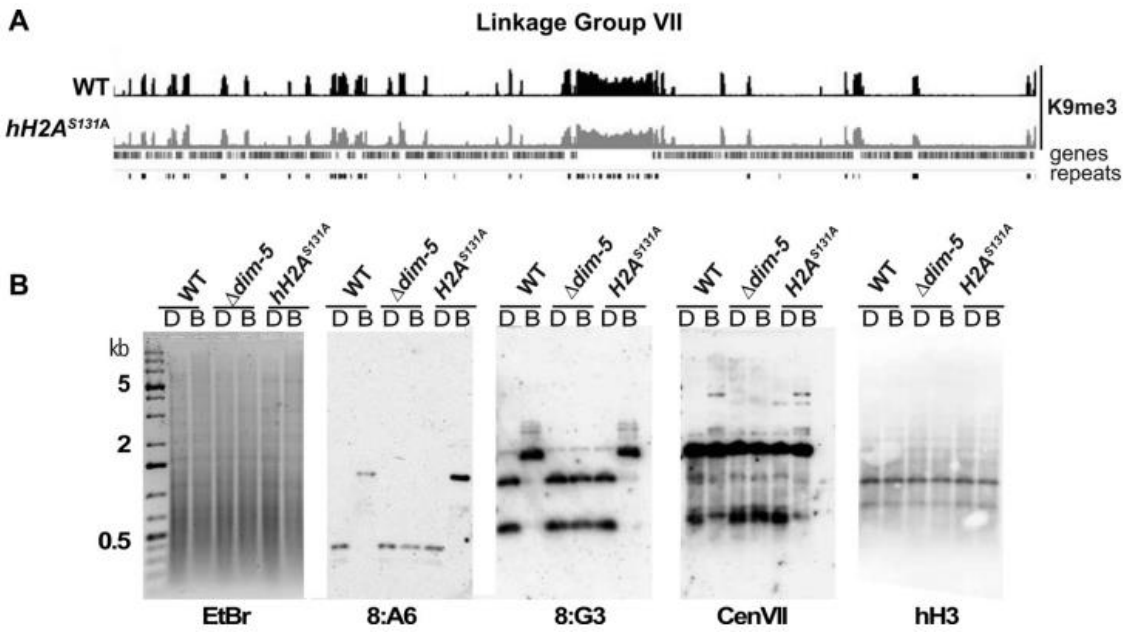

Figure 2.4 Heterochromatin formation is independent of γH2A. (**A**) ChIP-seq enrichment across Linkage Group VII is shown for H3K9me3 in the wildtype strain and the *hH2A*^{S131A} strain. The strain is indicated on the left of the histogram. Genes are shown in grey and degenerate DNA repeats are shown in black at the bottom of the plot. (**B**) Genomic DNA from wildtype, □*dim-5*, and *hH2A*^{S131A} was digested with methylation-sensitive and -insensitive isoschizomers DpnII ("D") and BfuCI ("B"). Cytosine methylation levels were analyzed by visualizing digested DNA with Ethidium Bromide (EtBr) and by probing Southern blots with the indicated methylated (8:A6, 8:G3, and CenVII), and unmethylated (*hH3*) regions.

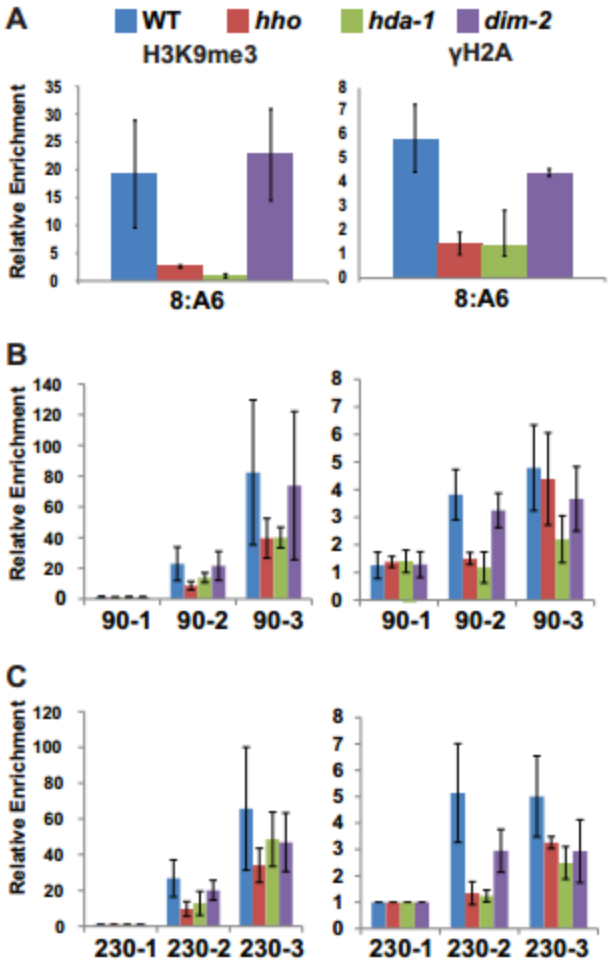

Figure 2.5 γH2A enrichment is reduced in the *hpo* and *hda-1* strains. ChIP was performed for the indicated strains using antibodies to H3K9me3 (left) and γH2A (right). Relative enrichment levels were determined by qPCR at the 8:A6 region (**A**) and at sites within and adjacent to peak 90 (**B**) and peak 230 (**C**). Enrichment at 8:A6 is shown relative to the euchromatic hH4 gene. Enrichment in peak 90 and 230 is shown relative to the euchromatin region adjacent to each peak (PCR amplicon 90-1 and 230-1, respectively).

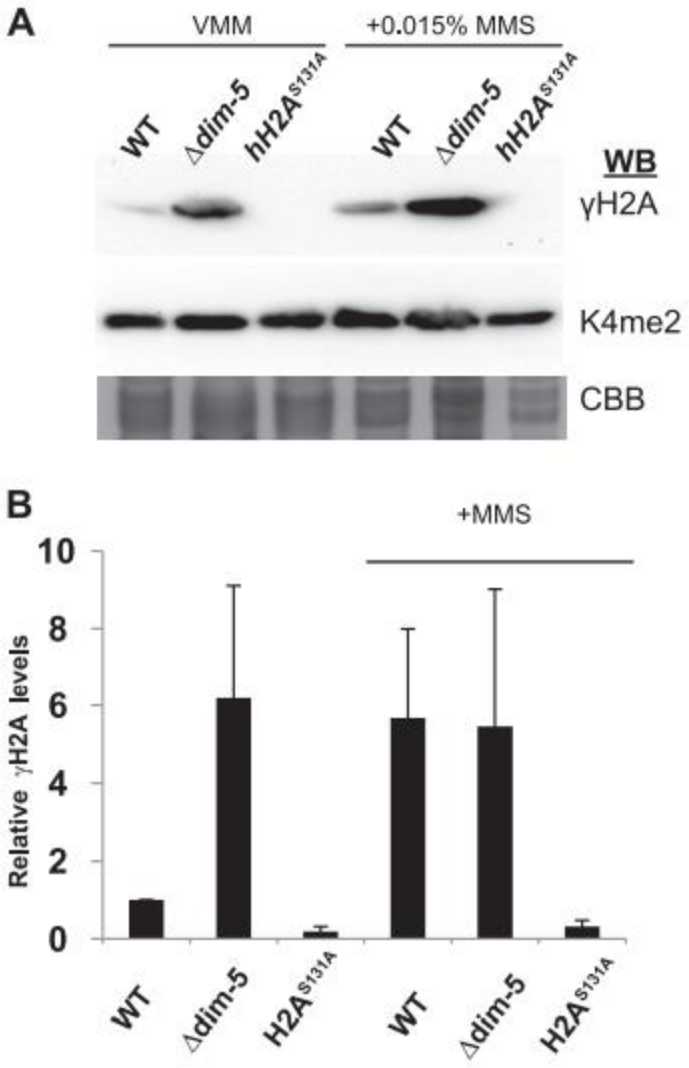

Figure 2.6 γH2A levels are elevated in the *Δdim-5* strain. (**A**) Histones were isolated from the indicated strains grown in VMM or VMM + MMS and subjected to western blot analyses for γH2A. Western blots were also performed using antibodies to H3K4me2, which serves as a loading control. (**B**) The levels of γH2A for each strain were determined by densitometry and normalized to H3K4me2 for each strain grown in VMM and VMM+MMS medium.

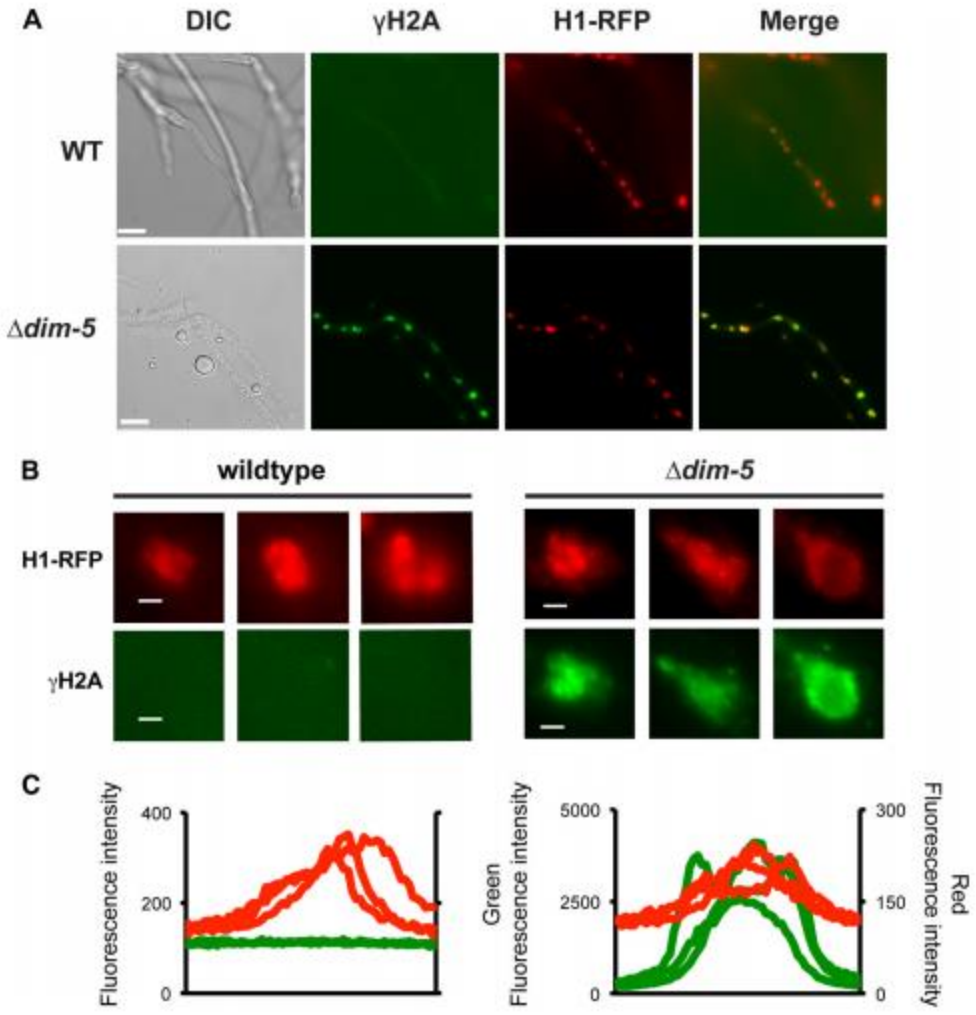

Figure 2.7 γH2A levels are elevated throughout *Δdim-5* nuclei. (**A**) Immunofluorescence of γH2A is shown for wildtype and *Δdim-5* cells. Both strains are expressing an H1-dTomato fusion protein to allow visualization of nuclei (H1-RFP). Scale bars indicate 10μm. (**B**) Immunofluorescence data for three individual nuclei from each strain are shown. Scale bars indicate 1μm. (**C**) Red and green fluorescence was quantified for three representative nuclei using the SoftWorx Explorer "line profile" tool. The plots show fluorescence intensity measured along a 4μm line drawn across the center of the nucleus.

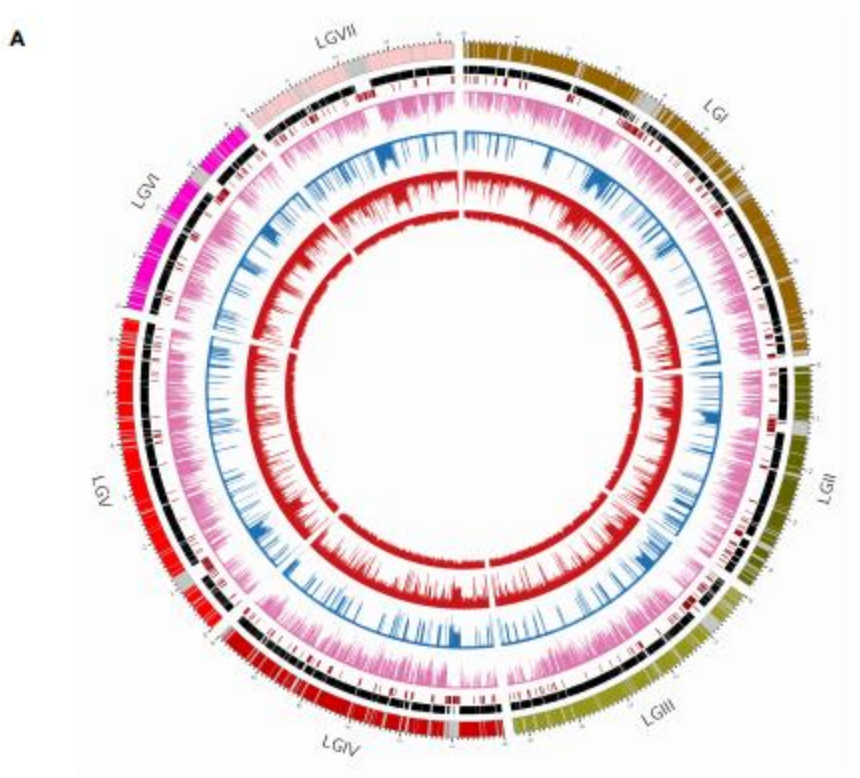

Figure S2.1 γH2A localizes with H3K9me3 to heterochromatin domains across the entire genome. ChIP-seq data for the seven Neurospora Linkage Groups were plotted with circos software. Chromosomes are plotted in different colors on the outside of the circle. Tick mark labels indicate each Megabases along the chromosomes. From outside moving toward the center, genes (black) and repeats (red) are shown, followed by histograms depicting wildtype enrichment patterns of K3K4me3 (pink), H3K9me3 (blue), and γH2A (red). The inner-most circle shows ChIP-seq enrichment data for the γH2A-deficient negative control strain, *hH2A*^{S131A}.

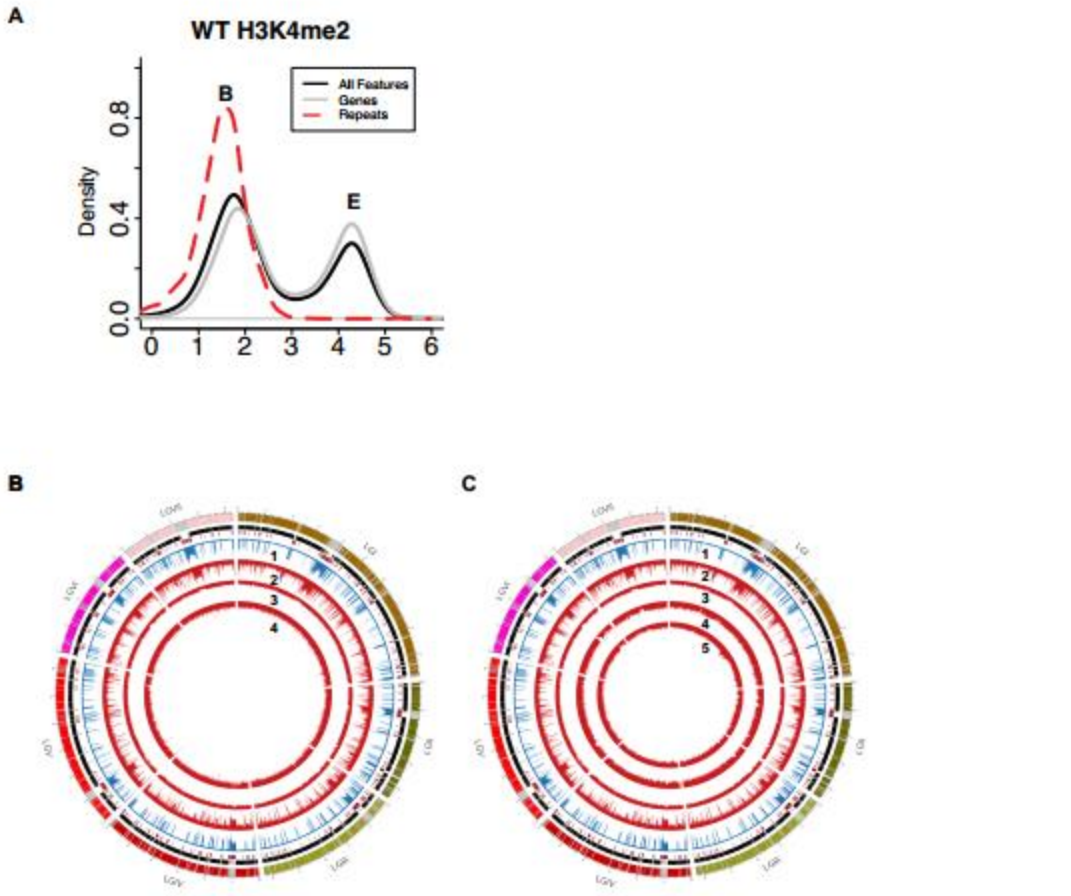

Figure S2.2 (A) H3K4me2 is enriched in a subset of genes, but not in repeats. (**A**) The distribution (kernel density estimation; density) of normalized read counts(NLCS) for H3K4me2 is shown for all genomic features (genes and repeats), genes only, and repeats only. Two peaks are observed corresponding to background enrichment (‘‘B’’) and enriched features. (**B**) **DIM-5 and H3K9 methylation are required for normal γH2A localization**. ChIP-seq data for the seven Neurospora Linkage Groups were plotted with circos software. Chromosomes are plotted in different colors on the outside of the circle. Tick mark labels indicate each Megabases along the chromosomes. From outside moving toward the center, genes (black) and repeats (red) are shown, followed by histograms depicting enrichment patterns of wildtype H3K9me3 (1; blue), wildtype γH2A (2; red), *hH2AS131A* γH2A (3; red), and Δ*dim-5* γH2A (4; red). (**C**) From

outside moving toward the center, genes (black) and repeats (red) are shown, followed by histograms depicting enrichment patterns of wildtype H3K9me3 (1; blue), wildtype γH2A (2; red), *hH2AS131A.*

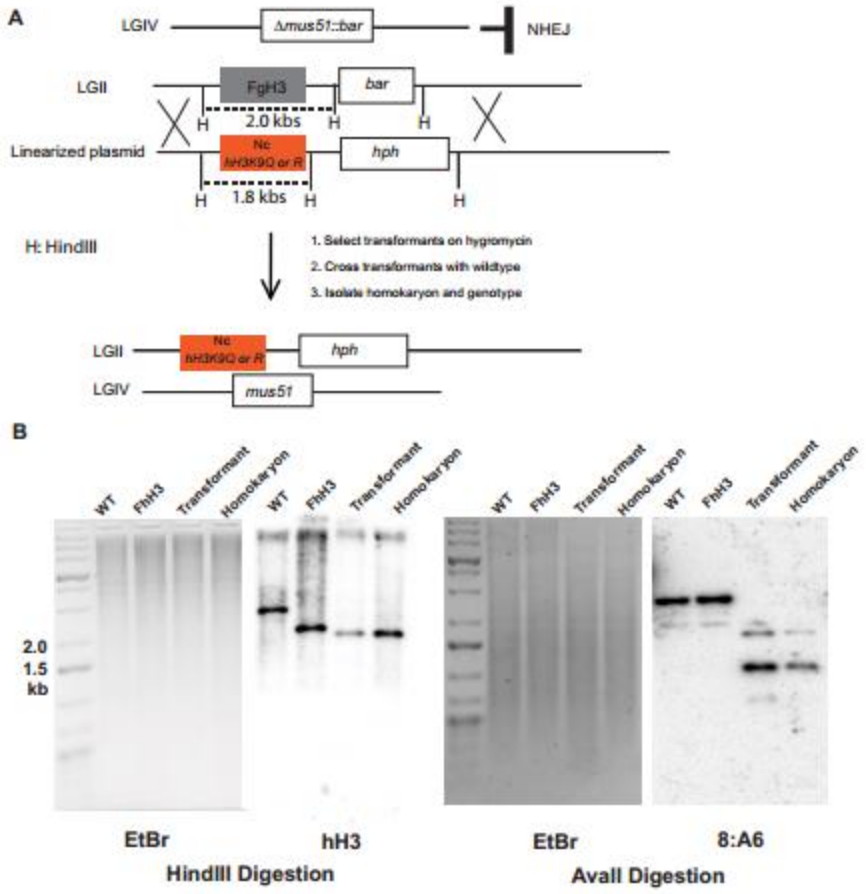

Figure S2.3 Strategy to introduce H3K9 substitution alleles into the native *hH3* locus. (**A**) A schematic diagram of experimental procedure is shown. The recipient Neurospora strain contains H3 coding sequence from *Fusarium graminearum* at the Neurospora hH3 locus and a deletion of the Neurospora *mus-51* gene. The DNA sequence of Fg *hH3* is different from Neurospora *hH3*, and thereby prevents recombination within coding sequence. Thus, most transformants are the result of a complete replacement of the Fg hH3 sequence with the engineered *hH3* allele and the 3' hygromycin-resistance cassette. (**B**) Genotyping by Southern blot. Genomic DNA was digestedby the indicated restriction enzymes overnight and run on 0.8% DNA gel. DNA was transfered to aNylon membrane and crosslinked by UV. Probes specific for hH3 was used to

confirm single-copyinsertion of hH3 in genome and probes for 8:A6 was used to test for DNA methylation at this heterochromatin locus.

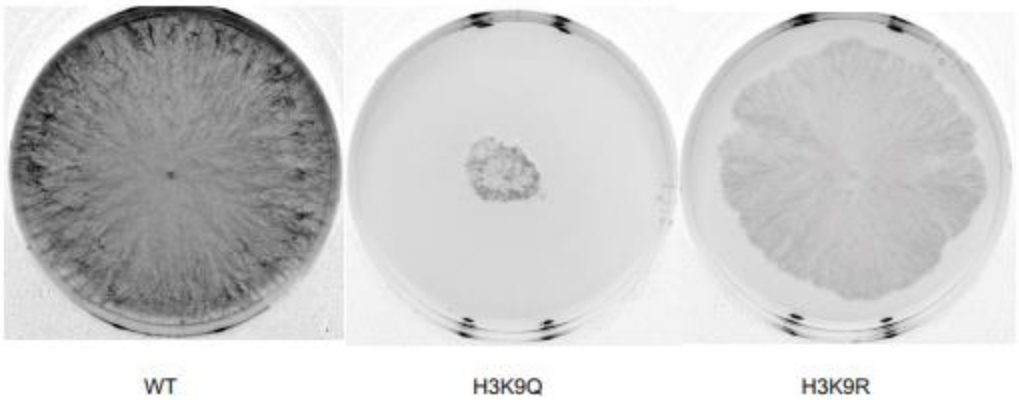

Figure S2.4 Growth of H3K9 substitution mutants on Vogel's minimal media. Conidia were spotted in the center of the plate and grown at 32 ˚C for 30 hrs. Pictures were taken using the FluorChem E Imager.

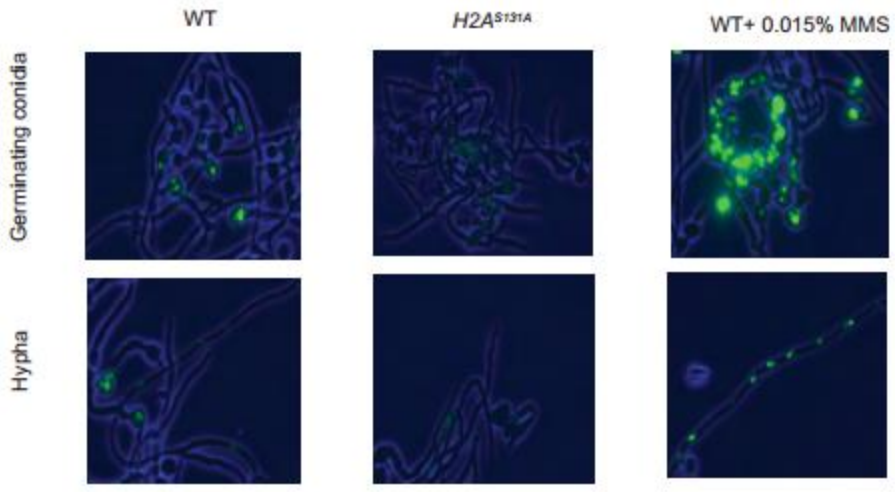

Figure S2.5 γH2A is induced in wildtype nuclei after induction with MMS Strains. Strains were grown in VMM for 15 hrs at 32 °C. MMS was added to yield a final concentration of 0.015%, and cells were grown for an additional 3 hours before fixation. Immunofluorescence analysis of γH2A revealed induction following MMS treatment in the wildype cells.

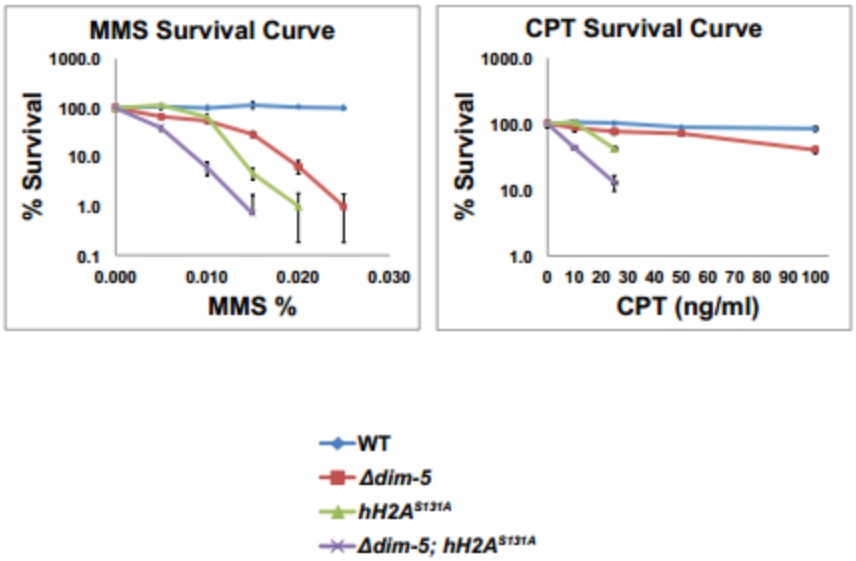

Figure S2.6. *Δdim-5; hH2A*^{S131A} double mutants exhibit increased sensitivity to DNA damaging agents. Spores were plated on media with increasing concentrations of genotoxic agent (MMS or camptothecin) and % Survival was determined as the number of colony forming units.

Table S2.1

Strains used in this study

Strain	Genotype	Source/reference
S2	Wildtype	FGSC# 2489
S132	*Δdim-5::bar+*	Reference # 15
S303	*hH3::hH3K9Q::hph+*	This study
S304	*hH3::hH3K9R::hph+*	This study
S181	*Δhpo-1::hph+*	FGSC #14522
S297	Δhda-1::hph+	FGSC #12003
S289	*hH2A::hH2AS131A::hph+*	S. Hatakeyamaand S. Tanaka; reference #66
S300	*his-3::hH1-dTomato*	P. Phatale and M. Freitag, in preparation
S301	*Δdim-5::bar+;his-3::hH1-dTomato*	This study
NMF679	*ΔhH3::FghH3::bar+; Δmus-51::bar+*	This study

Table S2.2

Primers used in this study

Primer Name	Sequence
8A6 5' FP2	CAATGGGCGAAAGATATAC
8A6 5' RP2	CCTTATAACCCAGACCTTCC
9e1 5' FP1	GAAGCTCTCGAACTATGTAAA
9e1 5' RP1	TCGCTATATTACCCAACAGG
Histone H4 5' FP2	CACACTTCACTTGGTCGCA
Histone H4 5' RP2	ATGACCCCTTGATGTGATGTA
Forward Primer for mid CDS of cfp gene	TGGGGACAAGTTAGCTCCGATG
Reverse Primer for mid CDS of cfp gene	ATCCGACCGTGCTGTAGTCGTT
Forward primer H3(K9Q)	CAGACCGCCCGCCAGTCCACCGGTGGCAAGGCCCCCCGTAAG
Reverse primer H3(K9Q)	CACCGGTGGACTGGCGGGCGGTCTGCTTAGTGCGGGCCATTGTG
Forward primer H3(K9R)	CAGACCGCCCGCCGCTCCACCGGTGGCAAGGCCCCCCGTAAG
Reverse primer H3(K9R)	CACCGGTGGAGCGGCGGGCGGTCTGCTTAGTGCGGGCCATTGTG
90-1 FP	CTAATCGGCTGGCTAGGAGAAG
90-1 RP	GACAACGAAACAAGCGACTCG
90-2 FP	GACCATGGCATTGTAGAGGTATG
90-2 RP	TACAAGTGCTTGCAAAACTAACC
90-3 FP	CTCTAAACCTTCTAATTATTCCATATACAC
90-3 RP	TTATACTAAGGAATTTAACCTATTGTACG
230-1 FP	GTATGGGGTTGGCGTGGTG
230-1 RP	GGGCACACAAGGACTGTTTACC
230-2 FP	TCCTACACACCCCTACAAACTAAC
230-2 RP	GAAGGATATCCCCTGGTCAAAC
230-3 FP	GAATTAGTAAGTTGGGTAATATTGTACG
230-3 RP	CCAAAAACATAATAGGCACAATTC
Cen VII probe FP	CTATAACTTAAATAGACCGCGGAG
Cen VII probe RP	TTTGAAAACTACTATAATACTCCATTTTAC
8:G3 probe FP1	GCGAGATTGAGATGTGAATGT
8:G3 probe RP2	CCAAAAAGAAGGGATTAGCTACC
9:E1 probe FP1	GAAGCTCTCGAACTATGTAAA
9:E1 probe RP2	GAGACAATCAGGTATAAGACCAG
H3 probe	GAAGTCCTGGGCAATCTC
H3 seq primer	TCCGCACATACATAAACCTCG
H3 seq primer 2	CTTCTAGTCATCAACCAGTC

Table S2.3

Genomic locations of H3K9me3-enriched domains identified by R-seg software.

Peak #	Contig	Peak Start	Peak Stop
1	Supercontig_12.1	0	1500
2	Supercontig_12.1	21000	34500
3	Supercontig_12.1	62700	89400
4	Supercontig_12.1	199200	208800
5	Supercontig_12.1	266400	289200
6	Supercontig_12.1	384000	385500
7	Supercontig_12.1	669900	697200
8	Supercontig_12.1	872100	925200
9	Supercontig_12.1	1182000	1186500
10	Supercontig_12.1	1219200	1229700
11	Supercontig_12.1	1337100	1350000
12	Supercontig_12.1	2273100	2343000
13	Supercontig_12.1	2381400	2404800
14	Supercontig_12.1	3062100	3065700
15	Supercontig_12.1	3378300	3378900
16	Supercontig_12.1	3476400	3495600
17	Supercontig_12.1	3552600	3566400
18	Supercontig_12.1	3579300	3580500
19	Supercontig_12.1	3595200	3638400
20	Supercontig_12.1	3640500	3664500
21	Supercontig_12.1	3679800	3698100
22	Supercontig_12.1	3699900	3709200
23	Supercontig_12.1	3714000	3730200
24	Supercontig_12.1	3735000	3972900
25	Supercontig_12.1	3974400	3987000
26	Supercontig_12.1	4005000	4007400
27	Supercontig_12.1	4009500	4040700
28	Supercontig_12.1	4042800	4098900
29	Supercontig_12.1	4162200	4167000
30	Supercontig_12.1	4169700	4195800
31	Supercontig_12.1	4212600	4214700
32	Supercontig_12.1	4314000	4356000
33	Supercontig_12.1	4375500	4377000
34	Supercontig_12.1	4531200	4544400
35	Supercontig_12.1	4878300	4883100
36	Supercontig_12.1	4923300	4925400

37	Supercontig_12.1	5006400	5010900
38	Supercontig_12.1	5078100	5082600
39	Supercontig_12.1	5262900	5265300
40	Supercontig_12.1	5317500	5340300
41	Supercontig_12.1	5394600	5400300
42	Supercontig_12.1	5481900	5499900
43	Supercontig_12.1	5529600	5545500
44	Supercontig_12.1	5734500	5773200
45	Supercontig_12.1	5805000	5808900
46	Supercontig_12.1	5919600	5944800
47	Supercontig_12.1	5955000	5977200
48	Supercontig_12.1	6197100	6200400
49	Supercontig_12.1	6249300	6262800
50	Supercontig_12.1	6298200	6330000
51	Supercontig_12.1	6331200	6333600
52	Supercontig_12.1	6383100	6458700
53	Supercontig_12.1	6469800	6474600
54	Supercontig_12.1	6501600	6505200
55	Supercontig_12.1	6520800	6528900
56	Supercontig_12.1	6600000	6601200
57	Supercontig_12.1	6998100	7002900
58	Supercontig_12.1	7373400	7374000
59	Supercontig_12.1	7423500	7427100
60	Supercontig_12.1	7506600	7511700
61	Supercontig_12.1	7710900	7712700
62	Supercontig_12.1	8226900	8267400
63	Supercontig_12.1	8279100	8293200
64	Supercontig_12.1	8893800	8895300
65	Supercontig_12.1	8991900	9000300
66	Supercontig_12.1	9163200	9175200
67	Supercontig_12.1	9286800	9337500
68	Supercontig_12.1	9358500	9360000
69	Supercontig_12.1	9406800	9408000
70	Supercontig_12.1	9481200	9515400
71	Supercontig_12.1	9697500	9701100
72	Supercontig_12.1	9705600	9758700
73	Supercontig_12.1	9772200	9798900
74	Supercontig_12.2	0	9000
75	Supercontig_12.2	12900	16500
76	Supercontig_12.2	108300	147600
77	Supercontig_12.2	390600	401100

78	Supercontig_12.2	516000	518400
79	Supercontig_12.2	572400	577500
80	Supercontig_12.2	684600	688500
81	Supercontig_12.2	699900	708300
82	Supercontig_12.2	874200	883200
83	Supercontig_12.2	1016100	1020900
84	Supercontig_12.2	1066200	1077000
85	Supercontig_12.2	1093500	1151400
86	Supercontig_12.2	1155000	1366500
87	Supercontig_12.2	1437000	1443000
88	Supercontig_12.2	1720500	1734600
89	Supercontig_12.2	1989300	2002200
90	Supercontig_12.2	2113200	2171100
91	Supercontig_12.2	2231400	2233800
92	Supercontig_12.2	2790900	2791500
93	Supercontig_12.2	2795400	2796300
94	Supercontig_12.2	2848500	2853600
95	Supercontig_12.2	2902500	2921400
96	Supercontig_12.2	3245700	3248100
97	Supercontig_12.2	3302700	3321600
98	Supercontig_12.2	3366000	3388500
99	Supercontig_12.2	3493200	3503100
100	Supercontig_12.2	3601800	3712800
101	Supercontig_12.2	3888600	3936600
102	Supercontig_12.2	4098300	4121400
103	Supercontig_12.2	4138500	4146000
104	Supercontig_12.2	4152600	4159200
105	Supercontig_12.2	4178400	4179600
106	Supercontig_12.2	4205700	4209600
107	Supercontig_12.2	4241400	4262700
108	Supercontig_12.2	4344600	4359900
109	Supercontig_12.2	4469700	4478700
110	Supercontig_12.20	0	1500
111	Supercontig_12.3	0	9600
112	Supercontig_12.3	61500	78300
113	Supercontig_12.3	132900	147900
114	Supercontig_12.3	180600	189000
115	Supercontig_12.3	267300	268800
116	Supercontig_12.3	301800	327900
117	Supercontig_12.3	346800	381300
118	Supercontig_12.3	430500	448500

119	Supercontig_12.3	474300	486600
120	Supercontig_12.3	563700	568200
121	Supercontig_12.3	672300	673200
122	Supercontig_12.3	683400	965700
123	Supercontig_12.3	1041900	1059600
124	Supercontig_12.3	1252200	1274700
125	Supercontig_12.3	1339800	1346400
126	Supercontig_12.3	1386600	1390200
127	Supercontig_12.3	1702200	1749900
128	Supercontig_12.3	1814400	1817100
129	Supercontig_12.3	2184900	2237100
130	Supercontig_12.3	2288400	2296500
131	Supercontig_12.3	2423400	2444700
132	Supercontig_12.3	2759700	2763600
133	Supercontig_12.3	2820900	2833500
134	Supercontig_12.3	2880900	2891100
135	Supercontig_12.3	2965500	2973900
136	Supercontig_12.3	3518400	3522000
137	Supercontig_12.3	3555600	3560400
138	Supercontig_12.3	3577800	3579000
139	Supercontig_12.3	4073100	4095900
140	Supercontig_12.3	4255200	4282200
141	Supercontig_12.3	4527900	4532700
142	Supercontig_12.3	4578300	4596900
143	Supercontig_12.3	4828200	4857300
144	Supercontig_12.3	5045700	5050500
145	Supercontig_12.3	5062200	5088600
146	Supercontig_12.3	5207100	5214900
147	Supercontig_12.3	5271300	5274600
148	Supercontig_12.4	0	1800
149	Supercontig_12.4	36600	47400
150	Supercontig_12.4	113400	141600
151	Supercontig_12.4	363300	373500
152	Supercontig_12.4	440100	444600
153	Supercontig_12.4	445200	455400
154	Supercontig_12.4	874200	1088700
155	Supercontig_12.4	1107000	1112100
156	Supercontig_12.4	1125000	1174200
157	Supercontig_12.4	1272900	1275300
158	Supercontig_12.4	1417800	1420500
159	Supercontig_12.4	1443000	1484700

160	Supercontig_12.4	1697100	1699800
161	Supercontig_12.4	1761000	1762200
162	Supercontig_12.4	1880700	1932600
163	Supercontig_12.4	2018100	2051400
164	Supercontig_12.4	2336100	2379600
165	Supercontig_12.4	2388300	2393400
166	Supercontig_12.4	2544900	2547600
167	Supercontig_12.4	2608200	2623200
168	Supercontig_12.4	2660400	2665200
169	Supercontig_12.4	2710500	2714400
170	Supercontig_12.4	2718000	2738100
171	Supercontig_12.4	2997000	2999700
172	Supercontig_12.4	3052200	3083700
173	Supercontig_12.4	3743100	3770400
174	Supercontig_12.4	4031400	4064100
175	Supercontig_12.4	4167900	4180500
176	Supercontig_12.4	4230600	4241100
177	Supercontig_12.4	4250100	4301700
178	Supercontig_12.4	4386900	4389600
179	Supercontig_12.4	4448100	4459800
180	Supercontig_12.4	4481400	4484400
181	Supercontig_12.4	4625100	4660500
182	Supercontig_12.4	4768800	4772700
183	Supercontig_12.4	5017500	5038500
184	Supercontig_12.4	5209500	5249400
185	Supercontig_12.4	5307900	5332200
186	Supercontig_12.4	5847600	5848800
187	Supercontig_12.4	5853000	5865600
188	Supercontig_12.4	5871600	5878800
189	Supercontig_12.4	5887800	5889300
190	Supercontig_12.4	5914200	5928600
191	Supercontig_12.4	5929800	5937600
192	Supercontig_12.4	5950800	6000600
193	Supercontig_12.5	0	19200
194	Supercontig_12.5	146400	147900
195	Supercontig_12.5	176700	196800
196	Supercontig_12.5	254400	266700
197	Supercontig_12.5	492900	508500
198	Supercontig_12.5	580500	615000
199	Supercontig_12.5	780900	796800
200	Supercontig_12.5	851100	856200

201	Supercontig_12.5	891000	1219200
202	Supercontig_12.5	1224000	1228200
203	Supercontig_12.5	1300800	1311900
204	Supercontig_12.5	1428600	1433400
205	Supercontig_12.5	1689300	1701900
206	Supercontig_12.5	1752900	1767900
207	Supercontig_12.5	1989900	1992600
208	Supercontig_12.5	2204400	2208300
209	Supercontig_12.5	2277900	2282400
210	Supercontig_12.5	2505600	2507100
211	Supercontig_12.5	2593500	2625900
212	Supercontig_12.5	2658900	2660700
213	Supercontig_12.5	2810700	2812200
214	Supercontig_12.5	2832600	2833500
215	Supercontig_12.5	3432300	3447900
216	Supercontig_12.5	3850800	3853200
217	Supercontig_12.5	3906900	3932100
218	Supercontig_12.5	4033200	4065900
219	Supercontig_12.5	4092900	4095600
220	Supercontig_12.5	4159200	4170900
221	Supercontig_12.5	4235100	4249500
222	Supercontig_12.5	4441500	4472700
223	Supercontig_12.5	4506600	4520100
224	Supercontig_12.5	4782900	4800600
225	Supercontig_12.5	5227200	5237400
226	Supercontig_12.5	5406300	5420700
227	Supercontig_12.5	5655900	5697600
228	Supercontig_12.5	5699400	5713500
229	Supercontig_12.5	5850300	5851800
230	Supercontig_12.5	5891100	5917200
231	Supercontig_12.5	5980500	6021900
232	Supercontig_12.5	6066900	6081600
233	Supercontig_12.5	6104400	6112800
234	Supercontig_12.5	6139800	6152100
235	Supercontig_12.5	6178200	6191100
236	Supercontig_12.5	6389100	6392100
237	Supercontig_12.5	6433800	6436200
238	Supercontig_12.6	0	1800
239	Supercontig_12.6	95700	99900
240	Supercontig_12.6	105000	120600
241	Supercontig_12.6	268800	275400

242	Supercontig_12.6	361500	391500
243	Supercontig_12.6	432900	444600
244	Supercontig_12.6	501300	506100
245	Supercontig_12.6	555900	560700
246	Supercontig_12.6	1069500	1088400
247	Supercontig_12.6	1171800	1193400
248	Supercontig_12.6	1329300	1339800
249	Supercontig_12.6	1756200	1760700
250	Supercontig_12.6	1765800	1777200
251	Supercontig_12.6	1794600	1824000
252	Supercontig_12.6	1843200	1865700
253	Supercontig_12.6	1867800	1874400
254	Supercontig_12.6	1904700	1908600
255	Supercontig_12.6	1935000	1958700
256	Supercontig_12.6	1983300	1991100
257	Supercontig_12.6	2031600	2032800
258	Supercontig_12.6	2384100	2387700
259	Supercontig_12.6	2419800	2423700
260	Supercontig_12.6	2724300	2747400
261	Supercontig_12.6	2783700	3080700
262	Supercontig_12.6	3237000	3240900
263	Supercontig_12.6	3334800	3339300
264	Supercontig_12.6	3406800	3415500
265	Supercontig_12.6	3415800	3420900
266	Supercontig_12.6	3488700	3493200
267	Supercontig_12.6	3507000	3538200
268	Supercontig_12.6	3630900	3645900
269	Supercontig_12.6	3781500	3794400
270	Supercontig_12.6	4010700	4020300
271	Supercontig_12.6	4067100	4071000
272	Supercontig_12.6	4162500	4218300
273	Supercontig_12.7	0	1800
274	Supercontig_12.7	49200	51000
275	Supercontig_12.7	78600	83400
276	Supercontig_12.7	135600	153000
277	Supercontig_12.7	185700	193200
278	Supercontig_12.7	259500	264300
279	Supercontig_12.7	273900	292800
280	Supercontig_12.7	326400	352500
281	Supercontig_12.7	502200	525900
282	Supercontig_12.7	610200	624000

283	Supercontig_12.7	810600	818100
284	Supercontig_12.7	890400	909600
285	Supercontig_12.7	1007400	1028100
286	Supercontig_12.7	1039500	1079400
287	Supercontig_12.7	1116900	1149900
288	Supercontig_12.7	1161900	1166700
289	Supercontig_12.7	1268400	1283400
290	Supercontig_12.7	1318500	1344600
291	Supercontig_12.7	1433700	1445400
292	Supercontig_12.7	1628700	1629900
293	Supercontig_12.7	1767300	1769700
294	Supercontig_12.7	1823100	1835700
295	Supercontig_12.7	1877400	1882200
296	Supercontig_12.7	2066100	2070000
297	Supercontig_12.7	2074800	2105400
298	Supercontig_12.7	2122800	2125200
299	Supercontig_12.7	2134500	2483400
300	Supercontig_12.7	2494200	2506500
301	Supercontig_12.7	2523300	2536500
302	Supercontig_12.7	2568900	2569500
303	Supercontig_12.7	2576100	2579400
304	Supercontig_12.7	2796600	2811300
305	Supercontig_12.7	2920200	2931900
306	Supercontig_12.7	3252000	3253800
307	Supercontig_12.7	3368100	3375000
308	Supercontig_12.7	3406200	3440700
309	Supercontig_12.7	3445800	3449100
310	Supercontig_12.7	3677700	3703800
311	Supercontig_12.7	4203300	4216500
312	Supercontig_12.7	4235400	4255200
313	Supercontig_12.8	0	79800
314	Supercontig_12.8	81300	192300
315	Supercontig_12.9	0	142500
316	Supercontig_12.10	0	125400
317	Supercontig_12.11	0	31500
318	Supercontig_12.12	0	19500
319	Supercontig_12.13	0	13500
320	Supercontig_12.14	0	11400
321	Supercontig_12.15	0	7800
322	Supercontig_12.15	8100	9300
323	Supercontig_12.16	0	9000

324	Supercontig_12.17	0	6600
325	Supercontig_12.18	0	6300
326	Supercontig_12.19	0	4800

References

1. **Grewal SI, Jia S.** 2007. Heterochromatin revisited. Nat Rev Genet **8:**35-46.

2. **McMurray CT.** 2010. Mechanisms of trinucleotide repeat instability during human development. Nat Rev Genet **11:**786-799.

3. **Lopez Castel A, Cleary JD, Pearson CE.** 2010. Repeat instability as the basis for human diseases and as a potential target for therapy. Nat Rev Mol Cell Biol **11:**165-170.

4. **Peng J, Karpen G.** 2008. Epigenetic regulation of heterochromatic DNA stability. Current Opinion in Genetics & Development**:**8.

5. **Mirkin EV, Mirkin SM.** 2007. Replication fork stalling at natural impediments. Microbiol Mol Biol Rev **71:**13-35.

6. **Mirkin SM.** 2006. DNA structures, repeat expansions and human hereditary disorders. Current opinion in structural biology **16:**351-358.

7. **Thompson SL, Compton DA.** 2011. Chromosomes and cancer cells. Chromosome Res **19:**433-444.

8. **Dillon LW, Burrow AA, Wang YH.** 2010. DNA instability at chromosomal fragile sites in cancer. Current genomics **11:**326-337.

9. **Hoskins RA, Carlson JW, Kennedy C, Acevedo D, Evans-Holm M, Frise E, Wan KH, Park S, Mendez-Lago M, Rossi F, Villasante A, Dimitri P, Karpen GH, Celniker SE.** 2007. Sequence finishing and mapping of *Drosophila melanogaster* heterochromatin. Science **316:**1625-1628.

10. **Rabinowicz PD, Bennetzen JL.** 2006. The maize genome as a model for efficient sequence analysis of large plant genomes. Current opinion in plant biology **9:**149-156.

11. **Galagan JE, Calvo SE, Borkovich KA, Selker EU, Read ND, Jaffe D, FitzHugh W, Ma LJ, Smirnov S, Purcell S, Rehman B, Elkins T, Engels R, Wang S, Nielsen CB, Butler J, Endrizzi M, Qui D, Ianakiev P, Bell-Pedersen D, Nelson MA, Werner-Washburne M, Selitrennikoff CP, Kinsey JA, Braun EL, Zelter A, Schulte U, Kothe GO, Jedd G, Mewes W, Staben C, Marcotte E, Greenberg D, Roy A, Foley K, Naylor J, Stange-Thomann N, Barrett R, Gnerre S, Kamal M, Kamvysselis M, Mauceli E, Bielke C, Rudd S, Frishman D, Krystofova S, Rasmussen C, Metzenberg RL, Perkins DD, Kroken S, Cogoni C, Macino G, Catcheside D, Li W, Pratt RJ, Osmani SA, DeSouza CP, Glass L, Orbach MJ, Berglund JA, Voelker R, Yarden O, Plamann M, Seiler S, Dunlap J, Radford A, Aramayo R, Natvig DO, Alex LA, Mannhaupt G, Ebbole DJ, Freitag M, Paulsen I, Sachs MS, Lander ES, Nusbaum C, Birren B.** 2003. The genome sequence of the filamentous fungus *Neurospora crassa*. Nature **422:**859-868.

12. **Lander ES, Linton LM, Birren B, Nusbaum C, Zody MC, Baldwin J, Devon K, Dewar K, Doyle M, FitzHugh W, Funke R, Gage D, Harris K, Heaford A, Howland J, Kann L, Lehoczky J, LeVine R, McEwan P, McKernan K, Meldrim J, Mesirov JP, Miranda C, Morris W, Naylor J, Raymond C, Rosetti M, Santos R, Sheridan A, Sougnez C, Stange-Thomann N, Stojanovic N, Subramanian A, Wyman D, Rogers J, Sulston J, Ainscough R, Beck S, Bentley D, Burton J, Clee C, Carter N, Coulson A, Deadman R, Deloukas P, Dunham A, Dunham I, Durbin R, French L, Grafham D, Gregory S, Hubbard T, Humphray S, Hunt A, Jones M, Lloyd C, McMurray A, Matthews L, Mercer S, Milne S, Mullikin JC, Mungall A, Plumb R, Ross M, Shownkeen R, Sims S, Waterston RH, Wilson RK, Hillier LW, McPherson JD, Marra MA, Mardis ER, Fulton LA, Chinwalla AT, Pepin KH, Gish WR, Chissoe SL, Wendl MC, Delehaunty KD, Miner TL, Delehaunty A, Kramer JB, Cook LL, Fulton RS, Johnson DL, Minx PJ, Clifton SW, Hawkins T, Branscomb E, Predki P, Richardson P, Wenning S, Slezak T, Doggett N, Cheng JF, Olsen A, Lucas S, Elkin C, Uberbacher E, Frazier M, Gibbs RA, Muzny DM, Scherer SE, Bouck JB, Sodergren EJ, Worley KC, Rives CM, Gorrell JH, Metzker ML, Naylor SL, Kucherlapati RS, Nelson DL, Weinstock GM, Sakaki Y, Fujiyama A, Hattori M, Yada T, Toyoda A, Itoh T, Kawagoe C, Watanabe H, Totoki Y, Taylor T, Weissenbach J, Heilig R, Saurin W, Artiguenave F, Brottier P, Bruls T, Pelletier E, Robert C, Wincker P, Smith DR, Doucette-Stamm L, Rubenfield M, Weinstock K, Lee HM, Dubois J, Rosenthal A, Platzer M, Nyakatura G, Taudien S, Rump A, Yang H, Yu J, Wang J, Huang G, Gu J, Hood L, Rowen L, Madan A, Qin S, Davis RW, Federspiel NA, Abola AP, Proctor MJ, Myers RM, Schmutz J, Dickson M, Grimwood J, Cox DR, Olson MV, Kaul R, Raymond C, Shimizu N, Kawasaki K, Minoshima S, Evans GA, Athanasiou M, Schultz R, Roe BA, Chen F, Pan H, Ramser J, Lehrach H, Reinhardt R, McCombie WR, de la Bastide M, Dedhia N, Blocker H, Hornischer K, Nordsiek G, Agarwala R, Aravind L, Bailey JA, Bateman A, Batzoglou S, Birney E, Bork P, Brown DG, Burge CB, Cerutti L, Chen HC, Church D, Clamp M, Copley RR, Doerks T, Eddy SR, Eichler EE, Furey TS, Galagan J, Gilbert JG, Harmon C, Hayashizaki Y, Haussler D, Hermjakob H, Hokamp K, Jang W, Johnson LS, Jones TA, Kasif S, Kaspryzk A, Kennedy S, Kent WJ, Kitts P, Koonin EV, Korf I, Kulp D, Lancet D, Lowe TM, McLysaght A, Mikkelsen T, Moran JV, Mulder N, Pollara VJ, Ponting CP, Schuler G, Schultz J, Slater G, Smit AF, Stupka E, Szustakowski J, Thierry-Mieg D, Thierry-Mieg J, Wagner L, Wallis J, Wheeler R, Williams A, Wolf YI, Wolfe KH, Yang SP, Yeh RF, Collins F, Guyer MS, Peterson J, Felsenfeld A, Wetterstrand KA, Patrinos A, Morgan MJ, de Jong P, Catanese JJ, Osoegawa K, Shizuya H, Choi S, Chen YJ.** 2001. Initial sequencing and analysis of the human genome. Nature **409:**860-921.

13. **Cleveland DW, Mao Y, Sullivan KF.** 2003. Centromeres and kinetochores: from epigenetics to mitotic checkpoint signaling. Cell **112:**407-421.

14. **Smith KM, Phatale PA, Sullivan CM, Pomraning KR, Freitag M.** 2011. Heterochromatin is required for normal distribution of *Neurospora crassa* CenH3. Mol Cell Biol **31:**2528-2542.

15. **Lewis ZA, Honda S, Khlafallah TK, Jeffress JK, Freitag M, Mohn F, Schubeler D, Selker EU.** 2009. Relics of repeat-induced point mutation direct heterochromatin formation in *Neurospora crassa*. Genome Res **19:**427-437.

16. **Lewis ZA, Adhvaryu KK, Honda S, Shiver AL, Knip M, Sack R, Selker EU.** 2010. DNA methylation and normal chromosome behavior in Neurospora depend on five components of a histone methyltransferase complex, DCDC. PLoS Genet **6:**e1001196.

17. **Lewis ZA, Adhvaryu KK, Honda S, Shiver AL, Selker EU.** 2010. Identification of DIM-7, a protein required to target the DIM-5 H3 methyltransferase to chromatin. Proc Natl Acad Sci U S A **107:**8310-8315.

18. **Xu H, Wang J, Hu Q, Quan Y, Chen H, Cao Y, Li C, Wang Y, He Q.** 2010. DCAF26, an adaptor protein of Cul4-based E3, is essential for DNA methylation in *Neurospora crassa*. PLoS Genet **6**.

19. **Zhao Y, Shen Y, Yang S, Wang J, Hu Q, Wang Y, He Q.** 2010. Ubiquitin ligase components Cullin4 and DDB1 are essential for DNA methylation in *Neurospora crassa*. J Biol Chem **285:**4355-4365.

20. **Allis CD, Berger SL, Cote J, Dent S, Jenuwien T, Kouzarides T, Pillus L, Reinberg D, Shi Y, Shiekhattar R, Shilatifard A, Workman J, Zhang Y.** 2007. New nomenclature for chromatin-modifying enzymes. Cell **131:**633-636.

21. **Freitag M, Hickey PC, Khlafallah TK, Read ND, Selker EU.** 2004. HP1 is essential for DNA methylation in Neurospora. Mol Cell **13:**427-434.

22. **Honda S, Lewis ZA, Shimada K, Fischle W, Sack R, Selker EU.** 2012. Heterochromatin protein 1 forms distinct complexes to direct histone deacetylation and DNA methylation. Nat Struct Mol Biol **19:**471-477.

23. **Honda S, Lewis ZA, Huarte M, Cho LY, David LL, Shi Y, Selker EU.** 2010. The DMM complex prevents spreading of DNA methylation from transposons to nearby genes in *Neurospora crassa*. Genes Dev **24:**443-454.

24. **Zaratiegui M, Castel SE, Irvine DV, Kloc A, Ren J, Li F, de Castro E, Marin L, Chang AY, Goto D, Cande WZ, Antequera F, Arcangioli B, Martienssen RA.** 2011. RNAi promotes heterochromatic silencing through replication-coupled release of RNA Pol II. Nature **479:**135-138.

25. **Cam HP, Sugiyama T, Chen ES, Chen X, FitzGerald PC, Grewal SI.** 2005. Comprehensive analysis of heterochromatin- and RNAi-mediated epigenetic control of the fission yeast genome. Nat Genet **37:**809-819.

26. **Peng JC, Karpen GH.** 2009. Heterochromatic genome stability requires regulators of histone H3 K9 methylation. PLoS Genet **5:**e1000435.

27. **Peng JC, Karpen GH.** 2007. H3K9 methylation and RNA interference regulate nucleolar organization and repeated DNA stability. Nat Cell Biol **9:**25-35.

28. **Paredes S, Maggert KA.** 2009. Ribosomal DNA contributes to global chromatin regulation. Proc Natl Acad Sci U S A **106:**17829-17834.

29. **Soria G, Almouzni G.** 2013. Differential contribution of HP1 proteins to DNA end resection and homology-directed repair. Cell Cycle **12:**422-429.

30. **Lee YH, Kuo CY, Stark JM, Shih HM, Ann DK.** 2013. HP1 promotes tumor suppressor BRCA1 functions during the DNA damage response. Nucleic Acids Res **41:**5784-5798.

31. **Bolderson E, Savage KI, Mahen R, Pisupati V, Graham ME, Richard DJ, Robinson PJ, Venkitaraman AR, Khanna KK.** 2012. Kruppel-associated Box (KRAB)-associated co-repressor (KAP-1) Ser-473 phosphorylation regulates heterochromatin protein 1beta (HP1-beta) mobilization and DNA repair in heterochromatin. J Biol Chem **287:**28122-28131.

32. **Chiolo I, Minoda A, Colmenares SU, Polyzos A, Costes SV, Karpen GH.** 2011. Double-strand breaks in heterochromatin move outside of a dynamic HP1a domain to complete recombinational repair. Cell **144:**732-744.

33. **Baldeyron C, Soria G, Roche D, Cook AJ, Almouzni G.** 2011. HP1alpha recruitment to DNA damage by p150CAF-1 promotes homologous recombination repair. J Cell Biol **193:**81-95.

34. **Luijsterburg MS, Dinant C, Lans H, Stap J, Wiernasz E, Lagerwerf S, Warmerdam DO, Lindh M, Brink MC, Dobrucki JW, Aten JA, Fousteri MI, Jansen G, Dantuma NP, Vermeulen W, Mullenders LH, Houtsmuller AB, Verschure PJ, van Driel R.** 2009. Heterochromatin protein 1 is recruited to various types of DNA damage. J Cell Biol **185:**577-586.

35. **Dinant C, Luijsterburg MS.** 2009. The emerging role of HP1 in the DNA damage response. Mol Cell Biol **29:**6335-6340.

36. **Quivy JP, Gerard A, Cook AJ, Roche D, Almouzni G.** 2008. The HP1-p150/CAF-1 interaction is required for pericentric heterochromatin replication and S-phase progression in mouse cells. Nat Struct Mol Biol **15:**972-979.

37. **Ayoub N, Jeyasekharan AD, Bernal JA, Venkitaraman AR.** 2008. HP1-beta mobilization promotes chromatin changes that initiate the DNA damage response. Nature **453:**682-686.

38. **Liu H, Galka M, Mori E, Liu X, Lin YF, Wei R, Pittock P, Voss C, Dhami G, Li X, Miyaji M, Lajoie G, Chen B, Li SS.** 2013. A method for systematic mapping of protein lysine methylation identifies functions for HP1beta in DNA damage response. Mol Cell **50:**723-735.

39. **Dickey JS, Redon CE, Nakamura AJ, Baird BJ, Sedelnikova OA, Bonner WM.** 2009. H2AX: functional roles and potential applications. Chromosoma **118:**683-692.

40. **Downs JA, Lowndes NF, Jackson SP.** 2000. A role for *Saccharomyces cerevisiae* histone H2A in DNA repair. Nature **408:**1001-1004.

41. **Paull TT, Rogakou EP, Yamazaki V, Kirchgessner CU, Gellert M, Bonner WM.** 2000. A critical role for histone H2AX in recruitment of repair factors to nuclear foci after DNA damage. Curr Biol **10:**886-895.

42. **Iacovoni JS, Caron P, Lassadi I, Nicolas E, Massip L, Trouche D, Legube G.** 2010. High-resolution profiling of gammaH2AX around DNA double strand breaks in the mammalian genome. The EMBO journal **29:**1446-1457.

43. **Szilard RK, Jacques PE, Laramee L, Cheng B, Galicia S, Bataille AR, Yeung M, Mendez M, Bergeron M, Robert F, Durocher D.** 2010. Systematic identification of fragile sites via genome-wide location analysis of gamma-H2AX. Nat Struct Mol Biol **17:**299-305.

44. **Rogakou EP, Pilch DR, Orr AH, Ivanova VS, Bonner WM.** 1998. DNA double-stranded breaks induce histone H2AX phosphorylation on serine 139. J Biol Chem **273:**5858-5868.

45. **Rozenzhak S, Mejia-Ramirez E, Williams JS, Schaffer L, Hammond JA, Head SR, Russell P.** 2010. Rad3 decorates critical chromosomal domains with gammaH2A to protect genome integrity during S-Phase in fission yeast. PLoS Genet **6:**e1001032.

46. **Davis RH.** 2000. Neurospora: Contributions of a Model Organism. Oxford: Oxford University Press.

47. **Pall ML.** 1993. The use of Ignite (Basta;glufosinate;phosphinothricin) to select transformants of bar-containing plasmids in Neurospora crassa. Fungal Genetics Newsletter **40:**58.

48. **Sambrook J, Russell DW.** 2001. Molecular cloning : a laboratory manual, 3rd ed. Cold Spring Harbor Laboratory Press, Cold Spring Harbor, N.Y.

49. **Liu H, Naismith JH.** 2008. An efficient one-step site-directed deletion, insertion, single and multiple-site plasmid mutagenesis protocol. BMC biotechnology **8:**91.

50. **Tamaru H, Selker EU.** 2001. A histone H3 methyltransferase controls DNA methylation in *Neurospora crassa*. Nature **414:**277-283.

51. **Adhvaryu KK, Berge E, Tamaru H, Freitag M, Selker EU.** 2011. Substitutions in the amino-terminal tail of neurospora histone H3 have varied effects on DNA methylation. PLoS Genet **7:**e1002423.

52. **Margolin BS, Freitag M, Selker EU.** 1997. Improved plasmids for gene targeting at the his-3 locus of *Neurospora crassa* by electroporation. Fungal Genetics Newsletter **44:**34-36.

53. **Pomraning KR, Smith KM, Freitag M.** 2009. Genome-wide high throughput analysis of DNA methylation in eukaryotes. Methods **47:**142-150.

54. **Honda S, Selker EU.** 2008. Direct interaction between DNA methyltransferase DIM-2 and HP1 is required for DNA methylation in *Neurospora crassa*. Mol Cell Biol **28:**6044-6055.

55. **Miao VP, Freitag M, Selker EU.** 2000. Short TpA-rich segments of the zeta-eta region induce DNA methylation in *Neurospora crassa*. J Mol Biol **300:**249-273.

56. **Langmead B, Salzberg SL.** 2012. Fast gapped-read alignment with Bowtie 2. Nature methods **9:**357-359.

57. **Thorvaldsdottir H, Robinson JT, Mesirov JP.** 2013. Integrative Genomics Viewer (IGV): high-performance genomics data visualization and exploration. Briefings in bioinformatics **14:**178-192.

58. **Robinson JT, Thorvaldsdottir H, Winckler W, Guttman M, Lander ES, Getz G, Mesirov JP.** 2011. Integrative genomics viewer. Nature biotechnology **29:**24-26.

59. **Price AL, Jones NC, Pevzner PA.** 2005. De novo identification of repeat families in large genomes. Bioinformatics **21 Suppl 1:**i351-358.

60. **Kent WJ.** 2002. BLAT--the BLAST-like alignment tool. Genome Res **12:**656-664.

61. **Hebenstreit D, Gu M, Haider S, Turner DJ, Lio P, Teichmann SA.** 2011. EpiChIP: gene-by-gene quantification of epigenetic modification levels. Nucleic Acids Res **39:**e27.

62. **Quinlan AR, Hall IM.** 2010. BEDTools: a flexible suite of utilities for comparing genomic features. Bioinformatics **26:**841-842.

63. **Momany M.** 2001. Using Microscopy to explore the duplication cycle, p. 119-125. *In* Talbot N (ed.), Molecular and Cell Biology of Filamentous Fungi: A Practical Approach. Oxford University Press, Oxford

64. **Scott JH, Schekman R.** 1980. Lyticase: endoglucanase and protease activities that act together in yeast cell lysis. Journal of bacteriology **142:**414-423.

65. **Ward IM, Chen J.** 2001. Histone H2AX is phosphorylated in an ATR-dependent manner in response to replicational stress. The Journal of biological chemistry **276:**47759-47762.

66. **Wakabayashi M, Saijyou N, Hatakeyama S, Inoue H, Tanaka S.** 2012. Neurospora mrc1 homologue is involved in replication stability and is required for normal cell growth and chromosome integrity in mus-9 and mus-21 mutants. Fungal Genet Biol **49:**263-270.

67. **Wakabayashi M, Ishii C, Hatakeyama S, Inoue H, Tanaka S.** 2010. ATM and ATR homologes of Neurospora crassa are essential for normal cell growth and maintenance of chromosome integrity. Fungal Genet Biol **47:**809-817.

68. **Oyola SO, Otto TD, Gu Y, Maslen G, Manske M, Campino S, Turner DJ, Macinnis B, Kwiatkowski DP, Swerdlow HP, Quail MA.** 2012. Optimizing Illumina next-generation sequencing library preparation for extremely AT-biased genomes. BMC genomics **13:**1.

69. **Aird D, Ross MG, Chen WS, Danielsson M, Fennell T, Russ C, Jaffe DB, Nusbaum C, Gnirke A.** 2011. Analyzing and minimizing PCR amplification bias in Illumina sequencing libraries. Genome Biol **12:**R18.

70. **Tamaru H, Zhang X, McMillen D, Singh PB, Nakayama J, Grewal SI, Allis CD, Cheng X, Selker EU.** 2003. Trimethylated lysine 9 of histone H3 is a mark for DNA methylation in *Neurospora crassa*. Nat Genet **34:**75-79.

71. **Selker EU, Tountas NA, Cross SH, Margolin BS, Murphy JG, Bird AP, Freitag M.** 2003. The methylated component of the *Neurospora crassa* genome. Nature **422:**893-897.

72. **Kitada T, Schleker T, Sperling AS, Xie W, Gasser SM, Grunstein M.** 2011. gammaH2A is a component of yeast heterochromatin required for telomere elongation. Cell Cycle **10:**293-300.

73. **Lee JH, Paull TT.** 2005. ATM activation by DNA double-strand breaks through the Mre11-Rad50-Nbs1 complex. Science **308:**551-554.

74. **Lee JH, Paull TT.** 2004. Direct activation of the ATM protein kinase by the Mre11/Rad50/Nbs1 complex. Science **304:**93-96.

75. **Byun TS, Pacek M, Yee MC, Walter JC, Cimprich KA.** 2005. Functional uncoupling of MCM helicase and DNA polymerase activities activates the ATR-dependent checkpoint. Genes Dev **19:**1040-1052.

76. **Zeman MK, Cimprich KA.** 2014. Causes and consequences of replication stress. Nat Cell Biol **16:**2-9.

77. **Kirkland JG, Kamakaka RT.** 2013. Long-range heterochromatin association is mediated by silencing and double-strand DNA break repair proteins. J Cell Biol **201:**809-826.

78. **Williams JS, Williams RS, Dovey CL, Guenther G, Tainer JA, Russell P.** 2010. gammaH2A binds Brc1 to maintain genome integrity during S-phase. EMBO J **29:**1136-1148.

79. **Li X, Liu K, Li F, Wang J, Huang H, Wu J, Shi Y.** 2012. Structure of C-terminal tandem BRCT repeats of Rtt107 protein reveals critical role in interaction with phosphorylated histone H2A during DNA damage repair. J Biol Chem **287:**9137-9146.

80. **Voineagu I, Narayanan V, Lobachev KS, Mirkin SM.** 2008. Replication stalling at unstable inverted repeats: interplay between DNA hairpins and fork stabilizing proteins. Proc Natl Acad Sci U S A **105:**9936-9941.

81. **Chicas A, Forrest EC, Sepich S, Cogoni C, Macino G.** 2005. Small interfering RNAs that trigger posttranscriptional gene silencing are not required for the histone H3 Lys9 methylation necessary for transgenic tandem repeat stabilization in *Neurospora crassa*. Mol Cell Biol **25:**3793-3801.

82. **Callen E, Di Virgilio M, Kruhlak MJ, Nieto-Soler M, Wong N, Chen HT, Faryabi RB, Polato F, Santos M, Starnes LM, Wesemann DR, Lee JE, Tubbs A, Sleckman BP, Daniel JA, Ge K, Alt FW, Fernandez-Capetillo O, Nussenzweig MC, Nussenzweig A.** 2013. 53BP1 mediates productive and mutagenic DNA repair through distinct phosphoprotein interactions. Cell **153:**1266-1280.

83. **Yan W, Shao Z, Li F, Niu L, Shi Y, Teng M, Li X.** 2011. Structural basis of gammaH2AX recognition by human PTIP BRCT5-BRCT6 domains in the DNA damage response pathway. FEBS letters **585:**3874-3879.

84. **Ichijima Y, Ichijima M, Lou Z, Nussenzweig A, Camerini-Otero RD, Chen J, Andreassen PR, Namekawa SH.** 2011. MDC1 directs chromosome-wide silencing of the sex chromosomes in male germ cells. Genes & development **25:**959-971.

85. **Zappulla DC, Maharaj AS, Connelly JJ, Jockusch RA, Sternglanz R.** 2006. Rtt107/Esc4 binds silent chromatin and DNA repair proteins using different BRCT motifs. BMC molecular biology **7:**40.

86. **Lee SY, Rozenzhak S, Russell P.** 2013. gammaH2A-binding protein Brc1 affects centromere function in fission yeast. Molecular and cellular biology **33:**1410-1416.

87. **Lee SY, Russell P.** 2013. Brc1 links replication stress response and centromere function. Cell cycle **12:**1665-1671.

88. **Li PC, Petreaca RC, Jensen A, Yuan JP, Green MD, Forsburg SL.** 2013. Replication fork stability is essential for the maintenance of centromere integrity in the absence of heterochromatin. Cell reports **3:**638-645.

89. **Lee CS, Lee K, Legube G, Haber JE.** 2014. Dynamics of yeast histone H2A and H2B phosphorylation in response to a double-strand break. Nat Struct Mol Biol **21:**103-109.

CHAPTER 3

PRC2 MODULATES THE CELLULAR RESPONSE TO GENOTOXIC STRESS IN *NEUROSPORA CRASSA*[2]

Takahiko Sasaki[*], Evelina Y. Basenko[*], Cameron Prybol, Rachel Burckhardt and Zachary A. Lewis

* These authors contributed equally to this work

[2] To be submitted to *Molecular Cell*

Abstract

Proper heterochromatin formation is required for normal growth and development in eukaryotes. Molecular components of heterochromatin include hypoacetylated histones, histone H3K9 methylation, heterochromatin protein-1 (HP1) and DNA methylation. In *Neurospora crassa*, H3K9me3 directs heterochromatin formation by recruiting multiple HP1-containing complexes that deacetylate histones and methylate cytosines. The Neurospora H3K9 methyltransferase, DCDC, is required for normal vegetative growth and is essential for meiosis. In addition, DCDC-deficient strains exhibit elevated γH2A and are hypersenstive to the DNA damaging agent MMS, linking defective heterochromatin to genotoxic stress. A number of human diseases are associated with mutations in heterochromatin components, but how heterochromatin disruption leads to defective growth is poorly defined. To understand the molecular consequences of heterochromatin disruption, we isolated a genetic suppressor of a DCDC-deficient strain and identified the causative mutation by combining Bulked Segregant Analysis with Illumina sequencing (BSA-seq). We found a mutation in the gene encoding EED, a component of the Polycomb Repressive Complex-2. In the absence of H3K9me3, H3K27me3 is redistributed to constitutive heterochromatin domains normally targeted by DCDC, suggesting that altered PRC2 activity leads to aberrant growth and genotoxic stress. Mutation of *set-7/kmt6,* encoding the PRC2 catalytic subunit, or introduction of an H3K27 missense mutation also suppressed the MMS-sensitivity phenotype of a DCDC-deficient strain. Moreover, strains lacking both SET-7/KMT1 and DIM-5/KMT1, the catalytic subunit of DCDC, grow at near wildtype rates and are able to undergo productive meiosis, in contrast to *dim-5/kmt1* single mutants. While most defects displayed by *dim-5/kmt1* are rescued by mutation of PRC2, strains lacking both H3K9me3 and H3K27me3 exhibit synthetic sensitivity to the topoisomerase I

inhibitor camptothecin. These data suggest that PRC2 modulates the cellular response to genotoxic stress.

Introduction

Modifications of histones and DNA partition genomes into discrete functional domains. Heterochromatin refers to highly condensed parts of the genome that are transcriptionally inert and rich in repeated DNA sequences (1). Failure to establish or maintain heterochromatin leads to catastrophic defects in chromosome segregation, DNA replication, and DNA repair, highlighting its functional importance (1, 2). At the molecular level heterochromatin domains are defined by hypoacetylated histones, histone H3K9 methylation (H3K9me), and DNA methylation (1). The model fungus *Neurospora crassa* shares these features with higher eukaryotes and is an established model to study the control and function of heterochromatin (3). In Neurospora the H3K9 methyltransferase DCDC (DIM-5,-7,-9, CUL4, DDB1, Complex) initiates heterochromatin formation at degenerate DNA repeat sequences that are products of the genome defense system RIP (repeat-induced point mutation) (4-6). DCDC tri-methylates H3K9 to create binding sites for multiple HP1-containing complexes, which in turn, direct methylation of cytosine bases in DNA and deacetylation of histones (7-9). As in other eukaryotes, heterochromatin formation is sufficient to silence transcription in *Neurospora*. Reporter genes flanked by RIP'd DNA are not expressed, and spreading of heterochromatin causes aberrant gene silencing in strains that lack DMM-1 (DNA methylation modulator-1) (10, 11). Together, heterochromatin domains comprise ~20% of the Neurospora genome and include structurally important loci such as the centromere (6).

In animals, plants, and some fungi, Polycomb (Pc) group proteins establish and maintain a second type of transcriptionally silent chromatin (12). In multicellular organisms Pc target sites are often referred to as facultative heterochromatin because these chromatin domains are transcriptionally repressed in some but not all cell lineages. Polycomb repressive complex-2 (PRC2) methylates H3K27, which in animals is bound by Polycomb Repressive Complex-1 (PRC1) to promote mitotically heritable gene silencing (12). Pc components are absent from the model yeasts *Saccharomyces cerevisiae* and *Schizosaccharyomyces pombe* and PRC1 appears to be absent from all fungi, but PRC2 is present in some fungi. Moreover, H3K27me3 is associated with transcriptional repression of large PRC2-target domains in *Neurospora*, *Fusarium graminearum* and *Cryptococcus neorformans* (13-15). This suggests that PRC2 is functionally equivalent in fungi, plants and animals. Thus, application of genetic approaches to study the Pc system in fungi can generate insights into the control and function of Pc components.

Although the Pc system is best known for its ability to repress developmentally regulated genes, recent studies in higher eukaryotes link H3K27 methylation to DNA replication and repair (16). In human cancer cells, PRC2 associates more stably with chromatin following oxidative DNA or UV-induced damage, and levels of both PRC2 and H3K27me3 are increased at induced double strand breaks (17-19). Moreover, knockdown of PRC2 increases sensitivity to ionizing radiation (19). It is possible that Pc proteins are recruited to silence transcription in the vicinity of a DNA lesion, but the precise roles of PRC2 and H3K27me3 in the DNA damage response are unclear.

Similarly, genome instability in heterochromatin-defective mutants suggests that heterochromatin components do not exclusively function to repress transcription. Replication fork stalling is observed in *S. pombe* heterochromatin domains (20), and $Clr4^{KMT1}$-deficient

mutants of *S. pombe* exhibit illegitimate mitotic recombination that is exacerbated by mutation of the replication fork protection complex (21, 22). In *Drosophila,* cytological studies revealed that H3K9me-deficient mutants exhibit spontaneous double strand breaks (DSBs) in heterochromatin, and it was proposed that this damage is due to defective DNA replication (2, 23-25). Mice lacking KMT1A (SUV39H1; Lysine (K) Methyltransferase 1) and KMT1B (SUV39H2) exhibit genome instability and high rates of lymphoma development (26, 27), and both KMT1 enzymes and HP1 proteins have been implicated in DNA repair in animals (28-37). These and other studies suggest that heterochromatin components have important roles during both DNA replication and DNA repair, but the heterochromatin-dependent mechanisms that maintain genome integrity are currently poorly defined.

Heterochromatin formation appears to be important for genome maintenance in *Neurospora* as well. H3K9 methylation is required for normal vegetative growth and for meiosis (5). DCDC-deficient mutants exhibit chromosome segregation defects and hypersensitivity to the DNA damaging agent MMS (Methyl methanesulfonate) (4), and mutants lacking the catalytic subunit of DCDC, *dim-5/kmt1* (*defective in methylation-5/lysine(K) methyltransferase-1*), exhibit increased rates of illegitimate recombination (38). In addition, *dim-5/kmt1* strains display induction and redistribution of the DNA damage marker γH2A during normal replicative growth (39). These data suggest that heterochromatin is critically important in *Neurospora*, but the cause of genotoxic stress and impaired growth in heterochromatin-defective mutants is not understood.

To understand the molecular consequences of heterochromatin depletion, we performed a genetic selection to identify suppressors of a DCDC-deficient strain. We identified a mutation in the PRC2 component *eed*. H3K9me3-deficient mutants exhibit redistribution of H3K27me3, leading to induction of PRC2 target genes. We show that gain of H3K27me3 in constitutive

heterochromatin domains is not compensatory for gene silencing, but rather, leads to growth defects and altered sensitivity to genotoxic agents. Our data suggest that PRC2 modulates the cellular response to genotoxic stress.

Materials and methods

Strains and growth media.

All Neurospora strains used in this study are listed in Table S3.1 Stains were grown at 32°C in Vogel's minimal medium (VMM) + 1.5% sucrose (40). Liquid cultures were shaken at 150 rpm. Crosses were performed on modified synthetic cross medium (40). For plating assays, Neurospora conidia were plated on VMM with 2.0% sorbose, 0.5% fructose, and 0.5% glucose. When relevant, plates included 200 µg/mL hygromycin or 400 µg/mL basta (41) or DNA damaging agents: methylmethane sulfonate (MMS; 0.025%), Etoposide (600ug/ml), Cisplatin (100ug/ml), Mitomycin C (60ug/ml), Bleomycin (0.15ug/ml), Camptothecin (CPT; 0.25ug/ml)..

Molecular analyses.

Neurospora transformation (42), DNA isolation (43), protein isolation, histone isolation and western blotting (9) were performed as previously described. Antibodies to γH2A-ChIP (Cat # ab15083, Abcam), H3K9me3 (Cat # 39161, Active Motif, USA), and H3K27 (Cat # 39535, Active motif), and RNA polymerase II CTD (Cat # MMS-126R, Covance) were used as indicated. Protein A/G beads (20 µl; Cat # sc-2003**,** Santa Cruz). ChIP-seq was performed as described (39).

Illumina sequencing.

For Illumina sequencing, ChIP-seq libraries were prepared using 10ng of immunoprecipitated DNA following the instructions supplied with Illumina Tru-seq ChIP-seq kits (Illumina Cat# FC-121-2002. RNA-seq libraries were prepared from 5ug total RNA. Ribosomal RNAs were depleted using the Epicentre yeast Ribo-zero kit and RNA libraries were generated with the Illumina Stranded RNA-seq kit PCR. For ChIP-seq, amplification was limited to 4-8 cycles to reduce PCR bias against A:T-rich DNA sequences (44). Illumina sequencing was performed using an Illumina Next-Seq Instrument at the University of Georgia Genomics Facility.

Data analysis.

Upon acceptance, Illumina sequence reads will be deposited into the NCBI short reads archive database. Short reads were mapped using bowtie2 (45) or TopHat for ChIP-seq or RNA-seq experiments, respectively, to the latest Neurospora genome annotation (version 12), available from the Neurospora genome database (46). Read numbers were counted for 25 base pair bins using igvtools, and the read density was visualized using the Integrated Genome Viewer available from the Broad website (47, 48). We used IGV to normalize data for total read number before plotting.

The HOMER software package (49) was used to identify H3K9me3 or H3K27me3 peaks and to construct histogram files to create heatmaps. We constructed a custom genome annotation file containing genes, repeats (39), H3K27me3 peaks, and H3K9me3 peaks and used HOMER to calculate FPKM values for each genomic feature or to construct heat maps of ChIP enrichment across H3K9me3 or H3K27me3 domains. HOMER “ghist” output was loaded into GENE-E

(http://www.broadinstitute.org/cancer/software/GENE-E/) to generate heat map images. To calculate normalized ChIP enrichment values (NCLS value) for each feature, we used EpiChIP software, which calculates enrichment values normalized for total read number and for length of the feature (50). Normalized H3K9me3, H3K4me3, and γH2A values for each feature were used to generate scatter plots and calculate Pearson's correlation coefficients in Microsoft Excel. FPKM values generated by HOMER were used to plot the Kernel Estimated Density for all features, genes, repeats, and H3K27me3 genes using R (http://www.r-project.org). When relevant, mapped reads were converted to bed format using bedtools software (51).

Results

dim-5 mutants exhibit hypersensitivity to the DNA damaging agent MMS, suggesting that the DIM-5^{KMT1} MTase is required for normal DNA replication or repair. We examined growth of the heterochromatin-defective mutants in the presence of additional DNA replication and repair inhibitors (**Figure 3.1A**). As controls, we included *mus-9*, lacking the Neurospora ATM homolog (52), and *mei-3*, lacking the homolog of the RAD51 required for homologous recombination (53). Elimination of DNA methylation did not impact growth on any of the tested genotoxic agents. When compared to wildtype, the deletion of genes encoding DCDC components DIM-5, DIM-7, and DIM-9 were hypersenstive to MMS, as previously described (4), and to other genotoxic agents including the topoisomerase II inhibitor etoposide, the topoisomerase I inhibitor Camptothecin, the interstrand cross-linking agent cisplatin, Mitomycin C, and Bleomycin, which are thought to cause oxidative damage and trigger double strand breaks. DCDC-cells were efficiently killed by low concentrations of MMS, whereas other agents only led to growth inhibition of *dim-5/kmt1*, *dim-7*, *dim-9*, and *hpo* strains. These strains showed

improved growth after prolonged incubation in the presence of these drugs (> 4 days), whereas growth of *mus-9* and *mei-3* did not improve. Mutants lacking the DCDC component CUL4 were more senstive to all genotoxic agents tested, which is expected given the established role of CUL4 in multiple complexes that regulate DNA replication and repair. The fact that heterochromatin-deficient mutants exhibit broad sensitivity to DNA damaging agents suggests that DCDC-deficient strains suffer from genotoxic stress, either due to defects in DNA repair or to failures during DNA replication. This conclusion is supported by our previous results that showed γH2A levels are elevated in the *dim-5* mutant.

Isolation and identification of a genetic suppressor of the *dim-9* mutant.

To understand how the absence of H3K9 methylation leads to genotoxic stress, we selected for genetic suppressors of a DCDC-deficient mutant. We mutagenized *dim-9* cells by exposure to UV light and plated cells on medium supplemented with 0.025% MMS. This concentration of MMS kills DCDC-deficient cells but not wildtype cells. MMS-resistant colonies were isolated and crossed to a wildtype strain (S1) to obtain homokaryons. A cross of one putative suppressor strain (*sup-24; suppressor-24*) yielded two classes of *dim-9* progeny in approximately equal numbers: MMS-tolerant and MMS-hypersensitive (**Figure 3.1B**). We quantified colony forming units to compare the level of MMS-sensitivity in wildtype, *dim-9*, and *dim-9; sup-24* strains and found that MMS-tolerance of *dim-9; sup-24* was similar to wildtype (**Figure 3.**1C). This suggested that a single mutation led to suppression of the *dim-9* MMS-hypersensitivity phenotype and that this mutation is unlinked to *dim-9*.

To identify the causative mutation, we performed bulked segregant analysis combined with Whole Genome Sequencing (BSA-seq) (54). We crossed a single *dim-9; sup-24*

homokaryon, generated in the Oak Ridge strain background (OR), to a polymorphic wildtype Neurospora strain (Mauriceville). Progeny were isolated and genotyped to identify *dim-9; sup-24* strains. We then isolated and pooled genomic DNA from 14 *dim-9; sup-24* progeny and sequenced the DNA in bulk. Analysis of the sequenced data revealed that regions on LGII and LGIV contained SNPs that were exclusively from the OR strain background and contained mutations (**Supplemental Figure 3.1**). The LGII region contained the *dim-9* deletion mutation. The region at the right end of Linkage Group IV contained a nonsense mutation in the gene encoding the single Neurospora EED homolog (**Figure 3.2A**). This mutation is predicted to introduce a stop codon in place of a tryptophan codon at position 252. We hereafter refer to this allele as *eed*$^{sup-24}$.

Neurospora EED is a component of PRC2 and is required for methylation of H3K27 (14). We therefore asked if H3K27 levels are altered in the *dim-9; eed*$^{sup-24}$ double mutant. We isolated total histones from wildtype, *dim-9*, and *dim-9*; *eed*$^{sup-24}$ strains and performed western blots using antibodies that recognize H3K9me3 and H3K27me3 (**Figure 3.2B**). As loading controls, we performed western blots with antibodies for H3K4me2 and stained total histones with coomassie blue. H3K9me3 was detected in wildtype but was absent in *dim-9* and *dim-9; eed*$^{sup-24}$ strains, demonstrating that the suppressor mutation is unable to restore H3K9 MTase activity in the *dim-9* background. Similarly, DNA methylation was absent from both *dim-9* and *dim-9; eed*$^{sup-24}$ strains (not shown). H3K27me3 was detected in wildtype and *dim-9* strains, but was not detected in the *dim-9; eed*$^{sup-24}$ double mutant, suggesting that *eed*$^{sup-24}$ allele encodes a non-functional protein. We detected a subtle increase in H3K27me3 levels in the *dim-9* strain. These data raised the possibility that PRC2 causes the MMS-sensitivity phenotype observed for DCDC-deficient mutants.

To test this, we crossed a *dim-5/kmt1* deletion strain to a *set-7/kmt6* deletion strain. The *dim-5/kmt1* and *set-7/kmt6* genes encode catalytic subunits of the DCDC H3K9 MTase and the PRC2 H3K27 MTase complex, respectively. We isolated 3 siblings of each genotype and determined the level of MMS-sensitivity for each strain by plating spores on increasing concentrations of the genotoxic agent (**Figure 3.2C**). Wildtype and *set-7/kmt6* displayed similar MMS-tolerance, whereas *dim-5/kmt1* was hypersensitive. In contrast, *dim-5/kmt1; set-7/kmt6* double mutant progeny displayed wildtype MMS-tolerance, confirming that elimination of PRC2 leads to genetic suppression of the MMS-hypersensitivity phenotype of DCDC-deficient mutants.

We next performed ChIP-seq to examine the distribution of H3K27me3 in wildtype and *dim-5/kmt1* mutant strains. As previously reported, H3K27me3 was localized to large chromatin domains of transcriptionally repressed genes (14). In the *dim-5/kmt1* mutant, however, H3K27me3 was detected exclusively at A:T-rich regions of the genome that are marked by H3K9 methylation in wildtype cells **(Figure 3.3A**). The enrichment of H3K27 methylation was highly reproducible in replicate experiments. We calculated normalized ChIP enrichment values for individual genomic features (genes or repeats; note that repeats in Neurospora share <80% identity) and generated scatter plots (**Figure 3.3B**). Replicate experiments for wildtype or *dim-5/kmt1* yielded correlation coefficients of 0.992 and 0.993, respectively. In contrast, no correlation was observed when comparing H3K27me3 enrichment values in wildtype and *dim-5/kmt1* ($R = 0.152$). We next examined the global changes in H3K27 methylation by creating heat maps of H3K9me3 and H3K27me3 at constitutive heterochromatin domains and at facultative heterochromatin domains (i.e. domains targeted in wildtype cells by DCDC or PRC2, respectively) (**Figure 3.3C**). In the *dim-5/kmt1* strain, H3K27me3 enrichment was abolished at

all regions that typically associate with this mark (**Figure 3.3**). In contrast, H3K37me3 enrichment was gained in all constitutive heterochromatin domains.

These data suggest that H3K9 methylation is required for normal H3K27me3 enrichment patterns. To confirm this, we tested strains in which the single H3 gene had been replaced with an $H3^{K9R}$ or an $H3^{K9Q}$ substitution allele. Normal H3K27 methylation patterns were abolished in these mutants, similar to the case for *dim-5/kmt1* strains. In animal cells, H3K9M substitutions are thought to act as dominant inhibitors of KMT1 enzymes. We therefore introduced an $H3^{K9M}$ substitution allele into the endogenous *hH3* locus. Although we were able to generate heterokaryons containing the $H3^{K9M}$ allele, crosses of transformants did not yield homokaryons. This suggests the H3K9M allele is lethal, in contrast to H3K9Q and H3K9R strains. Heterokaryons of *hH3;* $H3^{K9M}$ produced an intermediate distribution of H3K27me3, suggesting that the allele did not act in a dominant fashion as reported for animals. Our data suggest that caution should be used when interpreting phenotypes of histone lysine to M alleles.

Reduction of cytosine methylation in plant and animal cells produced a similar redistribution of H3K27 methylation (55-58). Positive feedback loops between H3K9 methylation and DNA methylation pathways complicate interpretation of these data, however. In plants and animals, DNA methylation is partly dependent on H3K9 methylation (59), and reduced DNA methylation can lead to a concomitant loss of H3K9 methylation in certain situations (60, 61). In Neurospora the heterochromatin formation pathway is primarily unidirectional. DNA methylation depends on H3K9me3 and HP1, but H3K9me3 patterns are not dramatically altered by loss of HP1 or DNA methylation (6, 9). We generated heat maps to ask if H3K27me3 patterns were altered in *hpo* mutants, which lack HP1, or *dim-2* mutants, which lack DNA methylation. Consistent with previous data, heat maps revealed that enrichment of

H3K9me3 was reduced at the boundaries of heterochromatin domains (8). Despite the presence of significant H3K9me3 in the *hpo* mutant, the pattern of H3K27 methylation was similar to the *dim-5/kmt1* mutant (**Figure 3.3C**). In contrast, H3K27me3 patterns in *dim-2* mutants were more similar to wildtype, although a subtle increase of H3K27me3 was observed in heterochromatin regions in the *dim-2* strain (**Figure 3.3C**). Thus, normal H3K27me3 patterns depend on DIM-5/KMT1 and HP1 in *Neurospora*. In C. elegans, spreading of H3K27me3 into adjacent chromatin is prevented by H3K36 methylation (62). We therefore asked if methylation of other H3 tail residues affects the distribution of H3K27 methylation in *Neurospora*. We performed ChIP-seq for H3K27me3 in *set-1* and *set-2* mutants, which are deficient for H3K4 and H3K36 methylation, respectively (**Figure S3.2**) (63). The pattern of H3K27me3 was similar to wildtype in both strains, indicating that defects in heterochromatin but not in other histone methylation pathways leads to altered PRC2-targeting.

It has been proposed that redistribution of H3K27me3 to constitutive heterochromatin domains is a compensatory response for maintenance of heterochromatic gene silencing (56). To test if this is the case in *Neurospora*, we asked if *dim-5/kmt1; set-7/kmt6* double mutants exhibit increased transcription from constitutive heterochromatin domains. We first performed strand-specific total RNA-seq in wildtype, *dim-5, set-7,* and *dim-5; set-7* double mutants. A significant number of H3K27me3-associated genes were upregulated in the *dim-5* mutant, consistent with the observed loss of H3K27me3 from these domains (**Figure 3.4A, and B)**. However, we did not detect RNAs originating from heterochromatin domains in any of the strains tested. We calculated FPKM values for repeats and for entire constitutive heterochromatin domains on both the plus and minus strand. It is possible that RNA surveillance pathways rapidly degrade heterochromatin-derived transcripts. We therefore performed ChIP-seq to examine RNA

polymerase II localization in wildtype, set-7, dim-5, and dim-5; set-7 double mutants. We did not detect an increase in RNA polymerase II at any heterochromatin regions in the mutants, consistent with RNA-seq analysis. Taken together, these data suggest that relocalization of H3K27me3 to heterochromatin in *Neurospora* is not part of a compensatory gene silencing pathway, although it is difficult to eliminate this possibility.

Aberrant H3K27me3 is responsible for growth defects and meiotic failure of *dim-5/kmt1* strains.

The fact that *set-7/kmt6* strains grow normally and are not hypersensitive to MMS (**Figure 3.2D**) suggests that loss of H3K27me3 from facultative heterochromatin does not lead to significant phenotypes. Rather, the data suggest that gain of H3K27me3 at constitutive heterochromatin domains is linked to genotoxic stress in DCDC-deficient mutants. To determine if MMS-sensitivity is caused by aberrant localization of H3K27me3, we replaced the wildtype *hH3* gene with an $hH3^{K27R}$ substitution allele and crossed the $hH3^{K27R}$ strain to *dim-5/kmt1*. *dim-5/kmt1;* $hH3^{K27R}$ double mutant progeny were resistant to MMS, suggesting that aberrant H3K27me3 triggers genotoxic stress in *dim-5/kmt1*.

We next asked if sensitivity to other DNA damaging agents was rescued in the *dim-5/kmt1; set-7/kmt6* double mutant (**Figure 3.5)**. The double mutant was more tolerant than *dim-5/kmt1* to all genotoxic agents with one exception. Cells that lacked both DCDC and PRC2 exhibited synthetic sensitivity to the topoisomerase I inhibitor camptothecin.

In addition to hypersensitivity to genotoxic agents, DCDC-deficient mutants display slow growth and meiotic failure (5). We asked if these defects were also rescued by removal of PRC2. Both vegetative and meiotic growth defects of *dim-5/kmt1* single mutants were rescued by

deletion of the *set-7/kmt6* gene. The linear growth rate of *dim-5/kmt1; set-7/kmt6* double mutants was significantly faster than *dim-5/kmt1* single mutants, yet slightly slower than wildtype (**Figure 3.6B**). In addition, homozygous crosses of *dim-5/kmt1; set-7/kmt6* double mutants were fertile, as evident by fruiting body structures filled with spores (**Figure 3.6C**). Although homozygous crosses of double mutants were fertile, spore production was delayed and the number of mature asci observed in squashed perithecia was reduced.

γH2A is a phosphorylated form of H2A that is induced by DNA damage (64). It is required for DNA repair, mediating the DNA damage response through interaction with kinases such ATM and ATR. We previously showed that γH2A is enriched in heterochromatin domains in wildtype cells and that γH2A is deposited throughout the genome in the *dim-5/kmt1* mutant, leading to loss of enrichment (39). We asked if γH2A localization was rescued in the *dim-5/kmt1; set-7/kmt6* double mutant. We performed ChIP-seq for γH2A in wildtype, *dim-5/kmt1*, *set-7/kmt6*, and *dim-5/kmt1; set-7/kmt6* double mutants (**Figure 3.6D**). As observed previously, γH2A was enriched in constitutive heterochromatin domains in wildtype, but enrichment was lost in the *dim-5/kmt1* strain. The pattern of γH2A enrichment in the *set-7/kmt6* mutant was equivalent to wildtype. In the *dim-5/kmt1; set-7/kmt6* double mutant, γH2A was enriched at constitutive heterochromatin domains (i.e. DCDC-target loci) with a distribution that was similar to wildtype. We created heat maps to visualize γH2A enrichment in all constitutive heterochromatin domains (**Figure 3.6E**). Wildtype and *set-7/kmt6* strains displayed higher levels of γH2A enrichment overall and γH2A exhibited the highest enrichment at the edges of RIP'd regions. In the *dim-5/kmt1; set-7/kmt6* double mutant strains, the levels of γH2A enrichment were lower and the boundaries of individual peaks were not as discrete as in wildtype. Together, the data suggest that in *dim-5/kmt1* strains, altered PRC2-targeting is responsible for γH2A

redistribution and for growth defects observed during vegetative and sexual phases of the life cycle in *Neurospora*.

Discussion

Heterochromatin components are required for normal growth and development and are important for maintenance of genome integrity. We found that defective growth of *Neurospora* H3K9me3-deficient mutants is caused by altered PRC2 function. Defective heterochromatin formation in *Neurospora* leads to global redistribution of H3K27me3 to repeat rich domains. Although the molecular signals that recruit PRC2 to constitutive heterochromatin are not understood, at least some of the responsible factors are likely to be conserved. PRC2 exhibits a similar antagonistic relationship with constitutive heterochromatin components in plants and animals. In Arabidopsis *met1* mutants, loss of 5mC in certain TEs is accompanied by gain of H3K27me3 at these regions. At the same time, H3K27me3 is lost from individual PRC2-target genes that gain 5mC (55). In animal cells, genomic (58), proteomic (56), and single-molecule approaches (57) show that 5mC prevents deposition of H3K27me3 at constitutive heterochromatin. Altered PRC2-targeting is linked to human diseases such as cancer. It is therefore possible that redistribution of H3K27me3 to heterochromatin may contribute to cancer development or progression. On the other hand, crosstalk between constitutive heterochromatin and PRC2 may also be important mechanisms for regulating of chromatin architecture in certain cell types. DNA demethylation in the Arabidobsis endosperm was correlated with redistribution of H3K27me3 to transposable elements (TEs) (65).

Although crosstalk between heterochromatin and PRC2 appears to be a shared feature of fungi, plants, and animals, there are subtle differences between systems. In the basidiomycete *C.*

neoformans, for example, normal H3K27me3 localization depends on the PRC2 component Ccc1, an H3K27me3-binding protein (13). Ccc1 prevents promiscuous H3K27 methylation at pericentromeric regions by tethering PRC2 to facultative heterochromatin domains adjacent to telomeres. Redistribution of H3K27me3 to constitutive heterochromatin in *C. neoformans* depends on H3K9 methylation, however, in contrast to *Neurospora* and to mammals. H3K27me3 redistribution occurs in *Neurospora* strains lacking H3K9me3 or HP1, but only limited redistribution was observed in the absence of 5mC. In animals, however, depletion of 5mC led to a dramatic redistribution of PRC2 to heterochromatin, whereas reduction of H3K9me3 led to only limited redistribution of PRC2. Despite these subtle differences, the fact that PRC2 is promiscuously targeted to constitutive heterochromatin in fungi, plants and animals suggests a shared mechanism. The only component required for PRC2 redistribution is the mammalian protein BEND3 (56), which is absent from *Neurospora*. Thus, additional studies are needed to understand the molecular signals leading to altered PRC2 recruitment to heterochromatin domains.

Regardless of the mechanism, altered PRC2 recruitment leads to dramatic phenotypic defects in Neurospora, highlighted by hypersensitivity to genotoxic agents. This result is somewhat surprising. H3K27me3 is a repressive chromatin modification capable of establishing facultative heterochromatin. It is therefore reasonable to assume that redistribution of H3K27me3 is part of a compensatory mechanism to assemble silent chromatin within repeat-rich regions of the genome. We found no evidence to support this idea. Even in the absence of both H3K9me3 and H3K27me3, we failed to detect increased transcripts from heterochromatin domains by RNA-seq. We also failed to detect an increase in RNA polymerase II localization by

ChIP-seq. Thus, our data suggest that redistribution of H3K27me3 to repeat-rich domains is deleterious rather than compensatory.

It is possible that aberrant recruitment of H3K27me3 causes genotoxic stress by interfering with normal DNA replication within heterochromatin domains. In plants, mono-methylation of H3K27 is required for normal DNA replication, although this modification does not depend on PRC2. Specifically, mutation of the *A. thanliana* H3K27 mono-methyltransferases AT leads to over-replication of heterochromatic DNA sequences (66, 67), whereas in *Tetrahymena thermophila*, loss of the H3K27 monomethylase TXR1 disrupts replication elongation (68). H3K27me1 is detected at constitutive heterochromatin domains in mammals, but its deposition and function are not understood (69). It is possible that aberrant conversion of H3K27me1 to H3K27me2/me3 leading to depletion of H3K27me1, which in turn could trigger replication defects.

Alternatively, H3K27me3 could function in a pathway that responds to DNA damage or replication stress. PRC2 localizes to double strand break regions in mammalian cells (19). Moreover, loss of H3K9me3 leads to spontaneous double strand breaks that arise during replication of repeat-rich heterochromatin domains in Drosophila (23). *S. pombe* lacks H3K27 methylation, but illegitimate recombination occurs in *S. pombe* heterochromatin-deficient mutants (22). Thus, it is possible that H3K27me3 relocalization is part of a DNA damage response and that growth defects could result from PRC2-dependent cell cycle arrest or apoptosis. Additional studies are needed to determine if H3K27me3 redistribution is the cause of genotoxic stress in *Neurospora* or a response to DNA damage arising during defective replication of repeat-rich heterochromatin domains.

Components of constitutive heterochromatin and Pc system components are frequently mutated or overexpressed in cancer cells (12). EZH2, the catalytic subunit of PRC2, has gained interest as a promising potential target for cancer therapeutics (70). Surprisingly, we found that *Neurospora* strains lacking both PRC2 and DCDC become more resistant to the topoisomerase II inhibitor etoposide and to other DNA damaging agents. In contrast, they display synthetic sensitivity to the topoisomerase I inhibitor CPT. These results suggest that PRC2 modulates the cellular sensitivity to DNA damaging agents and raises the possibility that EZH2 inhibition may have dramatically different consequences in different genetic backgrounds. Thus, understanding the relationship between Pc system and genotoxic stress has important implications for improved cancer treatment.

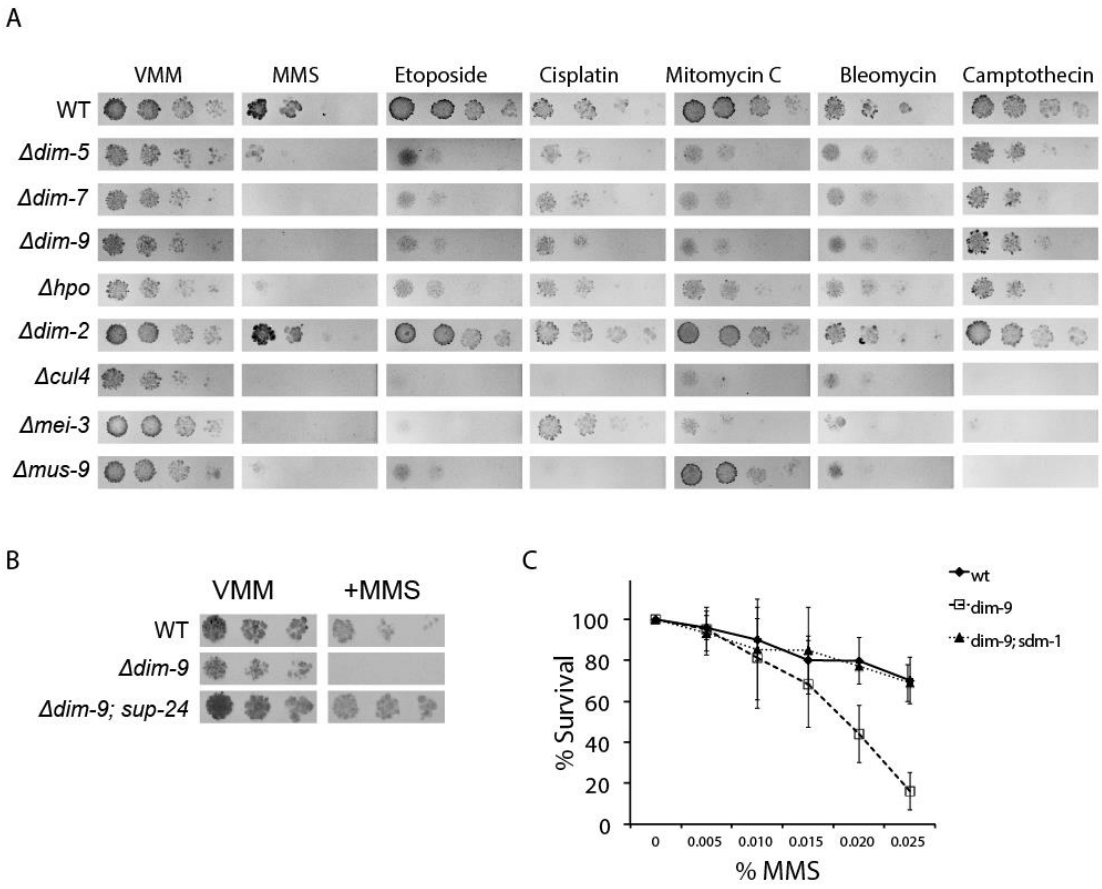

Figure 3.1 Drug sensitivity; suppressor isolation scheme. (**A**) Suspensions of 10^4, 10^3 or 10^2 conidia of the indicated strains were spot-tested on Vogel's Minimal Medium (VMM) with or without the indicated genotoxic agent: methylmethane sulfonate (MMS; 0.025%), Etoposide (600ug/ml), Cisplatin (100ug/ml), Mitomycin C (60ug/ml), Bleomycin (0.15ug/ml), Camptothecin (CPT; 0.25ug/ml). (**B**) Suspensions of conidia were spot-tested on VMM with or without 0.25%MMS. (**C**) Viability of spores on the indicated MMS-concentration is shown for wildtype, *dim-9,* and the *dim-9; sup-24* strain.

A

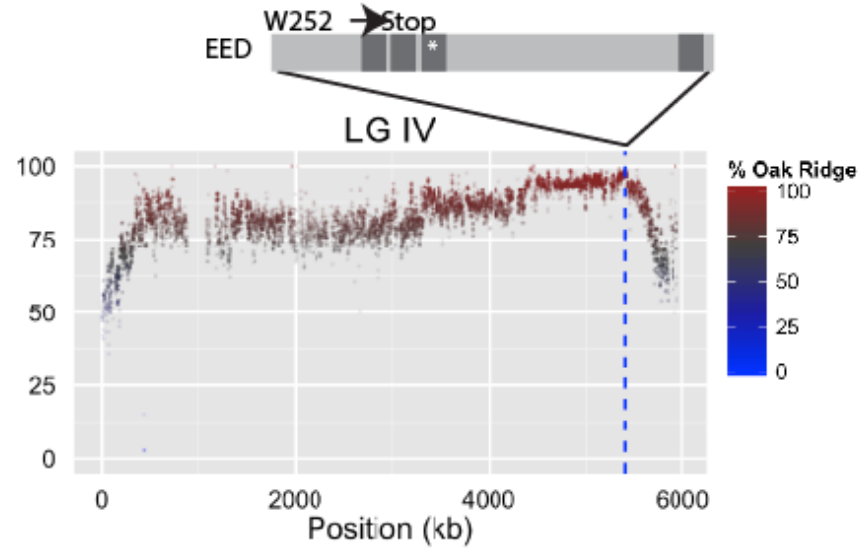
W252 → Stop
EED
LG IV
100
75
50
25
0
0
2000
4000
6000
Position (kb)
% Oak Ridge
100
75
50
25
0

B

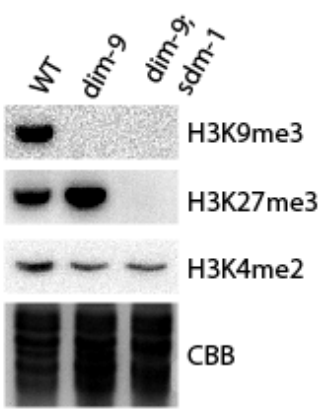
WT
dim-9
dim-9; sdm-1
H3K9me3
H3K27me3
H3K4me2
CBB

C

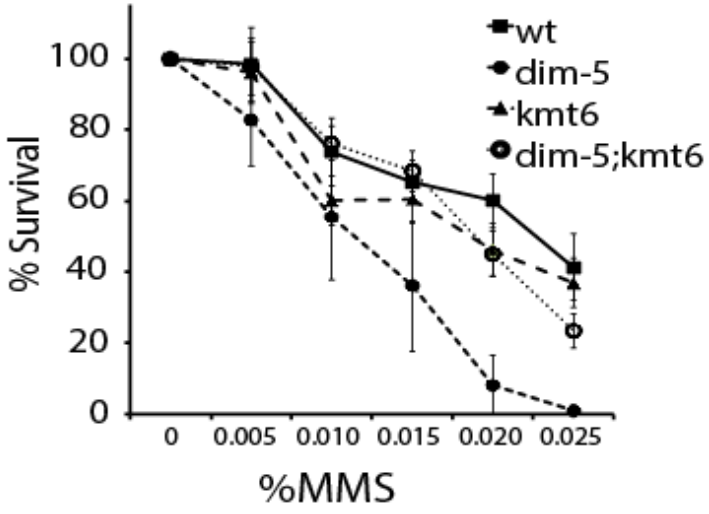
100
80
60
40
20
0
% Survival
0
0.005
0.010
0.015
0.020
0.025
%MMS
wt
dim-5
kmt6
dim-5;kmt6

Figure 3.2 *eed* is a genetic suppressor of DCDC-deficient mutants. (**A**) The frequency of OR and MA SNPs in progeny from a *dim-9; sup-24* x MA cross are shown for LGIV. An OR-specific region on the right arm of LGIV harbors a non-sense mutation in the Neurospora *eed* gene. (**B**) Western blots of acid-extracted histones are shown from wildtype, *dim-9,* and *dim-9; sup-24* probed with antibodies for H3K9me3 and H3K27me3. A gel stained with Coomassie Blue and a western blot probed with antibodies to H3K4me2 are shown as loading controls. (**C**) Viability of spores on the indicated MMS-concentrations is shown for wildtype, *dim-5, set-7* and the *dim-5; set-7* double mutant.

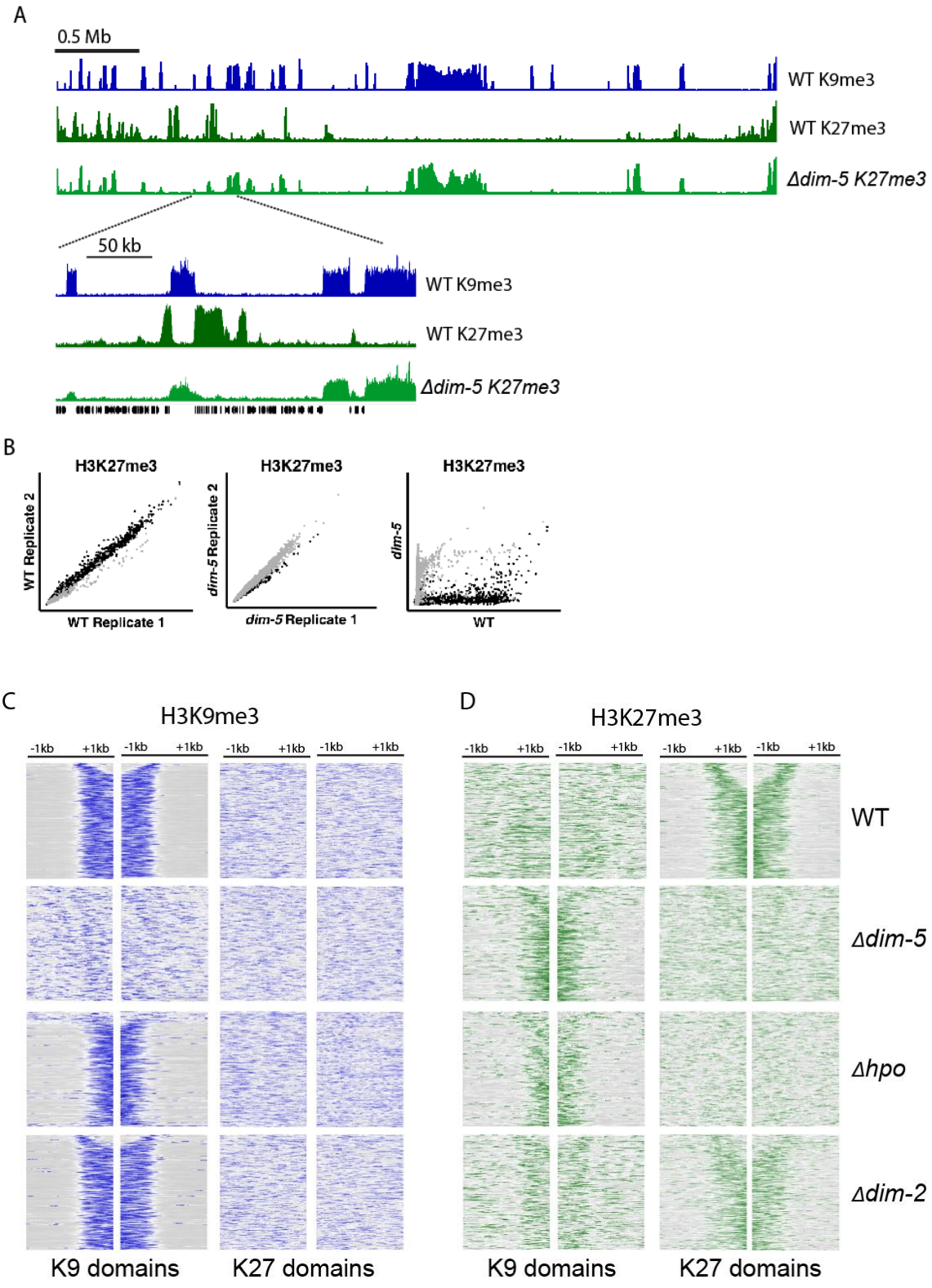
A
0.5 Mb
WT K9me3
WT K27me3
Δdim-5 K27me3
50 kb
WT K9me3
WT K27me3
Δdim-5 K27me3
B
H3K27me3
WT Replicate 2
WT Replicate 1
H3K27me3
dim-5 Replicate 2
dim-5 Replicate 1
H3K27me3
dim-5
WT
C
H3K9me3
-1kb +1kb -1kb +1kb -1kb +1kb -1kb +1kb
K9 domains
K27 domains
D
H3K27me3
-1kb +1kb -1kb +1kb -1kb +1kb -1kb +1kb
WT
Δdim-5
Δhpo
Δdim-2
K9 domains
K27 domains

Figure 3.3 Loss of H3K9 methylation leads to global redistribution of H3K27me3. (**A**) ChIP-seq enrichment across the entire Linkage Group VII (LGVII) is shown for H3K9me3 in wildtype and both H3K9me3 and H3K27me3 in the *dim-5* mutant. The scale bar indicates 0.5Mb or 50kb. (**B**) Scatter plots of H3K27me3 enrichment were generated to examine reproducibility between wildtype replicates (left), *dim-5* replicates (middle), or wildtype and *dim-5* samples (right). The plot depicts the normalized ChIP enrichment value (NLCS) obtained for each genomic feature is plotted. Genes and tRNAs are shown in black and repeats are shown in grey. (**C**) Heat maps show H3K9me3 enrichment for the indicated strains. Each heat map row depicts a 2kb window centered at the left or right boundary of each constitutive heterochromatin domain (K9me3 domains; left) or each facultative heterochromatin domain (K27me3-domains; right). Domains are arranged from smallest (top) to largest (bottom). (**D**) Heat maps show H3K27me3 enrichment for the indicated strains at constitutive heterochromatin domains (K9me3 domains; left) and for facultative heterochromatin domains (K27me3-domains; right), as in B.

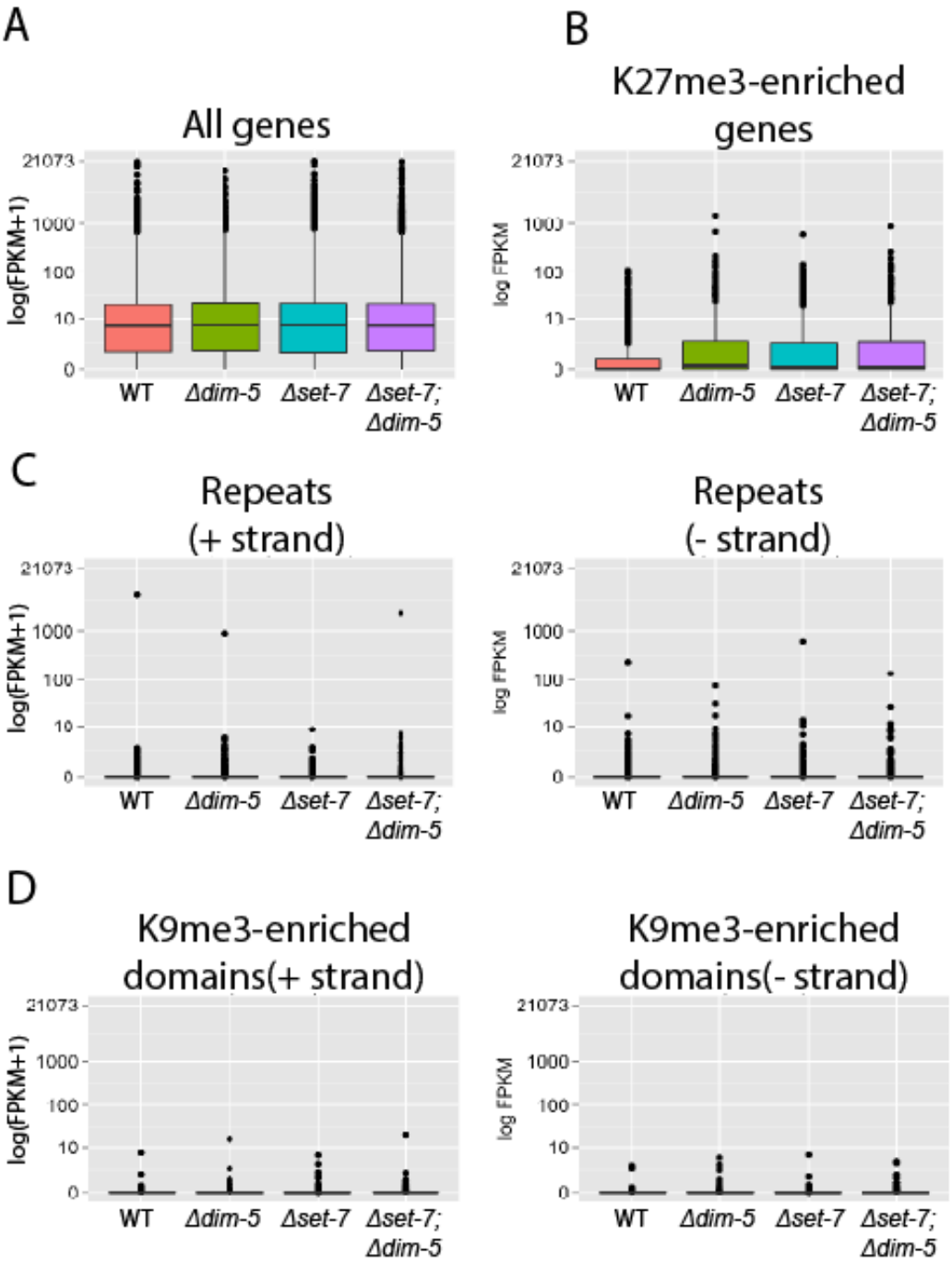

Figure 3.4 Loss of H3K27me3 leads to increased transcription from polycomb target genes but not from heterochromatin regions. Box plots of FPKM values in wildtype, *dim-5*, *set-7*,

and the *dim-5; set-7* double mutant for (**A**) all Neurospora genes, (**B**) H3K27me3-enriched genes, (**C**) repeated loci and (**D**) H3K9me3-enriched domains.

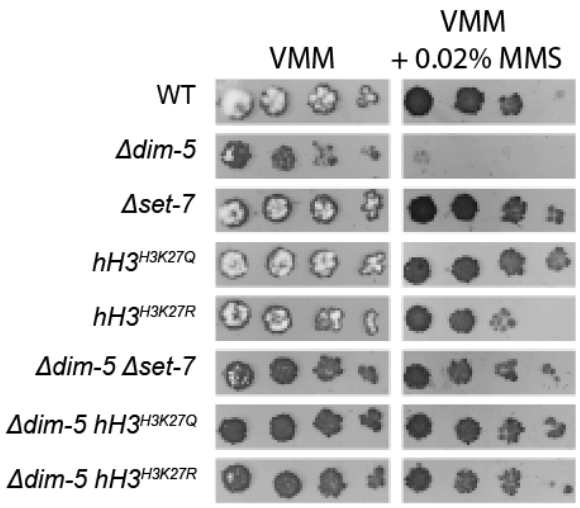

Figure 3.5 H3K27 methylation is responsible MMS-sensitivity and other phenotypic defects in H3K9-deficient strains. Suspensions of 10^4, 10^3 or 10^2 conidia of the indicated strains were spot-tested on media with or without methyl methanesulfonate (MMS).

A

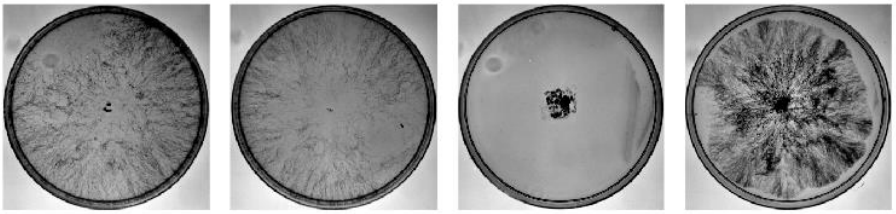
WT
Δset-7
Δdim-5
Δdim-5; Δset-7

B.

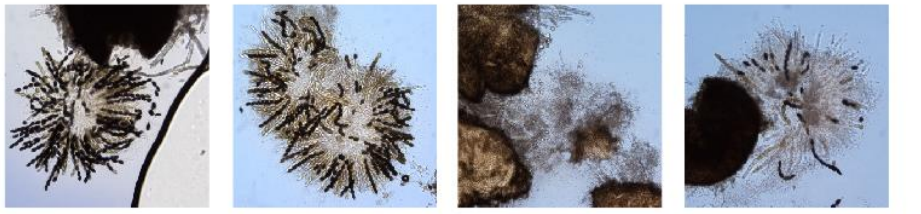
WT
Δset-7
Δdim-5
Δdim-5; Δset-7

C

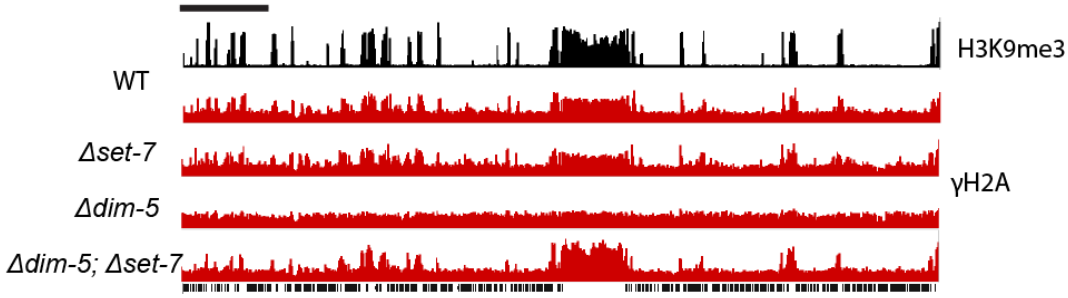
H3K9me3
WT
Δset-7
γH2A
Δdim-5
Δdim-5; Δset-7

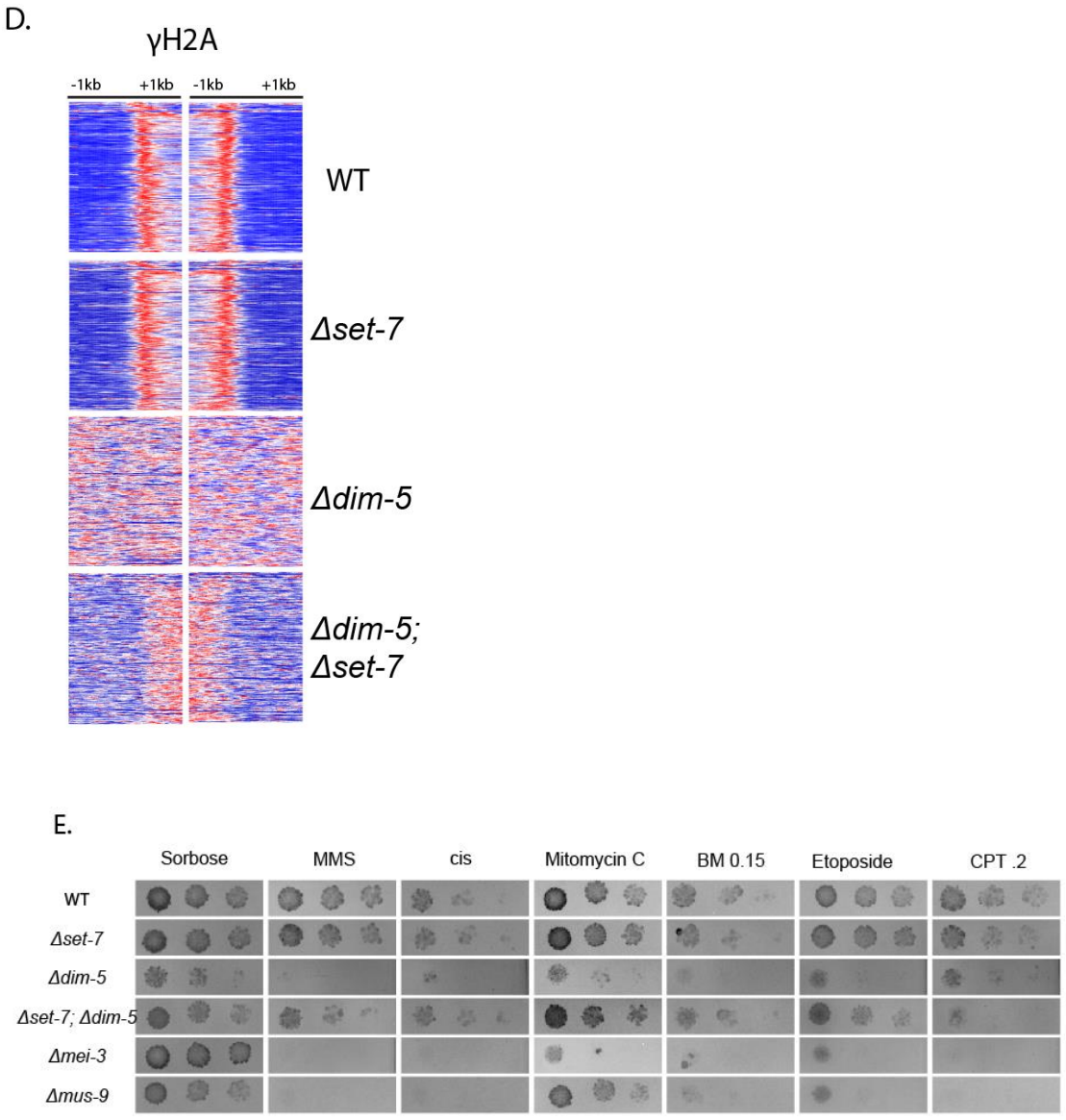

Figure 3.6 Elimination of H3K9me3 and H3K27me3 sensitizes cells to camptothecin. (**A**) Condia (10^3) produced by the indicated strains were inoculated in the center of a petri plate and cultures were allowed to grow for 24 hours. (**B**) Homozygous crosses were carried out for each of the indicated genotypes. Images of dissected fruiting bodies (perithecia) are shown revealing the presence or absence of meiotic products for each cross. (**C**) ChIP-seq enrichment across Linkage Group VII is shown for γH2A in wildtype, *dim-5*, *set-7*, and the *set-7; dim-5* double

mutant. (**D**) Heat maps show γH2A enrichment for the indicated strains. Each heat map depicts a 2kb window centered at the boundaries of all heterochromatin domains. Domains are arranged from smallest (top) to largest (bottom). (**E**) Suspensions of 10^4, 10^3 or 10^2 conidia of the indicated strains were spot-tested on Vogel's Minimal Medium (VMM) with or without the indicated genotoxic agent: methylmethane sulfonate (MMS; 0.025%), Etoposide (600ug/ml), Cisplatin (100ug/ml), Mitomycin C (60ug/ml), Bleomycin (0.15ug/ml), Camptothecin (CPT; 0.25ug/ml).

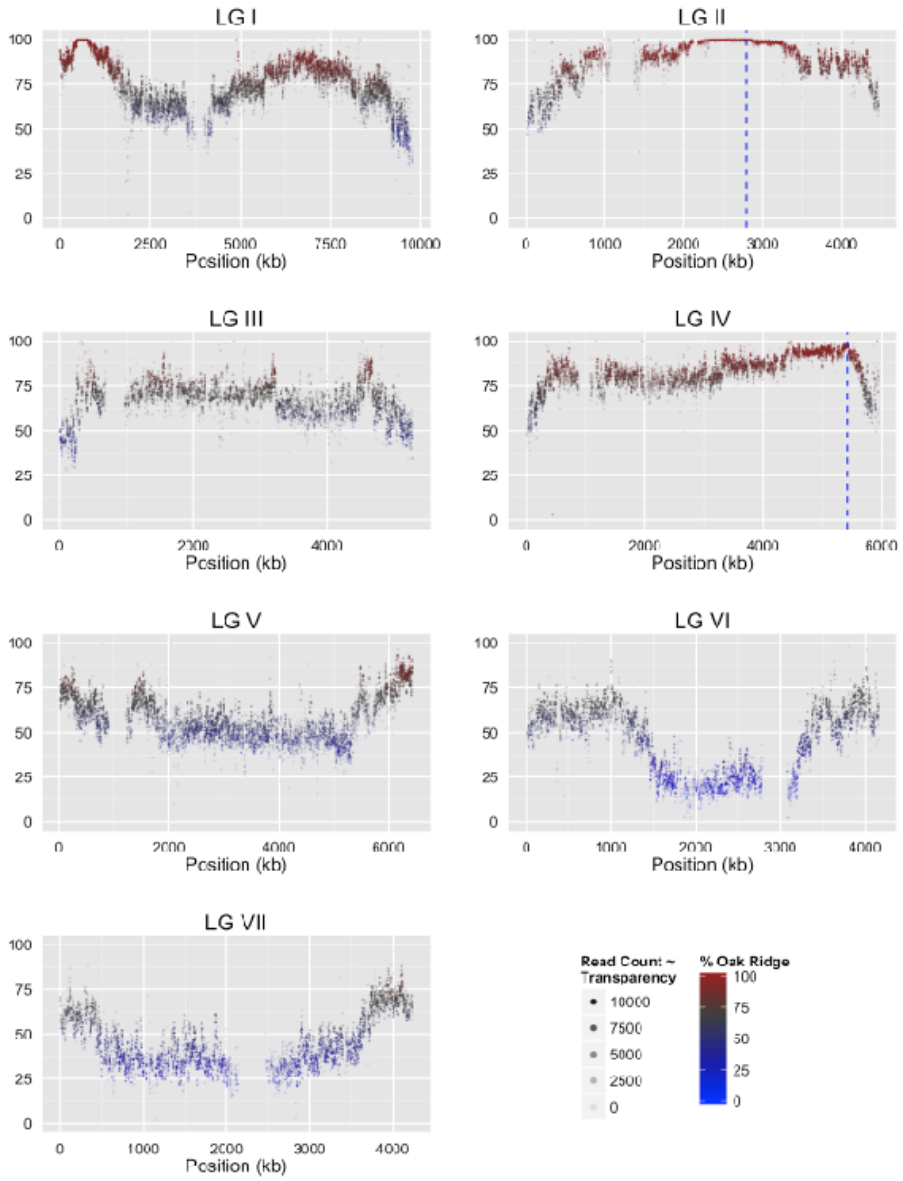

Figure S3.1 Bulk Segregant Analysis. A single *dim-9; sup-24* homokaryon, generated in the Oak Ridge strain background (OR), was crossed to a polymorphic wildtype Neurospora strain (Mauriceville). Genomic DNA was isolated from 14 progeny carrying both the *dim-9* deletion and the suppressor mutation, pooled and sequenced in bulk.

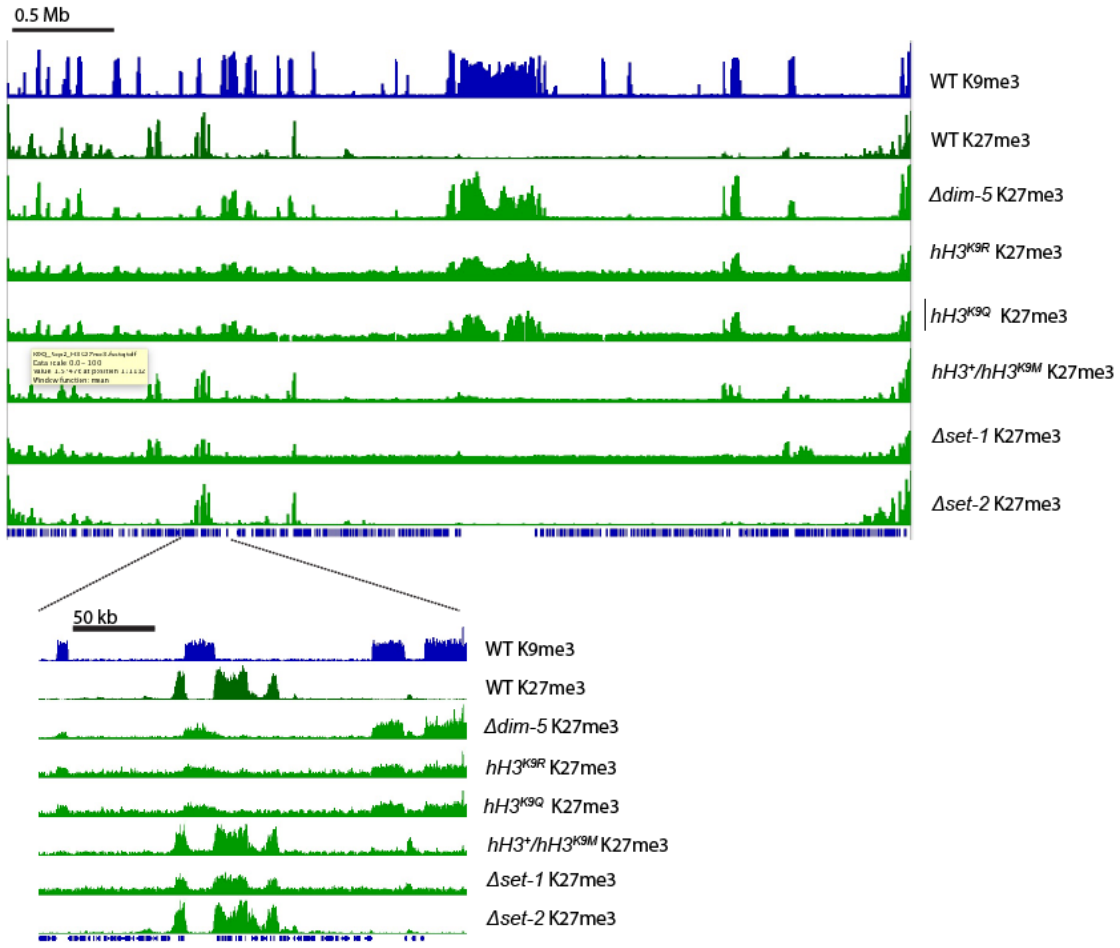

Figure S3.2 K27me3 distribution is normal in *Δset-1* and *Δset-2*. ChIP-seq was performed using the mutants. Germinating conidia grown in VMM with 1.5% sucrose at 32 °C for 6 hours were used in the experiments.

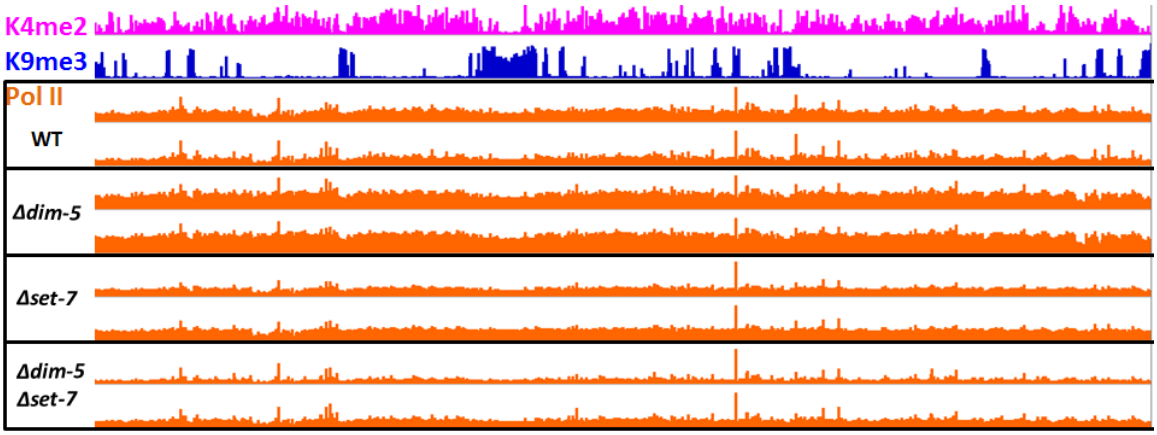

Figure S3.3 Pol II enrichment in wildtype, *Δdim-5*, *Δset-7*, and *Δdim-5; Δset-7*. ChIP-seq was performed to identify Pol II binding sites across the genome. Pol II distribution of the Linkage Group 7 is shown.

Table S3.1

Strains used in this study

Strain	Genotype	Source/reference
S2	Wildtype	FGSC# 2489
S132	*Δdim-5::bar+*	Ref (4)
S146	*Δdim-7::hph+*	Ref (4)
S147	*Δdim-7::hph+*	Ref (4)
S161	*Δdim-8:hph+*	Ref (4)
S175	*Δdim-8:hph+* Sad-1	Ref (4)
S239	*Δdim-9:hph+*	Ref (4)
S343	Wildtype	This study
S344	Wildtype	This study
S345	Wildtype	This study
S346	Δdim-5::bar+	This study
S347	Δdim-5::bar+	This study
S348	Δdim-5::bar+	This study
S349	Δdim-5::bar+	This study
S350	*Δset-7::hph+*	This study
S351	*Δset-7::hph+*	This study
S352	*Δset-7::hph+*	This study
S353	*Δdim-5::bar+, Δset-7::hph+*	This study
S354	*Δdim-5::bar+, Δset-7::hph+*	This study
S355	*Δdim-5::bar+, Δset-7::hph+*	This study

S365	dim9su#24 (Δdim-9:hph+, mutagenized with UV)	This study
S398	*hH3::hH3K27Q::hph+*	This study
S402	*hH3::hH3K27R::hph+*	This study

References

1. **Grewal SI, Jia S.** 2007. Heterochromatin revisited. Nature reviews. Genetics **8:**35-46.

2. **Peng J, Karpen G.** 2008. Epigenetic regulation of heterochromatic DNA stability. Current opinion in genetics & development**:**8.

3. **Aramayo R, Selker EU.** 2013. Neurospora crassa, a model system for epigenetics research. Cold Spring Harbor perspectives in biology **5:**a017921.

4. **Lewis ZA, Adhvaryu KK, Honda S, Shiver AL, Knip M, Sack R, Selker EU.** 2010. DNA methylation and normal chromosome behavior in Neurospora depend on five components of a histone methyltransferase complex, DCDC. PLoS genetics **6:**e1001196.

5. **Tamaru H, Selker EU.** 2001. A histone H3 methyltransferase controls DNA methylation in Neurospora crassa. Nature **414:**277-283.

6. **Lewis ZA, Honda S, Khlafallah TK, Jeffress JK, Freitag M, Mohn F, Schubeler D, Selker EU.** 2009. Relics of repeat-induced point mutation direct heterochromatin formation in Neurospora crassa. Genome research **19:**427-437.

7. **Tamaru H, Zhang X, McMillen D, Singh PB, Nakayama J, Grewal SI, Allis CD, Cheng X, Selker EU.** 2003. Trimethylated lysine 9 of histone H3 is a mark for DNA methylation in Neurospora crassa. Nature genetics **34:**75-79.

8. **Honda S, Lewis ZA, Shimada K, Fischle W, Sack R, Selker EU.** 2012. Heterochromatin protein 1 forms distinct complexes to direct histone deacetylation and DNA methylation. Nature structural & molecular biology **19:**471-477.

9. **Honda S, Selker EU.** 2008. Direct interaction between DNA methyltransferase DIM-2 and HP1 is required for DNA methylation in Neurospora crassa. Molecular and cellular biology **28:**6044-6055.

10. **Lewis ZA, Adhvaryu KK, Honda S, Shiver AL, Selker EU.** 2010. Identification of DIM-7, a protein required to target the DIM-5 H3 methyltransferase to chromatin. Proceedings of the National Academy of Sciences of the United States of America **107:**8310-8315.

11. **Honda S, Lewis ZA, Huarte M, Cho LY, David LL, Shi Y, Selker EU.** 2010. The DMM complex prevents spreading of DNA methylation from transposons to nearby genes in Neurospora crassa. Genes & development **24:**443-454.

12. **Margueron R, Reinberg D.** 2011. The Polycomb complex PRC2 and its mark in life. Nature **469:**343-349.

13. **Dumesic PA, Homer CM, Moresco JJ, Pack LR, Shanle EK, Coyle SM, Strahl BD, Fujimori DG, Yates JR, 3rd, Madhani HD.** 2015. Product binding enforces the genomic specificity of a yeast polycomb repressive complex. Cell **160:**204-218.

14. **Jamieson K, Rountree MR, Lewis ZA, Stajich JE, Selker EU.** 2013. Regional control of histone H3 lysine 27 methylation in Neurospora. Proceedings of the National Academy of Sciences of the United States of America **110:**6027-6032.

15. **Connolly LR, Smith KM, Freitag M.** 2013. The Fusarium graminearum histone H3 K27 methyltransferase KMT6 regulates development and expression of secondary metabolite gene clusters. PLoS genetics **9:**e1003916.

16. **Campbell S, Ismail IH, Young LC, Poirier GG, Hendzel MJ.** 2013. Polycomb repressive complex 2 contributes to DNA double-strand break repair. Cell cycle **12:**2675-2683.

17. **O'Hagan HM, Wang W, Sen S, Destefano Shields C, Lee SS, Zhang YW, Clements EG, Cai Y, Van Neste L, Easwaran H, Casero RA, Sears CL, Baylin SB.** 2011. Oxidative damage targets complexes containing DNA methyltransferases, SIRT1, and polycomb members to promoter CpG Islands. Cancer cell **20:**606-619.

18. **O'Hagan HM, Mohammad HP, Baylin SB.** 2008. Double strand breaks can initiate gene silencing and SIRT1-dependent onset of DNA methylation in an exogenous promoter CpG island. PLoS genetics **4:**e1000155.

19. **Chou DM, Adamson B, Dephoure NE, Tan X, Nottke AC, Hurov KE, Gygi SP, Colaiácovo MP, Elledge SJ.** 2010. A chromatin localization screen reveals poly (ADP ribose)-regulated recruitment of the repressive polycomb and NuRD complexes to sites of DNA damage. Proceedings of the National Academy of Sciences of the United States of America **107:**18475-18480.

20. **Zaratiegui M, Castel SE, Irvine DV, Kloc A, Ren J, Li F, de Castro E, Marin L, Chang AY, Goto D, Cande WZ, Antequera F, Arcangioli B, Martienssen RA.** 2011. RNAi promotes heterochromatic silencing through replication-coupled release of RNA Pol II. Nature **479:**135-138.

21. **Cam HP, Sugiyama T, Chen ES, Chen X, FitzGerald PC, Grewal SI.** 2005. Comprehensive analysis of heterochromatin- and RNAi-mediated epigenetic control of the fission yeast genome. Nature genetics **37:**809-819.

22. **Li PC, Petreaca RC, Jensen A, Yuan JP, Green MD, Forsburg SL.** 2013. Replication fork stability is essential for the maintenance of centromere integrity in the absence of heterochromatin. Cell reports **3:**638-645.

23. **Peng JC, Karpen GH.** 2009. Heterochromatic genome stability requires regulators of histone H3 K9 methylation. PLoS genetics **5:**e1000435.

24. **Peng JC, Karpen GH.** 2007. H3K9 methylation and RNA interference regulate nucleolar organization and repeated DNA stability. Nature cell biology **9:**25-35.

25. **Paredes S, Maggert KA.** 2009. Ribosomal DNA contributes to global chromatin regulation. Proceedings of the National Academy of Sciences of the United States of America **106:**17829-17834.

26. **Peters AH, O'Carroll D, Scherthan H, Mechtler K, Sauer S, Schofer C, Weipoltshammer K, Pagani M, Lachner M, Kohlmaier A, Opravil S, Doyle M, Sibilia M, Jenuwein T.** 2001. Loss of the Suv39h histone methyltransferases impairs mammalian heterochromatin and genome stability. Cell **107:**323-337.

27. **Allis CD, Berger SL, Cote J, Dent S, Jenuwien T, Kouzarides T, Pillus L, Reinberg D, Shi Y, Shiekhattar R, Shilatifard A, Workman J, Zhang Y.** 2007. New nomenclature for chromatin-modifying enzymes. Cell **131:**633-636.

28. **Soria G, Almouzni G.** 2013. Differential contribution of HP1 proteins to DNA end resection and homology-directed repair. Cell cycle **12:**422-429.

29. **Lee YH, Kuo CY, Stark JM, Shih HM, Ann DK.** 2013. HP1 promotes tumor suppressor BRCA1 functions during the DNA damage response. Nucleic acids research **41:**5784-5798.

30. **Bolderson E, Savage KI, Mahen R, Pisupati V, Graham ME, Richard DJ, Robinson PJ, Venkitaraman AR, Khanna KK.** 2012. Kruppel-associated Box (KRAB)-associated co-repressor (KAP-1) Ser-473 phosphorylation regulates heterochromatin protein 1beta (HP1-beta) mobilization and DNA repair in heterochromatin. The Journal of biological chemistry **287:**28122-28131.

31. **Chiolo I, Minoda A, Colmenares SU, Polyzos A, Costes SV, Karpen GH.** 2011. Double-strand breaks in heterochromatin move outside of a dynamic HP1a domain to complete recombinational repair. Cell **144:**732-744.

32. **Baldeyron C, Soria G, Roche D, Cook AJ, Almouzni G.** 2011. HP1alpha recruitment to DNA damage by p150CAF-1 promotes homologous recombination repair. The Journal of cell biology **193:**81-95.

33. **Luijsterburg MS, Dinant C, Lans H, Stap J, Wiernasz E, Lagerwerf S, Warmerdam DO, Lindh M, Brink MC, Dobrucki JW, Aten JA, Fousteri MI, Jansen G, Dantuma NP, Vermeulen W, Mullenders LH, Houtsmuller AB, Verschure PJ, van Driel R.** 2009. Heterochromatin protein 1 is recruited to various types of DNA damage. The Journal of cell biology **185:**577-586.

34. **Dinant C, Luijsterburg MS.** 2009. The emerging role of HP1 in the DNA damage response. Molecular and cellular biology **29:**6335-6340.

35. **Ayoub N, Jeyasekharan AD, Bernal JA, Venkitaraman AR.** 2008. HP1-beta mobilization promotes chromatin changes that initiate the DNA damage response. Nature **453:**682-686.

36. **Liu H, Galka M, Mori E, Liu X, Lin YF, Wei R, Pittock P, Voss C, Dhami G, Li X, Miyaji M, Lajoie G, Chen B, Li SS.** 2013. A method for systematic mapping of protein lysine methylation identifies functions for HP1beta in DNA damage response. Molecular cell **50:**723-735.

37. **Ayrapetov MK, Gursoy-Yuzugullu O, Xu C, Xu Y, Price BD.** 2014. DNA double-strand breaks promote methylation of histone H3 on lysine 9 and transient formation of repressive chromatin. Proceedings of the National Academy of Sciences of the United States of America.

38. **Chicas A, Forrest EC, Sepich S, Cogoni C, Macino G.** 2005. Small interfering RNAs that trigger posttranscriptional gene silencing are not required for the histone H3 Lys9 methylation necessary for transgenic tandem repeat stabilization in Neurospora crassa. Molecular and cellular biology **25:**3793-3801.

39. **Sasaki T, Lynch KL, Mueller CV, Friedman S, Freitag M, Lewis ZA.** 2014. Heterochromatin controls gammaH2A localization in Neurospora crassa. Eukaryotic cell **13:**990-1000.

40. **Davis RH.** 2000. Neurospora: Contributions of a Model Organism. Oxford: Oxford University Press.

41. **Pall ML.** 1993. The use of Ignite (Basta;glufosinate;phosphinothricin) to select transformants of bar-containing plasmids in Neurospora crassa. Fungal Genetics Newsletter **40:**58.

42. **Margolin BS, Freitag M, Selker EU.** 1997. Improved plasmids for gene targeting at the his-3 locus of Neurospora crassa by electroporation. Fungal Genetics Newsletter **44:**34-36.

43. **Pomraning KR, Smith KM, Freitag M.** 2009. Genome-wide high throughput analysis of DNA methylation in eukaryotes. Methods **47:**142-150.

44. **Ji L, Sasaki T, Sun X, Ma P, Lewis ZA, Schmitz RJ.** 2014. Methylated DNA is over-represented in whole-genome bisulfite sequencing data. Frontiers in genetics **5:**341.

45. **Langmead B, Salzberg SL.** 2012. Fast gapped-read alignment with Bowtie 2. Nature methods **9:**357-359.

46. **Galagan JE, Calvo SE, Borkovich KA, Selker EU, Read ND, Jaffe D, FitzHugh W, Ma LJ, Smirnov S, Purcell S, Rehman B, Elkins T, Engels R, Wang S, Nielsen CB, Butler J, Endrizzi M, Qui D, Ianakiev P, Bell-Pedersen D, Nelson MA, Werner-**

Washburne M, Selitrennikoff CP, Kinsey JA, Braun EL, Zelter A, Schulte U, Kothe GO, Jedd G, Mewes W, Staben C, Marcotte E, Greenberg D, Roy A, Foley K, Naylor J, Stange-Thomann N, Barrett R, Gnerre S, Kamal M, Kamvysselis M, Mauceli E, Bielke C, Rudd S, Frishman D, Krystofova S, Rasmussen C, Metzenberg RL, Perkins DD, Kroken S, Cogoni C, Macino G, Catcheside D, Li W, Pratt RJ, Osmani SA, DeSouza CP, Glass L, Orbach MJ, Berglund JA, Voelker R, Yarden O, Plamann M, Seiler S, Dunlap J, Radford A, Aramayo R, Natvig DO, Alex LA, Mannhaupt G, Ebbole DJ, Freitag M, Paulsen I, Sachs MS, Lander ES, Nusbaum C, Birren B. 2003. The genome sequence of the filamentous fungus Neurospora crassa. Nature **422:**859-868.

47. **Thorvaldsdottir H, Robinson JT, Mesirov JP.** 2013. Integrative Genomics Viewer (IGV): high-performance genomics data visualization and exploration. Briefings in bioinformatics **14:**178-192.

48. **Robinson JT, Thorvaldsdottir H, Winckler W, Guttman M, Lander ES, Getz G, Mesirov JP.** 2011. Integrative genomics viewer. Nature biotechnology **29:**24-26.

49. **Heinz S, Benner C, Spann N, Bertolino E, Lin YC, Laslo P, Cheng JX, Murre C, Singh H, Glass CK.** 2010. Simple combinations of lineage-determining transcription factors prime cis-regulatory elements required for macrophage and B cell identities. Molecular cell **38:**576-589.

50. **Hebenstreit D, Gu M, Haider S, Turner DJ, Lio P, Teichmann SA.** 2011. EpiChIP: gene-by-gene quantification of epigenetic modification levels. Nucleic acids research **39:**e27.

51. **Quinlan AR, Hall IM.** 2010. BEDTools: a flexible suite of utilities for comparing genomic features. Bioinformatics **26:**841-842.

52. **Wakabayashi M, Ishii C, Hatakeyama S, Inoue H, Tanaka S.** 2010. ATM and ATR homologes of Neurospora crassa are essential for normal cell growth and maintenance of chromosome integrity. Fungal genetics and biology : FG & B **47:**809-817.

53. **Hatakeyama S, Ishii C, Inoue H.** 1995. Identification and expression of the Neurospora crassa mei-3 gene which encodes a protein homologous to Rad51 of Saccharomyces cerevisiae. Molecular & general genetics : MGG **249:**439-446.

54. **Liti G, Schacherer J.** 2011. The rise of yeast population genomics. Comptes rendus biologies **334:**612-619.

55. **Deleris A, Stroud H, Bernatavichute Y, Johnson E, Klein G, Schubert D, Jacobsen SE.** 2012. Loss of the DNA Methyltransferase MET1 Induces H3K9 Hypermethylation at PcG Target Genes and Redistribution of H3K27 Trimethylation to Transposons in Arabidopsis thaliana. PLoS genetics **8:**e1003062.

56. **Saksouk N, Barth TK, Ziegler-Birling C, Olova N, Nowak A, Rey E, Mateos-Langerak J, Urbach S, Reik W, Torres-Padilla ME, Imhof A, Dejardin J, Simboeck E.** 2014. Redundant mechanisms to form silent chromatin at pericentromeric regions rely on BEND3 and DNA methylation. Molecular cell **56:**580-594.

57. **Murphy PJ, Cipriany BR, Wallin CB, Ju CY, Szeto K, Hagarman JA, Benitez JJ, Craighead HG, Soloway PD.** 2013. Single-molecule analysis of combinatorial epigenomic states in normal and tumor cells. Proceedings of the National Academy of Sciences of the United States of America **110:**7772-7777.

58. **Reddington JP, Perricone SM, Nestor CE, Reichmann J, Youngson NA, Suzuki M, Reinhardt D, Dunican DS, Prendegast JG, Mjoseng H, Ramsahoye BH, Whitelaw E, Greally JM, Adams IR, Bickmore WA, Meehan RR.** 2013. Redistribution of H3K27me3 upon DNA hypomethylation results in de-repression of Polycomb-target genes. Genome biology **14:**R25.

59. **Lehnertz B, Ueda Y, Derijck AA, Braunschweig U, Perez-Burgos L, Kubicek S, Chen T, Li E, Jenuwein T, Peters AH.** 2003. Suv39h-mediated histone H3 lysine 9 methylation directs DNA methylation to major satellite repeats at pericentric heterochromatin. Current biology : CB **13:**1192-1200.

60. **Smallwood A, Esteve PO, Pradhan S, Carey M.** 2007. Functional cooperation between HP1 and DNMT1 mediates gene silencing. Genes & development **21:**1169-1178.

61. **Esteve PO, Chin HG, Smallwood A, Feehery GR, Gangisetty O, Karpf AR, Carey MF, Pradhan S.** 2006. Direct interaction between DNMT1 and G9a coordinates DNA and histone methylation during replication. Genes & development **20:**3089-3103.

62. **Yuan W, Xu M, Huang C, Liu N, Chen S, Zhu B.** 2011. H3K36 methylation antagonizes PRC2-mediated H3K27 methylation. The Journal of biological chemistry **286:**7983-7989.

63. **Adhvaryu KK, Morris SA, Strahl BD, Selker EU.** 2005. Methylation of Histone H3 Lysine 36 Is Required for Normal Development in Neurospora crassa. Eukaryotic cell **4:**1455-1464.

64. **Rogakou EP, Pilch DR, Orr AH, Ivanova VS, Bonner WM.** 1998. DNA double-stranded breaks induce histone H2AX phosphorylation on serine 139. The Journal of biological chemistry **273:**5858-5868.

65. **Weinhofer I, Hehenberger E, Roszak P, Hennig L, Kohler C.** 2010. H3K27me3 profiling of the endosperm implies exclusion of polycomb group protein targeting by DNA methylation. PLoS genetics **6**.

66. **Stroud H, Hale CJ, Feng S, Caro E, Jacob Y, Michaels SD, Jacobsen SE.** 2012. DNA methyltransferases are required to induce heterochromatic re-replication in Arabidopsis. PLoS genetics **8:**e1002808.

67. **Jacob Y, Stroud H, LeBlanc C, Feng S, Zhuo L, Caro E, Hassel C, Gutierrez C, Michaels SD, Jacobsen SE.** 2010. Regulation of heterochromatic DNA replication by histone H3 lysine 27 methyltransferases. Nature **466:**987-991.

68. **Gao S, Xiong J, Zhang C, Berquist BR, Yang R, Zhao M, Molascon AJ, Kwiatkowski SY, Yuan D, Qin Z, Wen J, Kapler GM, Andrews PC, Miao W, Liu Y.** 2013. Impaired replication elongation in Tetrahymena mutants deficient in histone H3 Lys 27 monomethylation. Genes & development **27:**1662-1679.

69. **Jacob Y, Michaels SD.** 2009. H3K27me1 is E(z) in animals, but not in plants. Epigenetics : official journal of the DNA Methylation Society **4:**366-369.

70. **Hock H.** 2012. A complex Polycomb issue: the two faces of EZH2 in cancer. Genes & development **26:**751-755.

CHAPTER 4

MOLECULAR DISSECTION OF COMPONENTS REQUIRED FOR TOLERANCE TO DNA DAMAGING AGENTS IN NEUROSPORA CRASSA[4]

Takahiko Sasaki, Mallorie Lee Huff, Zachary A. Lewis

[4] To be submitted to *G3*

Introduction

DNA replication is a conserved process in all organisms used to duplicate their chromosomes. In eukaryotes replisomes initiate DNA replication at multiple origins by unwinding the double stranded DNA to synthesize the new complimentary DNA strands. Many factors are associated with the replication forks that help to ensure the accurate and timely completion of DNA duplication. Physical tension around the replication fork caused by positive supercoiling in front and negative supercoiling behind are relieved by specialized factors such as topoisomerases (1, 2). Checkpoint systems function as a surveillance mechanism to detect DNA damage and activate the DNA repair pathway (3). These events are tightly coordinated in order to safeguard genome integrity and to relieve the biotic stress that is generated during DNA replication. Loss of this coordination can lead to genome instabilities arising from increased mutation rate, accelerated frequency of homologous recombination, and global chromosomal rearrangements (4). Examples of this type of instability can be seen when a component of the replisome is missing. In yeasts, deletion of the replisome components, Tof1, Mrc1, or Cms3 destabilizes the association of the replisome with replication fork (5). In humans, mutations in MCM4 and RPA14 32 and 70 have been linked to diseases such as cancer (4). In addition inverted repeats have been demonstrated to impede DNA replication (6). Thus, DNA replication needs to be tightly coordinated amongst a myriad of factors to successfully complete the duplication of the chromosomes while preserving normal genome structure.

DNA damaging agents have previously been used to identify genes involved in the DNA replication and repair pathways (7). One commonly used agent, Methyl methanesulfonate (MMS), is a DNA alkylating agent that causes both DNA base mispairing and stalling of the DNA replication fork through methylation of guanine and adenine bases (8). These modified

bases can be tolerated during S-phase replication through the utilization of the translesion synthesis (TLS) pathway (9). During TLS the normal replicative DNA polymerases in the replication fork are exchanged for specialized TLS DNA polymerases that allow replication to continue past the the methylated bases. These bypassed methylated bases are then ultimately repaired by the base excision repair machinery (9). MMS screens were performed on the *Saccharomyces cerevisiae* to discover components that played a major role in MMS-induced DNA damage repair. The screens indicated that the base excision repair machinery, factors required for homologous recombination, and a DNA alkyltransferases played a major role in MMS-induced DNA damage repair (7).

Another commonly used DNA damaging agent, Camptothecin (CPT), is a topoisomerase I (Topo1) inhibitor that leads to accumulation of the Topo1-DNA complex (10). The accumulation of this complex is believed to cause the stalled replication forks and transcriptional arrests. A screen for CPT-hypersensitive mutants uncovered components of several DNA repair pathways , some of which are also required for growth on MMS. However, some required components are only critical for growth in the presence of CPT such as transcription factors, histone acetyltransferases, and chromatin remodelers (7). Hydroxyurea can also be used to induce replicative stress as it inhibits ribonucleotide reductases which in turn leads to decrease in the available dNTP pool (11). DNA polymerase stalls when the dNTP level falls below a certain threshold which can then lead to replication fork collapse. ATR and its downstream components are important in the HU-induced stress response (12). The activation of kinases such as ATM and ATR, and the resulting signal transduction through the phosphorylation of their targets, are the common DNA damage responses when an organism is subjected to MMS, CPT, and HU-induced replicative stress (7, 12).

Previous research in *Neurospora* suggests that DCDC, a histone lysine methyltransferase complex required for heterochromatin formation, plays a role in DNA replication and DNA repair (13). DCDC is composed of 5 subunits, DIM-5, DIM-7, DIM-8, DIM-9, and CUL4. DIM-5, which is the catalytic subunit of the complex, is responsible for the tri-methylation of H3K9 (14). DIM-7 is required for interaction between DIM-5 and the histone substrate at A:T-rich sequences (15). DIM-8, DIM-9 and CUL4 are also required for H3K9 methylation, although how these three components facilitate H3K9 methylation through DIM-5 is not clear (13). Tri-methylated H3K9 residues (H3K9me3) are in turn recognized by HP1, which leads to DNA cytosine methylation and the heterochromatin formation and domain silencing (16, 17).

The knockout mutation of any individual DCDC subunits has been shown to lead to a hypersensitivity to MMS. In contrast, DNA methylation deficient mutants (*Δhpo* and *Δdim-2*) were shown to have normal sensitivity (13). In addition, loss of the DIM-5 subunit activates the DNA damage response in the absence of exogenous damaging agents, indicated by increased γH2A across the entire genome (18). *Δdim-5* also suffers from aberrant facultative heterochromatin formation at A:T-rich repetitive domains where H3K9 methylation would normally occur. H3K27 methylation also does not occur at the normal facultative heterochromatin domains in the *Δdim-5*, which indicates that chromatin structure in *Δdim-5* is disorganized.

The studies suggest that either the DCDC complex or H3K9me3 are required for maintaining genome integrity. Importantly, the MMS-hypersensitivity of *Δdim-5* is suppressed upon the removal of H3K27 methylation. It is currently unknown whether aberrant facultative heterochromatin itself is the cause of MMS-hypersensitivity as *Δhpo* is not MMS-hypersensitive

in spite of the H3K27me3 redistribution. However, the exact molecular mechanism that allow DIM-5 to play a role in MMS-tolerance remains a mystery.

The DIM-5 catalytic reaction depends on its SET domain and the N-terminal tail of H3. DIM-5 is composed of 318 amino acid residues and contains a SET domain that is conserved across most eukaryotic histone lysine methyltransferases (19). Structures of DIM-5 co-crystalized with a methyl-donor mimic (S-adenosyl-homocytosine) and the H3 N-terminal peptide (15 AA residues) suggest that this SET domain is the catalytically active site on DIM-5 (20, 21). The SET domain has been shown to fold into a binding pocket where both the methyl-donor and the histone substrate are bound. *In vitro* biochemical assays indicate that DIM-5 AA residues N241, Y283, L317, and W318 are required for interaction with the methyl-donor, whereas AA residues D209 and F281 are utilized for the histone substrate recognition (20-22). While the catalytic pocket is required for interaction with both the histone substrate and the methyl-donor, the H3 peptide sequence has been shown to affect the catalysis of the methyltransferase reaction (23). Mutations at the H3 histone residues R8, S10, T11, and G12 significantly lowered the level of H3K9 methylation by DIM-5 *in vitro* (23). Histone mutants $hH3^{R8A}$ and $hH3^{S10A}$ are both defective for DNA methylation, which suggests that these alleles have reduced levels of H3K9me3 *in vivo* (24).

Materials and methods

Stains and growth media

Strains used in this study are listed in Table 4.1. Vogel's minimal medium with 1.5% sucrose was used to grow strains in a 32 °C incubator. Crosses were performed on modified

synthetic cross medium at room temperature for 2 to 3 weeks. Plating assays were performed according to previously described methods in (18).

Construction of DIM-5 catalytic mutants

Primers and plasmids used in this study are listed in Table 4.2. The *dim-5* gene was amplified by PCR using the Phusion DNA polymerase including its native promoter region. Fragments were digested by NotI and PacI and cloned into pCCG::C-3xFLAG using the T4 DNA Ligase (25). The cloned *dim-5* was mutated by the site-directed mutagenesis using the Phusion DNA polymerase. The DNA sequence of each mutant was sequenced by Genewiz and the point mutations were confirmed. For *Neurospora* transformation, plasmids were linearized by NdeI and electroporated into a histidine auxotroph of *Δdim-5*. Transformants were selected on VMM+1.5% sucrose. Insertion of the dim-5 gene at the his-3 locus was confirmed by PCR and Southern blot.

W**estern blot**

Cells were grown in VMM with 1.5% sucrose for 2 days. Mycelia were harvested, washed with PBS, and placed in 500 µL of protein extraction buffer (50 mM HEPES pH 7.5, 150 mm NaCl, 1 mm EDTA, 0.02% NP-40,1 mM PMSF, 1 tablet per 10 mL of protease inhibitor cocktail). Cells were lysed by sonication at following setting (output 3.5; duty cycle 80; 1 second pulses) for 30 pulses. SDS-PAGE was performed using a 10% acrylamide gel (Acrylamide: Bis-Acrylamide ratio 29:1), and proteins were transferred onto a PDVF membrane using Tris-glycine transfer buffer (25 mM Tris, 192 mM glycine, 20% methanol). The PDVF membrane was incubated with PBS containing 3% non-fat powdered milk for 30 minutes at room temperature

on a rotation platform, rinsed with PBS, and incubated in PBS with 1:10000 dilution of FLAG® M2 monoclonal antibody overnight at 4 ˚C on a rotating platform. The membrane was washed with PBS two times, and incubated with anti-mouse secondary antibody conjugated with HRP for 30 min at room temperature on a rotation platform. Thermo Scientific™ SuperSignal™ West Femto Chemiluminescent Substrate was used to visualize FLAG-tagged proteins. The signal was detected using a FluorChem™ E System.

Chromatin Immunoprecipitation (ChIP),Quantitative PCR, and Illumina sequencing.

ChIP and qPCR were performed according to previously described methods {Sasaki, 2014 #4588}. For K27me3, one microliter of the K27 methylation specific antibody (Cat# 39535, Active motif) was used. Primers used for the qPCR are described in (18) and . Real-time quantitative PCR was performed using iTaq Universal SYBR green Supermix (Bio-Rad) and CFX96 Touch Real-Time PCR Detection System (Bio-Rad) according to manufacturer's instructions. Illumina sequencing libraries were constructed using the TruSeq ChIP Sample Prep Kit A and B (Catalog #: IP-202-1012 and IP-202-1024, respectively) according to the manufacturer's instructions. For K27me3 samples, twelve cycles of PCR were performed at the PCR-enrichment step. Bioinfomatic analysis on ChIP-seq data were performed as previously described (18).

Results

DIM-5 catalytic activity is required for MMS tolerance.

To determine if DIM-5 catalytic activity is required for normal MMS-tolerance, we first constructed DIM-5 catalytic mutants. The *dim-5* constructs were driven by the native *dim-5*

promoter at *his-3* locus and coupled to a 3xFLAG-tag at the C-terminus. Wild-type DIM-5-FLAG was transformed into the *Δdim-5* strain and was shown to have normal expression of DIM-5 and to complement the growth defect and loss of DNA methylation to the normal level (Fig 4.1). This confirms that WT DIM-5-FLAG is expressed the *his-3* locus at native levels and that it has fully functional histone H3 methyltransferase activity sufficient for directing DNA methylation. Catalytic mutants were also shown to be expressed when integrated at the *his-3* locus, but were unable complement the loss of DNA methylation (Fig 4.1). This suggests that the DIM-5 catalytic mutants are unable to perform H3K9 methylation.

We then examined the DIM-5 catalytic mutants for sensitivity to 0.025% MMS. All DIM-5 catalytic mutants except *dim-5*^{W318A} showed hypersensitivity to MMS, indicating that functional DIM-5 catalytic activity is required for growth in the presence of MMS (Fig 4.2). It is unknown why *dim-5*^{W318A} did not demonstrate MMS hypersensitivity and exhibited better growth phenotype relative to the other DIM-5 catalytic mutants. We hypothesized that there is a low level of H3K9 methylation occurring sufficient to relieve the MMS-induced stress and growth defect in this strain.

To test this possibility, we performed ChIP to examine the levels of H3K9 methylation in *dim-5*^{W318A}. Despite the fact that there was no detectable DNA methylation by Southern blot, *dim-5*^{W318A} was found to be able to catalyze H3K9 methylation (Fig 4.3). The level of H3K9 methylation was found to be reduced in the *dim-5*^{W318A} in comparison to wild-type. This suggests that the reduced H3K9 level was not sufficient to direct DNA methylation. It also suggests that there is a threshold of H3K9 methylation required for HP1 binding and subsequent DIM-2 recruitment. In addition, we tested the H3K27me3 levels at constitutive heterochromatin domains to see if PRC2 components are misregulated in in *dim-5*^{W318A} strain. Indeed, H3K27

methylation was observed at H3K9me3 locus peak 90 (Fig 4.3). Thus, reduced H3K9 methylation level and aberrant H3K27 methylation lead to the intermediate phenotypes in *dim-5*^{W318A}.

H3 K9 methylation is required for a normal response to MMS and CPT induced replicative stress.

To test if the MMS hypersensitivity of *Δdim-5* is caused by a loss of H3K9me3, we next examined the sensitivity of H3K9 deficient mutants to MMS. Although an *hH3*^{K9L} allele was reported to be lethal in a homokaryotic strain of Neurospora{Adhvaryu, 2011 #402}, mutation of H3K9 to glutamine (Q) and arginine (R) are both viable. Both *hH3*^{K9Q} and *hH3*^{K9R} are hypersensitive to MMS but to a lesser extent than is found in *Δdim-5* (Fig. 4.4). This indicates that both H3K9 methylation and DIM-5 catalytic activity are required for normal tolerance to MMS-induced stress. It also suggests that DIM-5 may play an additional role in the MMS-induced stress tolerance. Interestingly, *hH3*^{K9R} is more susceptible to CPT than *hH3*^{K9Q} or *Δdim-5*. This may indicate that factors required for response to CPT-induced stress are not properly functioning in the *hH3*^{K9R} mutant but are functional in *hH3*^{K9Q} mutant.

Removal of H3K27me3 in *hH3*^{K9Q} suppresses MMS hypersensitivity but sensitizes cells to CPT.

Since it has been shown previously that SET-7 deletion suppresses the MMS-hypersensitivity of *Δdim-5,* we constructed the double mutants *hH3*^{K9Q}*;Δset-7*, *hH3*$^{K9Q:K27Q}$, and *hH3*$^{K9Q:K27R}$ and tested them on 0.02% MMS plates. As expected, MMS-hypersensitivity was suppressed in all of the double mutants (Fig 4.5). Interestingly these double mutants were shown

to be hypersensitive to CPT, but to have a normal level of sensitivity to hydroxyurea (Fig 4.5). Mutants of H3K27, *hH3*^{K9Q} and *hH3*^{K9R} were not hypersensitive to MMS, CPT or hydroxyurea (Fig. 4.5). To test if facultative heterochromatin formation occurs normally in these mutants, we performed ChIP-seq to map distribution of H3K27me3 in *hH3*^{K9Q} and *hH3*^{K9R}. As was seen in *Δdim-5*, H3K27me3 was shown to be redistributed to A:T-rich domains where constitutive heterochromatin usually occurs in wild-type (Fig 4.6).

Chromodomain proteins are not required for tolerance of MMS induced-DNA damage.

Due to the observed redistribution of H3K27 methylation found in both the *hH3*^{K9Q} *and Δdim-5* strains, we hypothesized that chromatin components functioning at the normal H3K27me3 domains are aberrantly recruited to constitutive heterochromatin domains where they inhibit normal cell growth and cause MMS-hypersensitivity. To test this hypothesis we introduced deletion alleles of genes whose products contain methyl-lysine binding motifs, such as tudor and chromo domains into the *Δdim-5* background. The resulting double mutants lacked both DIM-5 and one of the 10 predicted methyl-lysine binding proteins. It was expected that removal of any methyl-lysine binding protein interacting with H3K27me3 would reduce or abolish MMS-hypersensitivity in the *Δdim-5* background. However, none of the double mutants were shown to have any suppression or decrease in MMS-hypersensitivity (Fig 4.7). Though no decrease in MMS-hypersensitivity was found, a number of other intriguing effects were noted. The *Δmi-2;Δdim-5* double mutant was shown to have synthetic growth defects (data not shown), and the *Δcrf-6;Δdim-5* was unable to be isolated indicating that it may be synthetically lethal.

Discussion

DIM-5 catalytic activity and H3K9me3 are necessary to cellular MMS response.

Eukaryotic cells are exposed to various biotic stresses resulting from basic cellular activities. Many components required for the normal response to such endogenous stresses have been identified through high-throughput screens of mutants utilizing various DNA damaging agents (7, 26). Interestingly, the DCDC complex has been found to be required for cellular tolerance of MMS induced stress, but not to the stresses induced by CPT and HU (13).

Since each subunit of the DCDC complex is required for normal H3K9 methylation, we decided to examine MMS-hypersensitivity in the *Δdim-5*strain to by ascertaining if this sensitivity depends on DIM-5 catalytic activity or on proper H3K9 methylation. To do this we constructed three H3K9 mutants, $hH3^{K9Q}$, $hH3^{K9R}$, and $hH3^{K9A}$ to test for hypersensitivity to the MMS-induced stress. These specific AA residue mutations were chosen as Arginine and glutamine mimic unacetylated and acetylated lysine respectively.

The $hH3^{K9A}$ strain was shown to be hypersensitive to MMS, but had a severe growth defect (data not shown) that made it difficult to determine whether this hypersensitivity was caused by a defect in the MMS stress response pathway or by pleiotrophic affects caused by the more dramatic change in N-terminal tail structure. Both the $hH3^{K9Q}$ and $hH3^{K9R}$ strains were shown to be more sensitive to MMS than WT, however the $hH3^{K9Q}$ strain had only a relatively minor sensitivity to MMS. These results indicate that MMS-hypersensitivity is at least partialy dependent on the H3K9 residue and that H3K9 methylation is required for normal MMS-induced stress tolerance. More Importantly, DIM-5 catalytic activity has also been shown to play a role in MMS induced replicative stress tolerance as the *Δdim-5* strain is slightly more sensitive to MMS

than *hH3*^{K9R} strain. This seems to indicate that DIM-5 catalytic activity promotes MMS-tolerance through the methylation of non-histone substrates.

Mutant strains deficient in HP1 and DIM-2 (*Δhpo and Δdim-2 respectivley)* are not hypersensitive to MMS as these proteins function downstream of H3K9me3 deposition and they retain both normal DIM-5 catalytic activity and H3K9me3 level in most of constitutive heterochromatin domains. It should also be noted that, in *S. pombe,* heterochromatin components are required for normal MMS-induced stress tolerance. *Δclr4*, a mutant of *dim-5* homolog, is hypersensitive to MMS whereas *Δswi6*, HP1 counterpart, is not (26). This indicates that the mechanism by which both CLR4 catalytic activity and H3K9 methylation play a role in MMS-tolerance in *S. pombe* might be similar to the ones in *Neurospora*. However, *Δclr4* is also hypersensitive to HU and tetrabenazine (TBZ) whereas *Δdim-5* is not (26). This suggests that the functionally diverged role of heterochromatin components on genome integrity among fungi.

Role of H3K9 residue to CPT-tolerance

Interestingly, *hH3*^{K9R} is hypersensitive to CPT but *Δdim-5* and *hH3*^{K9Q} are not. It suggests that H3K9 acetylation might be required for CPT-induced stress response pathway such as removal of the topo1-DNA complex. It is supported by the fact that loss of Gcn5 causes hypersensitivity to CPT in both *S. cerevisiae* and *S. pombe* (26). Further genetic analysis is needed to characterize the acetylation-dependent role in the CPT-induced stress.

Genetic interaction between H3K9 and H3K27

PRC2 is aberrantly recruited to A:T-rich domains in the absence of H3K9 methylation. Given the observations that redistribution of K27me3 occurs in *hH3*^{K9Q} and *hH3*^{K9R}, these strains

suffer from the aberrant facultative domains. Indeed, removal of the H3K27 methylation suppresses MMS-hypersensitivity of *hH3*^{K9Q}. A study has shown that redistribution of K27me3 also occurs in *Δhpo*, indicating that HP1 interacts with H3K9me3 and prevents PRC2 from associating with A:T-rich domains, restricting facultative heterochromatin at the normal location. Why H3K27 positioned in A:T-rich domains become preferred substrates for PRC2 in the absence of HP1 localization at constitutive heterochromatin remains elusive. Based on the fact that *Δhpo* exhibits normal sensitivity to MMS, redistribution of K27me3 is not the cause of MMS hypersensitivity. MMS-tolerance appears to depend on both DIM-5 catalytic activity and H3K9 residue.

Loss of methylation at both K9 and K27 of H3 N-terminal tail dramatically affect tolerance of *Neurospora* to MMS and CPT. This is perhaps because some DNA repair machineries can properly respond to the MMS-induced genotoxic stress whereas others do not function optimally to CPT-induced damage in the absence of both H3K9 and H3K27 methylation. In other words, mutations in the histone N-terminal tail might lead to pleiotropic effects on various DNA damage response pathways: Some pathways are intact and others are not. H3 N-terminal tails on an array of nucleosomes serve as an important platform to regulate DNA repair factors to maintain genome integrity.

Putative methyl-lysine binding proteins may not be involved in recognition of K27me3

AT-rich DNA repetitive sequence of *Neurospora* directs constitutive heterochromatin formation through H3K9me3. HP1 brings a lot of factors to the domains, such as CDP-2, HDA-1, CHAP, DMM complex, and DIM-2 (17, 27). In the absence of H3K9 methylation, the PRC2 complex is recruited to the same A:T-rich domains catalyzing H3K27 methylation. This leads to

formation of repressive heterochromatin distinctive from the one directed by H3K9 methylation, causing the growth defect. However, components required for the abnormal PRC2 recruitment are not known. We therefore attempted to identify factors associating with the aberrant facultative heterochromatin domains in *Δdim-5* to elucidate the molecular mechanism of the toxicity. We selected 7 proteins with a putative chromodomain and 2 with a tudor domain, and crossed with *Δdim-5*. Both single mutants of the putative methyl-lysine binding proteins and double mutants with *Δdim-5* were isolated and tested on MMS plates. None of the double mutants exhibited suppression of MMS hypersensitivity whereas all single mutants showed a normal level of sensitivity to MMS. It suggests that the putative methyl-binding proteins are not the cause of toxicity in *Δdim-5*. The results also indicate that they are not required for aberrant PRC2 recruitment.

MI-2 is critical for growth in *Δdim-5*

Importantly, *Δmi-2*;*Δdim-5* showed synthetic growth defect, whereas *Δmi-2* shows normal growth. MI-2 is a well conserved protein required for normal growth and development in *Caenorhabditis elegans*, plants and animals. The genetic interaction between MI-2 and DIM-5 might indicate that MI-2 plays an important role in promoting cell growth in *Δdim-5* background. In mammalian cells, CHD3 and CHD4, homologs of MI-2, make a complex with a histone deacetylase complex NuRD (28) . The MI-2/NuRD complex is required for normal S-phase progression, proper pericentromeric heterochromatin formation and genome integrity (29). NuRD contains metastatic tumor antigen 1 (MTA1) that is required for its repression function. Interestingly, MTA1 is methylated by a H3K9 methylatransferase G9a at K532. Interaction between CHD4 and the methylated MTA1 is required for repression function of MI-2/NuRD. A

point mutant of MTA1^{K532R} loses its interaction with CHD4, leading to derepression of subset of genes targeted by MI-2/NuRD (30). In *C. elegans*, MI-2 homologs are associated with vulval development, modulating Ras signaling pathway (31). In *Neurospora*, MI-2 has not been characterized and its binding partners have not been identified. Hence, it would be interesting to see whether *Neurospora* MI-2 interacts with histone deacetylases and if so what genes are repressed by the complex. Also, given the fact that G9a targets a subunit of MI-2/NuRD in mammalian cell, MI-2 and its interacting partners might be non-histone substrates of DIM-5 and the interaction could contribute to genome integrity, although Neurospora does not have homologous proteins to MTA1 and NuRD complex.

MI-2 could play a role in DNA damage response or genome maintenance since its function appears to play a pivotal role in growth of *Δdim-5*. In a human cell, CHD4 localizes to a DNA region damaged by the ionized radiation. Remarkably, PRC2 (EZH2, SUZ12, and EED) and other NuRD components (HDAC1 and MTA1) also accumulate at the damaged sites (32-34). Accumulation of HDAC1 is reduced in the absence of CHD4 (34). In addition, in a mouse embryonic stem cell, both PRC2 and MI-2/NuRD localize to A:T-rich satellite repeats upon removal of DNA methylation (35). These observations suggest that MI-2 might localize to constitutive heterochromatin domains in *Δdim-5* due to loss of DNA methylation at A:T-rich sequence or as a part of DNA damage response. Then MI-2 could function to maintain genome integrity at the constitutive heterochromatin domains. We are tempted to speculate that, in the absence of heterochromatin components, A:T-rich sequences might be recognized as the damaged DNA. In fact, spontaneous activation of the DNA damage response is observed in *Δdim-5* (18). This could explain the synthetic growth defect in *Δmi-2*;*Δdim-5*. Further

characterization of *Δmi-2*;*Δdim-5* is required to test the hypothesis and will uncover the functional role of the conserved chromatin remodeler MI-2 on genome integrity in *Neurospora*.

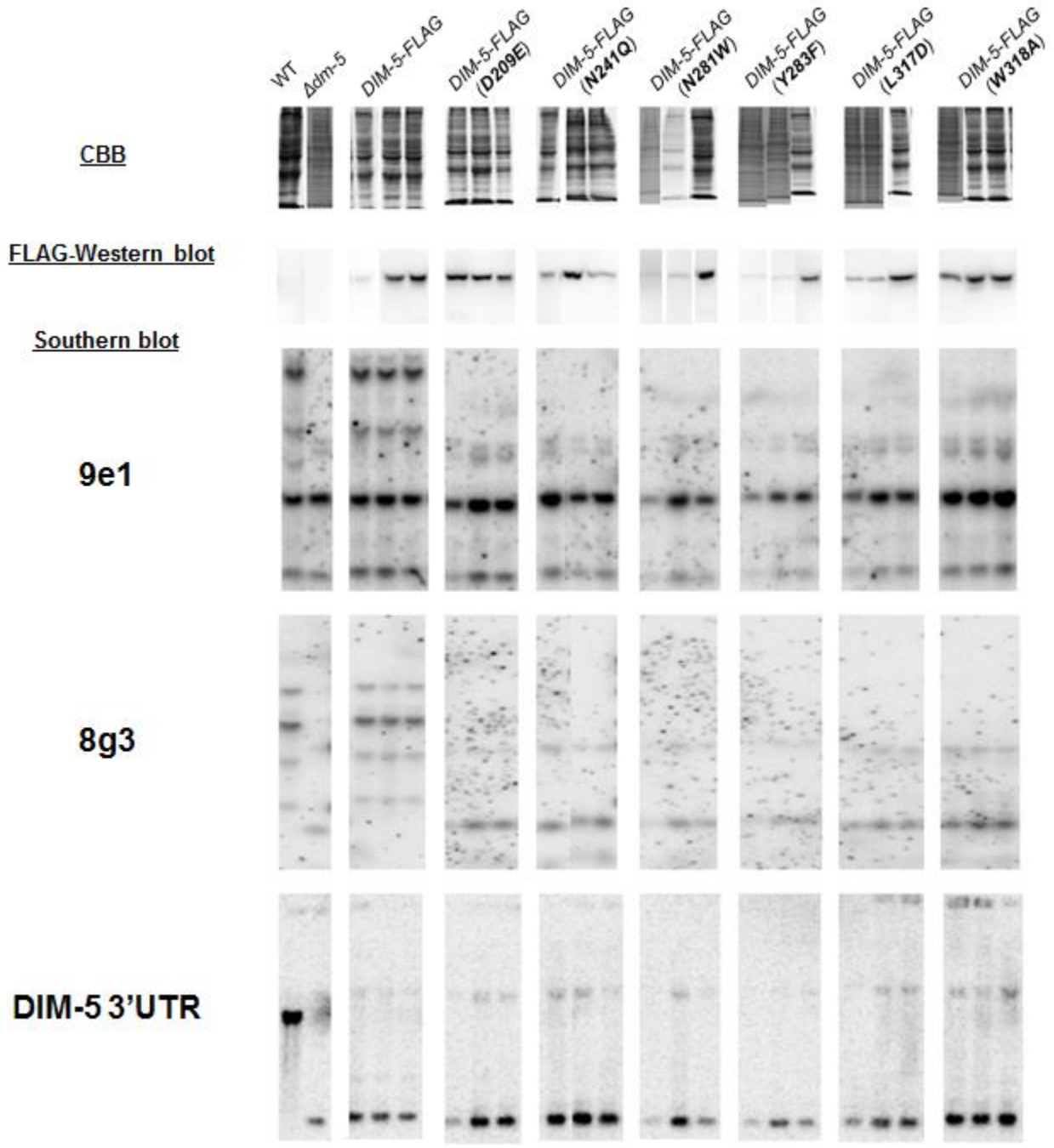

Figure. 4.1 DIM-5 catalytic mutants abolish DNA methylation. Cells were lysed by sonication and centrifuged. Soluble proteins in the supernatant were loaded into proteins gels and transferred onto a PDVF membrane. Western blot was performed to detect FLAG-tagged DIM-5 and its mutants to assess the protein expression at his-3 locus. To look at the DNA methylation level, genomic DNA was isolated from each strain. DNA digested with the methyl-sensitive

enzyme AvaII was probed with 9e1 (methylated region) or digested with the methyl-sensitive enzyme HpaII and probed with 8g3 (methylated region). To confirm the endogenous *dim-5* gene was absent, DNA was digested with ApaL1 and KpnI and probed for the *dim-5* 3'UTR. Southern blot was performed using a probe labeled with P32.

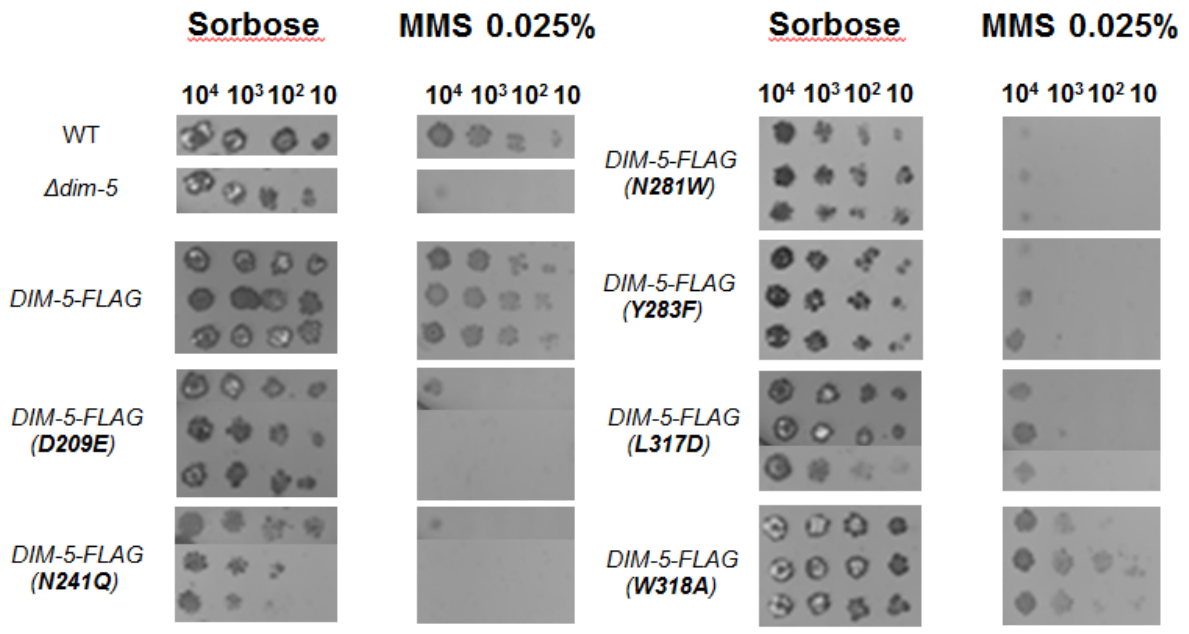

Figure. 4.2 DIM-5 catalytic activity is required for growth on MMS. Suspensions of 10^4, 10^3, 10^2 or 10 conidia of the indicated strains were spot-tested on media with or without methyl methanesulfonate (MMS). Strains were grown three days at 32 °C.

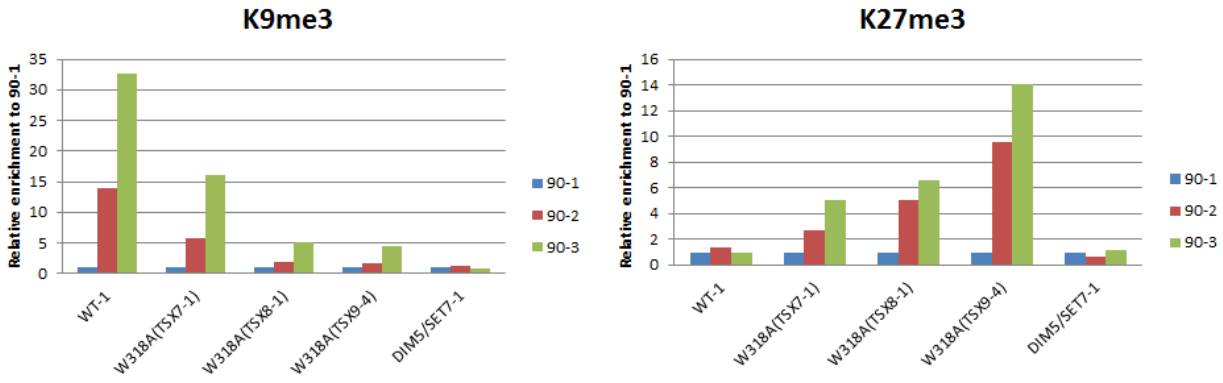

Figure 4.3 DIM-5(W318A) has a reduced catalytic activity but sufficient to induce PRC2 mislocalization. ChIP was performed using indicated strains pulling down nucleosomes containing H3K9me3 or H3K27me3. The, qPCR was performed to look at the relative enrichment of a constitutive heterochromatin locus peak 90. Locus 90-1 (euchromatin), 90-2 (boundary between euchromatin and constitutive heterochromatin) and 90-3 (constitutive heterochromatin) were amplified to examine the H3K9me3 or H3K27me3 level. Enrichment was normalized to locus 90-1.

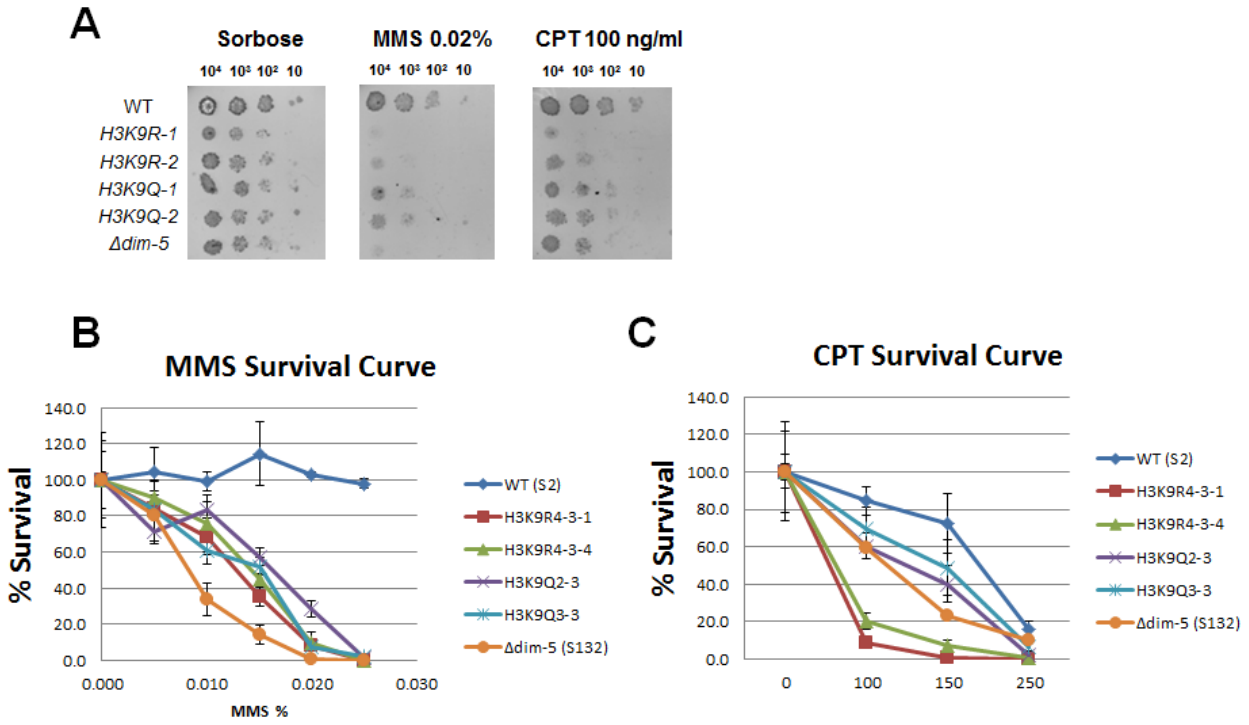

Figure 4.4 Replicative stress tolerance of H3K9 mutants. (A) Suspensions of 10^4, 10^3, 10^2 or 10 conidia of the indicated strains were spot-tested on media with or without methyl methanesulfonate (MMS) or camptothecin (CPT). Strains were grown three days at 32 °C. Approximately 200 conidia were spread on a series of (B) MMS or (C) CPT to examine the sensitivity of the indicated strains to the DNA damaging agents.

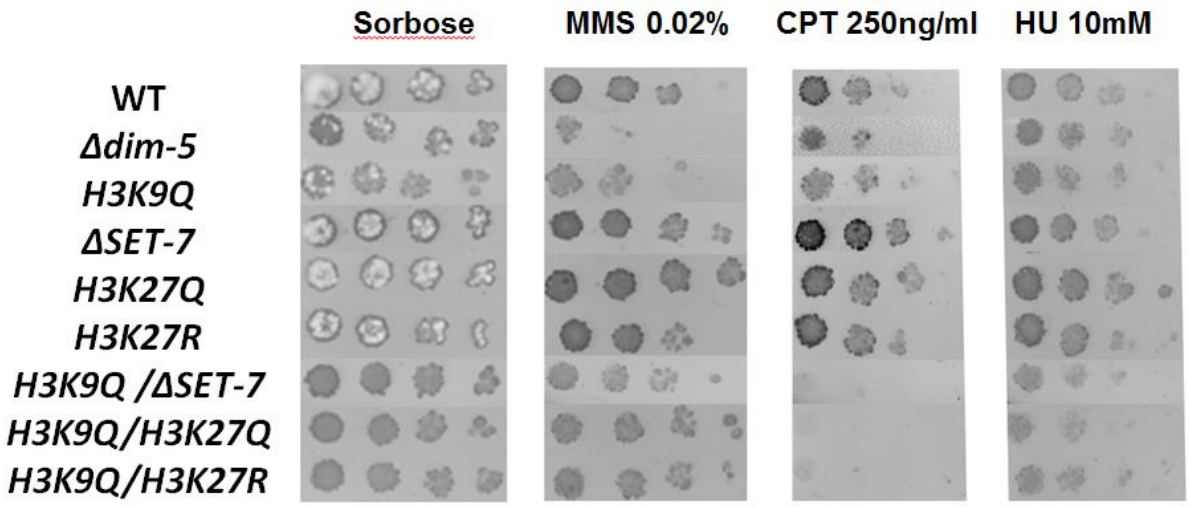

Figure 4.5 Removal of H3K27 methylation can suppress the MMS hypersensitivity in H3K9Q but induce hypersensitivity to CPT. Suspensions of 10^4, 10^3, 10^2 or 10 conidia of the indicated strains were spot-tested on media with or without methyl methanesulfonate (MMS), camptothecin (CPT), or hydroxyurea (HU).

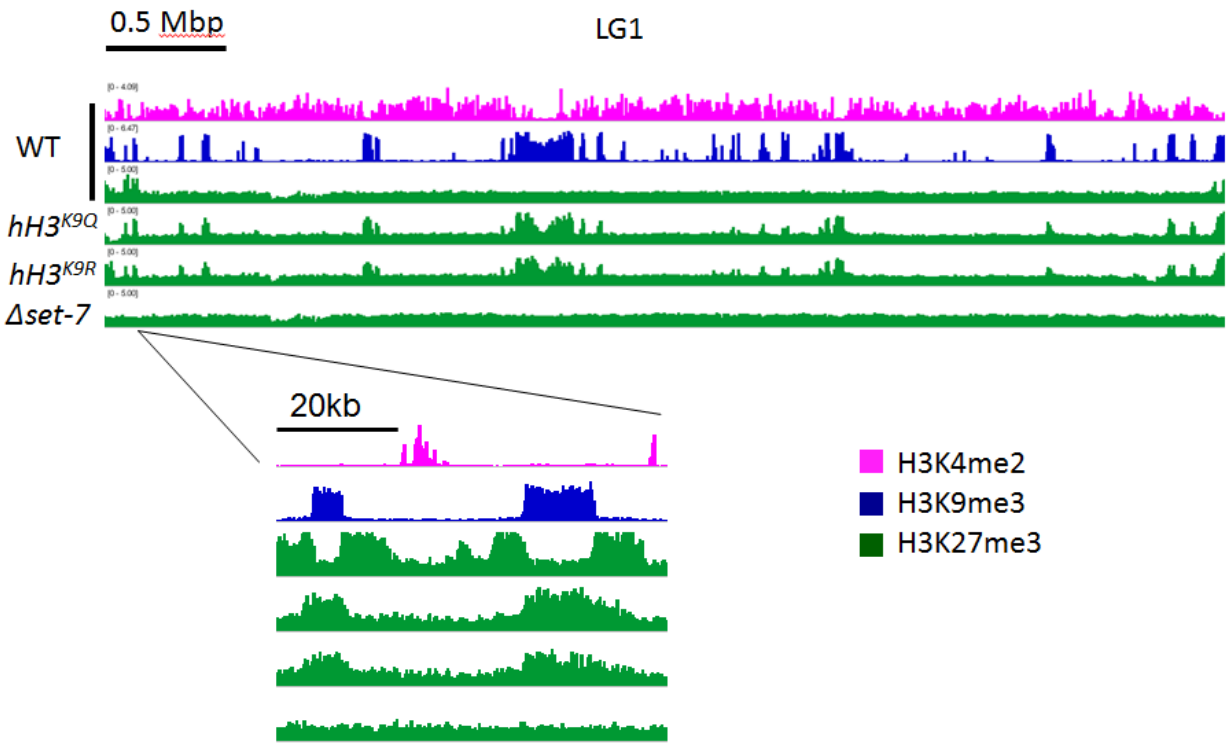

Figure 4.6 *hH3*^{K9Q} and *hH3*^{K9R} have aberrant facultative chromatin. H3K27me3 ChIP-seq was performed using the indicated strains. Reads from Illumina sequencing were mapped to Neurospora genome (V12).

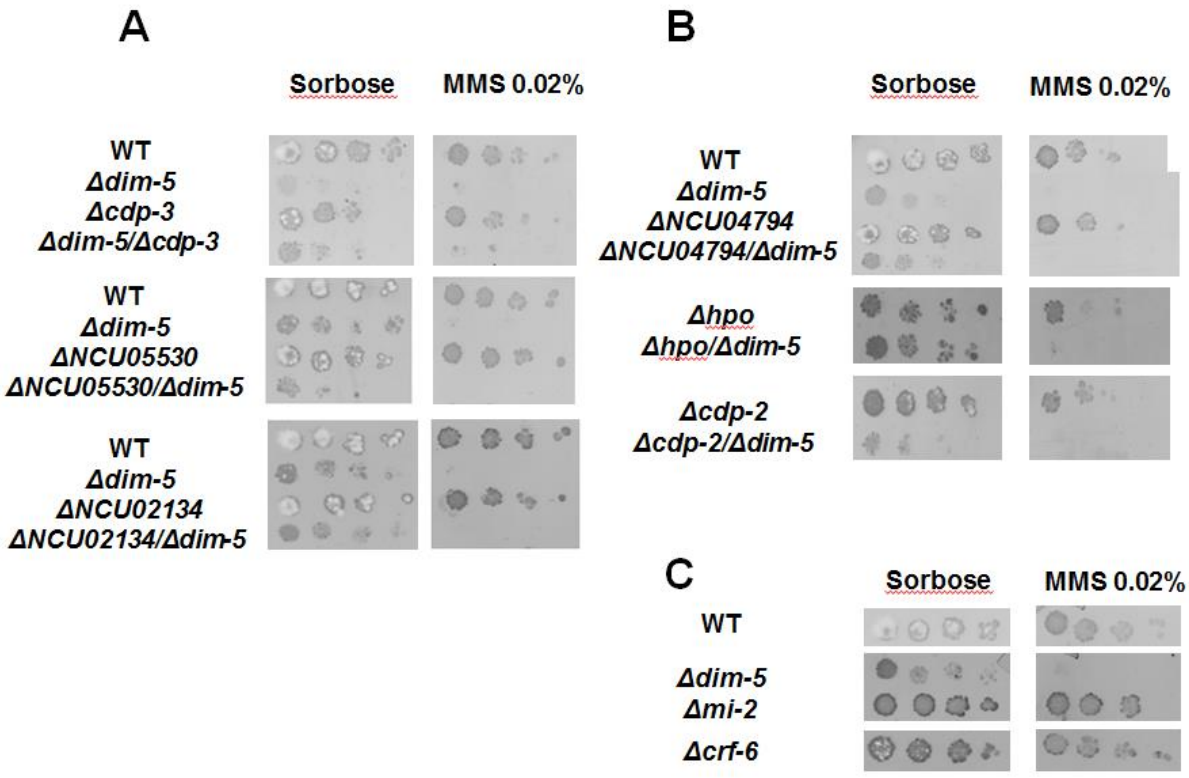

Figure 4.7 MMS sensitivity of mutants of methyl-lysine binding proteins in wild-type and *Δdim-5* background. Suspensions of 10^4, 10^3, 10^2 or 10 conidia of the indicated strains were spot-tested on media with or without methyl methanesulfonate (MMS)

Table S4.1
Strains used in this study

Strain	Genotype	Source/reference
S2	Wildtype	FGSC# 2489
S181	*Δhpo-1::hph+*	FGSC # 14522
S242	*Δdim-5::bar+, his-3::dim-5-FLAG*	This Study
S243	*Δdim-5::bar+, his-3::dim-5-FLAG*	This Study
S244	*Δdim-5::bar+, his-3::dim-5-FLAG*	This Study
S246	*Δdim-5::bar+, his-3::dim-5-FLAG*	This Study
S247	*Δdim-5::bar+, his-3::dim-5-FLAG(209E)*	This Study
S248	*Δdim-5::bar+, his-3::dim-5-FLAG(209E)*	This Study
S249	*Δdim-5::bar+, his-3::dim-5-FLAG(N241Q)*	This Study
S250	*Δdim-5::bar+, his-3::dim-5-FLAG(N241Q)*	This Study
S251	*Δdim-5::bar+, his-3::dim-5-FLAG(N241Q)*	This Study
S252	*Δdim-5::bar+, his-3::dim-5-FLAG(N241Q)*	This Study
S253	*Δdim-5::bar+, his-3::dim-5-FLAG(F281W)*	This Study
S254	*Δdim-5::bar+, his-3::dim-5-FLAG(F281W)*	This Study
S255	*Δdim-5::bar+, his-3::dim-5-FLAG(Y283F)*	This Study
S256	*Δdim-5::bar+, his-3::dim-5-FLAG(Y283F)*	This Study
S257	*Δdim-5::bar+, his-3::dim-5-FLAG(Y283F)*	This Study
S258	*Δdim-5::bar+, his-3::dim-5-FLAG(L317A)*	This Study
S259	*Δdim-5::bar+, his-3::dim-5-FLAG(L317A)*	This Study
S260	*Δdim-5::bar+, his-3::dim-5-FLAG(W318A)*	This Study
S261	*Δdim-5::bar+, his-3::dim-5-FLAG(W318A)*	This Study
S262	*Δdim-5::bar+, his-3::dim-5-FLAG(W318A)*	This Study
S263	*Δdim-5::bar+, his-3::dim-5-FLAG*	This Study
S264	*Δdim-5::bar+, his-3::dim-5-FLAG(209E)*	This Study
S265	*Δdim-5::bar+, his-3::dim-5-FLAG(N241Q)*	This Study
S266	*Δdim-5::bar+, his-3::dim-5-FLAG(F281W)*	This Study
S267	*Δdim-5::bar+, his-3::dim-5-FLAG(F281W)*	This Study
S268	*Δdim-5::bar+, his-3::dim-5-FLAG(Y283F)*	This Study
S268	*Δdim-5::bar+, his-3::dim-5-FLAG(Y283F)*	This Study
S269	*Δdim-5::bar+, his-3::dim-5-FLAG(L317A)*	This Study
S270	*Δdim-5::bar+, his-3::dim-5-FLAG(W318A)*	This Study
S271	*Δdim-5::bar+, his-3::dim-5-FLAG(W318A)*	This Study
S272	*Δdim-5::bar+, his-3::dim-5-FLAG(W318A)*	This Study
S273	*Δdim-5::bar+, his-3::dim-5-FLAG*	This Study
S274	*Δdim-5::bar+, his-3::dim-5-FLAG(209E)*	This Study
S275	*Δdim-5::bar+, his-3::dim-5-FLAG(Y283F)*	This Study
S276	*Δdim-5::bar+, his-3::dim-5-FLAG(L317A)*	This Study

S277	*Δdim-5::bar+, his-3::dim-5-FLAG*	This Study
S278	*Δdim-5::bar+, his-3::dim-5-FLAG(N241Q)*	This Study
S279	*Δdim-5::bar+, his-3::dim-5-FLAG(Y283F)*	This Study
S280	*Δdim-5::bar+, his-3::dim-5-FLAG(N241Q)*	This Study
S302	*FgH3::bar+*	(18)
S303	*hH3::hH3K9Q::hph+*	(18)
S304	*hH3::hH3K9R::hph+*	(18)
S305	*hH3::hH3K9Q::hph+*	(18)
S306	*hH3::hH3K9R::hph+*	(18)
S394	*hH3::hH3K9A::hph+*	This Study
S395	*hH3::hH3K9A::hph+*	This Study
S396	*hH3::hH3K9Q;K27R:hph+*	This Study
S397	*hH3::hH3K9Q;K27R:hph+*	This Study
S398	*hH3::hH3K27Q::hph+*	This Study
S399	*hH3::hH3K27Q::hph+*	This Study
S400	*hH3::hH3K27Q::hph+*	This Study
S401	*hH3::hH3K27Q::hph+*	This Study
S402	*hH3::hH3K27R::hph+*	This Study
S403	*hH3::hH3K9Q;K27Q:hph+*	This Study
S404	*hH3::hH3K9Q;K27Q:hph+*	This Study
S405	*hH3::hH3K27Q::hph+*	This Study
NCU00738.7	Δcdp-2::hph	FGSC #11771
NCU00738.7;Δdim-5	Δcdp-2::hph, Δdim-5::bar+	This Study
NCU01522.7	Δcdp-3::hph	FGSC #11772
NCU01522.7;Δdim-5	Δcdp-3::hph, Δdim-5::bar+	This Study
NCU04017.7	*Δhpo-1::hph, Δdim-5::bar+*	This Study
NCU05530.7	ΔNCU05530.7::hph	FGSC #12173
NCU05530.7;Δdim-5	ΔNCU05530.7::hph,Δdim-5::bar+	This Study
NCU03060.7	crf6-1/chd1	FGSC #14805
NCU10337.7	Δmi-2::hph,	This Study
NCU10337.7;Δdim-5	Δmi-2::hph,Δdim-5::bar+	This Study
NCU02134	ΔNCU02134::hph	FGSC # 12751
NCU02134 ;Δdim-5	ΔNCU02134::hph, Δdim-5::bar+	This Study
NCU04794	ΔNCU04794 ::hph	FGSC # 18163
NCU04794 ;Δdim-5	ΔNCU04794 ::hph, Δdim-5::bar+	This Study

References

1. **Vos SM, Tretter EM, Schmidt BH, Berger JM.** 2011. All tangled up: how cells direct, manage and exploit topoisomerase function. Nature reviews. Molecular cell biology **12:**827-841.

2. **Champoux JJ.** 2001. DNA topoisomerases: structure, function, and mechanism. Annual review of biochemistry **70:**369-413.

3. **Lopes M, Cotta-Ramusino C, Pellicioli A, Liberi G, Plevani P, Muzi-Falconi M, Newlon CS, Foiani M.** 2001. The DNA replication checkpoint response stabilizes stalled replication forks. Nature **412:**557-561.

4. **Aguilera A, Gomez-Gonzalez B.** 2008. Genome instability: a mechanistic view of its causes and consequences. Nature reviews. Genetics **9:**204-217.

5. **Bando M, Katou Y, Komata M, Tanaka H, Itoh T, Sutani T, Shirahige K.** 2009. Csm3, Tof1, and Mrc1 form a heterotrimeric mediator complex that associates with DNA replication forks. The Journal of biological chemistry **284:**34355-34365.

6. **Voineagu I, Narayanan V, Lobachev KS, Mirkin SM.** 2008. Replication stalling at unstable inverted repeats: interplay between DNA hairpins and fork stabilizing proteins. Proceedings of the National Academy of Sciences of the United States of America **105:**9936-9941.

7. **Chang M, Bellaoui M, Boone C, Brown GW.** 2002. A genome-wide screen for methyl methanesulfonate-sensitive mutants reveals genes required for S phase progression in the presence of DNA damage. Proceedings of the National Academy of Sciences of the United States of America **99:**16934-16939.

8. **Wyatt MD, Pittman DL.** 2006. Methylating agents and DNA repair responses: Methylated bases and sources of strand breaks. Chemical research in toxicology **19:**1580-1594.

9. **Johnson RE, Yu SL, Prakash S, Prakash L.** 2007. A role for yeast and human translesion synthesis DNA polymerases in promoting replication through 3-methyl adenine. Molecular and cellular biology **27:**7198-7205.

10. **Liu LF, Desai SD, Li TK, Mao Y, Sun M, Sim SP.** 2000. Mechanism of action of camptothecin. Annals of the New York Academy of Sciences **922:**1-10.

11. **Koc A, Wheeler LJ, Mathews CK, Merrill GF.** 2004. Hydroxyurea arrests DNA replication by a mechanism that preserves basal dNTP pools. The Journal of biological chemistry **279:**223-230.

12. **Abraham RT.** 2001. Cell cycle checkpoint signaling through the ATM and ATR kinases. Genes & development **15:**2177-2196.

13. **Lewis ZA, Adhvaryu KK, Honda S, Shiver AL, Knip M, Sack R, Selker EU.** 2010. DNA methylation and normal chromosome behavior in Neurospora depend on five components of a histone methyltransferase complex, DCDC. PLoS genetics **6:**e1001196.

14. **Tamaru H, Selker EU.** 2001. A histone H3 methyltransferase controls DNA methylation in Neurospora crassa. Nature **414:**277-283.

15. **Lewis ZA, Adhvaryu KK, Honda S, Shiver AL, Selker EU.** 2010. Identification of DIM-7, a protein required to target the DIM-5 H3 methyltransferase to chromatin. Proceedings of the National Academy of Sciences of the United States of America **107:**8310-8315.

16. **Tamaru H, Zhang X, McMillen D, Singh PB, Nakayama J, Grewal SI, Allis CD, Cheng X, Selker EU.** 2003. Trimethylated lysine 9 of histone H3 is a mark for DNA methylation in Neurospora crassa. Nature genetics **34:**75-79.

17. **Honda S, Lewis ZA, Shimada K, Fischle W, Sack R, Selker EU.** 2012. Heterochromatin protein 1 forms distinct complexes to direct histone deacetylation and DNA methylation. Nature structural & molecular biology **19:**471-477.

18. **Sasaki T, Lynch KL, Mueller CV, Friedman S, Freitag M, Lewis ZA.** 2014. Heterochromatin controls gammaH2A localization in Neurospora crassa. Eukaryotic cell **13:**990-1000.

19. **Dillon SC, Zhang X, Trievel RC, Cheng X.** 2005. The SET-domain protein superfamily: protein lysine methyltransferases. Genome biology **6:**227.

20. **Zhang X, Yang Z, Khan SI, Horton JR, Tamaru H, Selker EU, Cheng X.** 2003. Structural basis for the product specificity of histone lysine methyltransferases. Molecular cell **12:**177-185.

21. **Zhang X, Tamaru H, Khan SI, Horton JR, Keefe LJ, Selker EU, Cheng X.** 2002. Structure of the Neurospora SET domain protein DIM-5, a histone H3 lysine methyltransferase. Cell **111:**117-127.

22. **Adhvaryu KK, Gessaman JD, Honda S, Lewis ZA, Grisafi PL, Selker EU.** 2015. The cullin-4 complex DCDC does not require E3 ubiquitin ligase elements to control heterochromatin in Neurospora crassa. Eukaryotic cell **14:**25-28.

23. **Rathert P, Zhang X, Freund C, Cheng X, Jeltsch A.** 2008. Analysis of the substrate specificity of the Dim-5 histone lysine methyltransferase using peptide arrays. Chemistry & biology **15:**5-11.

24. **Adhvaryu KK, Berge E, Tamaru H, Freitag M, Selker EU.** 2011. Substitutions in the amino-terminal tail of neurospora histone H3 have varied effects on DNA methylation. PLoS genetics **7:**e1002423.

25. **Honda S, Selker EU.** 2009. Tools for fungal proteomics: multifunctional neurospora vectors for gene replacement, protein expression and protein purification. Genetics **182:**11-23.

26. **Pan X, Lei B, Zhou N, Feng B, Yao W, Zhao X, Yu Y, Lu H.** 2012. Identification of novel genes involved in DNA damage response by screening a genome-wide Schizosaccharomyces pombe deletion library. BMC genomics **13:**662.

27. **Honda S, Lewis ZA, Huarte M, Cho LY, David LL, Shi Y, Selker EU.** 2010. The DMM complex prevents spreading of DNA methylation from transposons to nearby genes in Neurospora crassa. Genes & development **24:**443-454.

28. **Denslow SA, Wade PA.** 2007. The human Mi-2/NuRD complex and gene regulation. Oncogene **26:**5433-5438.

29. **Sims JK, Wade PA.** 2011. Mi-2/NuRD complex function is required for normal S phase progression and assembly of pericentric heterochromatin. Molecular biology of the cell **22:**3094-3102.

30. **Nair SS, Li DQ, Kumar R.** 2013. A core chromatin remodeling factor instructs global chromatin signaling through multivalent reading of nucleosome codes. Molecular cell **49:**704-718.

31. **von Zelewsky T, Palladino F, Brunschwig K, Tobler H, Hajnal A, Muller F.** 2000. The C. elegans Mi-2 chromatin-remodelling proteins function in vulval cell fate determination. Development **127:**5277-5284.

32. **Campbell S, Ismail IH, Young LC, Poirier GG, Hendzel MJ.** 2013. Polycomb repressive complex 2 contributes to DNA double-strand break repair. Cell cycle **12:**2675-2683.

33. **Chou DM, Adamson B, Dephoure NE, Tan X, Nottke AC, Hurov KE, Gygi SP, Colaiacovo MP, Elledge SJ.** 2010. A chromatin localization screen reveals poly (ADP ribose)-regulated recruitment of the repressive polycomb and NuRD complexes to sites of DNA damage. Proceedings of the National Academy of Sciences of the United States of America **107:**18475-18480.

34. **Dobbin MM, Madabhushi R, Pan L, Chen Y, Kim D, Gao J, Ahanonu B, Pao PC, Qiu Y, Zhao Y, Tsai LH.** 2013. SIRT1 collaborates with ATM and HDAC1 to maintain genomic stability in neurons. Nature neuroscience **16:**1008-1015.

35. **Saksouk N, Barth TK, Ziegler-Birling C, Olova N, Nowak A, Rey E, Mateos-Langerak J, Urbach S, Reik W, Torres-Padilla ME, Imhof A, Dejardin J, Simboeck E.** 2014. Redundant mechanisms to form silent chromatin at pericentromeric regions rely on BEND3 and DNA methylation. Molecular cell **56:**580-594.

CHAPTER 5

CONCLUSIONS

The goal of these studies was to elucidate the molecular mechanisms by which heterochromatin components regulate genome integrity in the tractable model organism for chromatin research *Neurospora crassa*. Heterochromatin is required for normal growth and development in many eukaryotes. However, how heterochromatin maintains genome integrity is complex because many chromatin associated factors are associated with the densely packaged form of chromatin. Despite the fact that heterochromatin has been extensively studied using various model systems and current understanding of heterochromatin is expanding at fast pace, we still do not fully understand a role of heterochromatin in genome integrity. *Neurospora* is suited for chromatin research because of its genetically tractable nature and chromatin components resembling ones in plants and animals. Also, *Neurospora* allows us to do experiments that are difficult or impossible to do in other model organisms. Using this tractable model, I investigated a role of heterochromatin components in genome integrity. My work provides insights into how heterochromatin components facilitate normal chromosomal architecture. Also, my dissertation research is relevant to understanding of cancer cells and contributes to provide the basic knowledge of heterochromatin function that should serve as a foundation for development of therapeutics for cancer treatment.

Previous research in *Neurospora* has provided the conclusive model for DNA cytosine methylation pathway directed by H3K9me3. The H3K9 methylation is mediated by the KMT complex composed of DIM-5, DIM-7, DIM-9, DDB1, and CUL4. All of the components are

essential for both H3K9 methylation and DNA methylation in *Neurospora*. Interestingly, single deletion mutants of each KMT complex become hypersensitive to MMS, an alkylating agent that causes the stalled DNA replication fork and double stranded breaks (DSBs). This indicates that the KMT complex is required for genome integrity and that the mutation of KMT complex might result in defective DNA replication, chromosomal segregation, or/and DNA repair. In Chapter 2, I demonstrated that *Δdim-5* has aberrant γH2A distribution whereas, in wild-type, γH2A is enriched in constitutive heterochromatin domains. It suggests that DNA damage checkpoint is activated in *Δdim-5* in the absence of the exogenous DNA damaging agent and γH2A spreads all over the genome. The aberrant γH2A induction appears to occur in other heterochromatin mutants, *hH3*^{K9Q}, *hH3*^{K9R}, *Δhpo, and Δ-hda1,* but not in *Δdim-2*. This illustrates the importance of heterochromatin components in maintaining normal genome integrity.

In order to understand the underlying mechanisms of the defects in *Δdim-5*, suppressors of the MMS hypersensitive mutants are isolated by the UV mutagenesis followed by screening on 0.025% MMS plates. After performing bulk segregate analysis followed by whole genome sequencing of suppressors, we identified suppressors of *Δdim-9*, which was EED, a component of PRC2 complex. As suppressors are lacking both K9 methylation and K27 methylation, we hypothesized that *Δdim-5* MMS hypersensitive phenotype would be suppressed by deletion of SET-7. In Chapter 3, I constructed the deletion of *set-7* in the *Δdim-5* background and tested if the double mutant grows on MMS. Indeed, removal of H3K27 methylation suppressed the MMS hypersensitive phenotype and partially rescued the cell growth defect of *Δdim-5*. Also, the aberrant γH2A formation observed in *Δdim-5* was also suppressed, although γH2A enrichment at the edge of heterochromatin domains was reduced. As growth defects and MMS hypersensitive phenotype of *Δdim-5* seems to be related to H3K27 methylation, we mapped H3K27me3

distribution in *Δdim-5* performing ChIP-Seq. I demonstrated the complete relocalization of H3K27me3 from facultative heterochromatin domains to constitutive heterochromatin domains. H3K27me3 at the constitutive heterochromatin domains is the cause of growth defects and MMS hypersensitivity. H3K27me3 is catalyzed by PRC2 that regulates a number of developmental processes in higher eukaryotes. PRC2 is required for normal cellular differentiation, and its dysregulation has a link to cancer such as glioma.

PRC2 is composed of SET-7, SUZ12, EED, and NRF in *Neurospora*. SET-7 is a catalytic subunit of PRC2 that catalyzes the tri-methylation of Lysine 27 of H3 (H3K27me3), directing the formation of facultative heterochromatin domains and silencing of the genes in these loci. SUZ12 and EED are required for the SET-7 catalytic activity, and NRF appears to have a minor role in PRC2 recruitment. Currently, how the PRC2 is recruited to certain chromosomal domains, how the H3K27 methylation is maintained, and how the boundary of the facultative domains is controlled is extensively studied by many researchers. In chapter 4, I tried to identify the components that function downstream of K27me3 at the constitutive heterochromatin domains in *Δdim-5*. I hypothesized that not only PRC2 but also other factors are mislocalized to the A:T-rich domains through H3K27me3. I, therefore, made double mutants of a putative methyl-binding protein and *Δdim-5* to see if it suppresses the MMS hypersensitivity of *Δdim-5*. However, Suppression of the MMS hypersensitivity was not observed in any of the double mutants. This suggests that the putative methyl-lysine binding proteins are not the cause of toxicity in *Δdim-5*.

Overall, I demonstrated that heterochromatin components are required to maintain normal chromosomal organization, such γH2A and H3K27 methylation. In the absence of heterochromatin components such as *Δdim-5* and H3K9 methylation, a number of factors start

functioning aberrantly. Checkpoint activation occurs in the absence of exogenous DNA damaging agents and PRC2 recruitment is completely changed. I speculate that not only PRC2 but also other chromatin associated factors are misregulated. In fact, in mice, upon removal of H3K9me3 or DNA methylation, PRC2 complex is recruited to constitutive heterochromatin domains of A:T-rich satellite repeats, transforming regions into facultative heterochromatin. At the same time, many factors, usually not present in the A:T-rich satellite repeats, start accumulating at the sites, leading to structurally different type of repressive chromatin. Therefore, my findings are relevant to heterochromatin regulation in animals and provide a strong foundation to investigate PRC2 recruitment.

Future directions

In Chapter 2, I demonstrated that γH2A a component of constitutive heterochromatin in *Neurospora* and heterochromatin components are required for normal distribution. This has been observed in *S. cerevisiae* and *S. pombe*. Currently, readers of γH2A are not known in *Neurospora*. In *S. pombe,* Brc1 mediate DNA damage response through its BRCT domain that specifically binds to the phosphorylated serine 129 of H2A. Since *Neurospora* has 10 proteins harboring a putative BRCT-domain, we asked if they can also bind γH2A and function as components of heterochromatin. Since we wanted to test if they localize to heterochromatin, I tagged the BRCT-domain proteins with RFP and observed their localization under fluorescent microscopy. Preliminary results suggest that RTT107, FCP1, and PES1 might be components of heterochromatin based on nuclear localization. Others did not show clear RFP signal in cells, possible due to the low expression level. PES1 appears to be highly induced upon MMS-induced damage. Future work will be to confirm if RFP-tagged proteins remain functional, as the bulky

nature of RFP might interfere with the native functions. Also, using a spin column with resins conjugated with RFP-antibody, ChIP-seq should be performed to identify the binding sites of BRCT-domain proteins. The pilot experiment using HP1-RFP was already done and enrichment of HP1-RFP at heterochromatin domain was confirmed by qPCR.

While γH2A mediates the DNA damage response, it is not clear what it biologically means by γH2A localization in constitutive heterochromatin. It has been shown in *S. cerevisiae* that γH2A enrichment correlate with DNA polymerase stall sites. Neurospora constitutive heterochromatin might be an impediment of DNA replication because it contains A:T-rich repetitive sequences that might be prone to make secondary structures. However, we currently do not have evidence that DNA polymerases stall at heterochromatin domains. I fused replisome components POLD, TOF1 and MRC1 with 3xFLAG and performed ChIP-Seq to identify the polymerase stalling sites in genome. However, we could not see enrichment of the proteins anywhere in genome, possible because POLD, TOF1 and MRC1 were not crosslinked with DNA. I also tagged these components with RFP to see if they localize at the heterochromatin domain in nucleus. However, I could not see any fluorescent signal inside cell probably because expression level of POLD, TOF1 and MRC1 was too low.

In Chapter 3, I demonstrate that K27me3 is redistributed in *Δdim-5*. However, how PRC2 is recruited to A:T-rich domains and how it is no longer recruited to the normal domain are not clear. Also, how PRC2 is targeted to the normal domains remains elusive. PRC2 is highly conserved and plays an important role in normal development in plants and animals. Despite PRC2 recruitment has been extensively studies in *Drosophila* and mammals, molecular determinants of targeting are still elusive. *Δdim-5* has the excellent phenotype to study PRC2 recruitment process. One of the hypotheses we try to test is if R-loop is responsible for

recruitment of PRC2 to A:T-rich domains in *Δdim-5*. Because the silencing in the constitutive heterochromatin domains is presumably lost in the absence of H3K9me3 and DNA methylation, AU-rich repetitive transcripts from constitutive heterochromatin domain might be prone to form DNA-RNA duplex that could attract PRC2 complex. In *S. pombe* and mammal, R-loop has been shown to direct constitutive heterochromatin formation. I made constructs overexpressing RNase H in the *Δdim-5* background to see if it inhibits PRC2 recruitment through elimination of the DNA-RNA duplex. Preliminary results show that Rnase H overexpression causes a subtle growth defect in wild-type and appears to be lethal in *Δdim-5*. Whether or not Rnase H is overexpressed needs to be confirmed. Elucidation of PRC2 mechanism will expand our knowledge of facultative heterochromatin formation and how a single cell differentiates into many cell types in animals.

In Chapter 4, I found *Δmi-2;Δdim-5* has a synthetic growth defect, indicating that MI-2 plays an important role in facilitating growth in *Δdim-5*. As described above *Δdim*-5 has aberrant facultative heterochromatin and the spontaneous DNA damage checkpoint induction. I speculate that the constitutive heterochromatin in the absence of DIM-5 is recognized as a "damage" activating the DNA damage checkpoint. As it has been shown that PRC2 and MI2/NuRD components localize to double stranded break sites in mammalian cells, I hypothesize that MI-2 plays a role in DNA damage response. It would be interesting to see if the same synthetic growth defect is observed in DNA repair mutants in *Δdim-5* background. Not only PRC2 but also other components are like to be redistributed to constitutive heterochromatin in *Δdim-5*. The important question is if they are causing toxic effects or actually promoting the growth. H3K27me3 is obviously the former. Identification of components recruited to the A:T-rich domain in *Δdim-5* will be a key to understand the molecular mechanism of genome maintenance.